# ASSESSMENT OF HYDROPOWER POTENTIAL USING GIS FOR SOUTHERN MIZORAM

## A DISSERTATION

*Submitted in partial fulfillment of the*
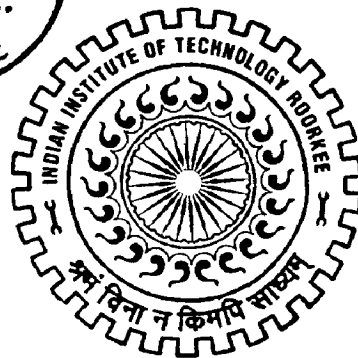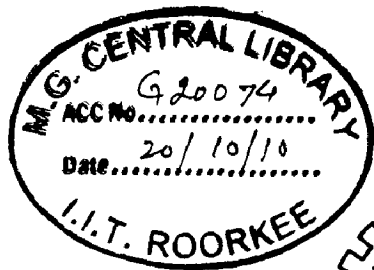*requirements for the award of the degree*
*of*

MASTER OF TECHNOLOGY

*in*

WATER RESOURCES DEVELOPMENT AND MANAGEMENT

*By*

## DANIEL LALREMPUIA

DEPARTMENT OF WATER RESOURCES DEVELOPMENT & MANAGEMENT
INDIAN INSTITUTE OF TECHNOLOGY ROORKEE
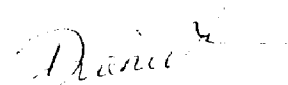ROORKEE-247 667 (INDIA)
JUNE, 2010

# CANDIDATE'S DECLARATION

I hereby certify that the work being presented in this Dissertation entitled "ASSESSMENT OF HYDRO POWER POTENTIAL USING GIS IN SOUTHERN MIZORAM" in partial fulfillment of the requirement for the award of degree of MASTER OF TECHNOLOGY in Water Resources Development and submitted in the Department of Water Resources Development and management, Indian Institute of Technology Roorkee, Roorkee is an authentic record of my work carried out during the period from August 2009 to June 2010 under the supervision and guidance of Dr. Ashish Pandey, Assistant Professor and Prof. S.K. Jain, Chair Professor NEEPCO, Department of Water Resource Development and Management, Indian Institute of Technology Roorkee, Roorkee, Uttarakhand, India.

The matter embodied in this dissertation has not been submitted by me for the award of any other degree.
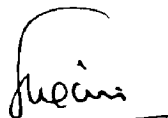
Dated : ....June, 2010

Place : Roorkee.

**(Daniel Lalrempuia)**

Enrollment No : 08548006

This is to certify that the above mentioned statement made by the candidate is correct to the best of our knowledge.

**(Prof. S.K. Jain)**
*Chair Proessor, NEEPCO*
Department of Water Resources
Development and Management
Indian Institute of Technology Roorkee
Roorkee-247667, Uttarakhand
INDIA

**(Dr. Ashish Pandey)**
*Assistant Professor*
Department of Water Resources
Development and Management
Indian Institute of Technology Roorkee
Roorkee-247667, Uttarakhand
INDIA

# ACKNOWLEDGEMENTS

Roorkee,

**( Daniel Lalrempuia )**

M. Tech ( WRD&M )

Date : 25th June, 2010

IIT Roorkee

# ABSTRACT

In this study, Geographical Information System (GIS), Remote Sensing (RS) and the SWAT (Soil and Water Assessment Tool) model are used for assessment of hydropower potential sites in the Mat watershed, Mizoram, India. The stream network was generated using Arc SWAT model. After locating the required elevation for the Digital Elevation Model (DEM), the stream length was measured from the outlet to check for the distance criteria. The subbasin outlet was then added manually in the stream network at each identified sites and the subwatershed was delineated again. The site was selected as potential hydropower site when both the height and distance criteria are met. The remaining sites were assessed in the same manner starting from the last selected site till the stream ends.

Calibration of the SWAT model was done for the year 1988 by manually adjusting the model parameters within the prescribed range and simulated discharge was compared with the observed discharge. The calibrated model was validated using four established indices, the Coefficient of determination ($R^2$), Nash and Sutcliffe efficiency (NSE), index of agreement (d), and relative error of the stream flow volume (RE) for the year 1989, 1991 and 1994. The validation was carried out using the discharge data of the year 1988, 1989, 1991 and 1994 altogether, and separately for the dry and rainy periods.

The discharge at each selected potential sites were generated with the help of the calibrated SWAT model. The hydropower potential was estimated for different discharge dependability using Flow duration Curve (FDC). Thirty three hydropower potential sites are identified within 147.325 $km^2$ of the Mat river basin. A total of 3039.47 KW, 1127.16 KW and 804.98 KW can be harnessed at 50 %, 75 % and 90% dependability respectively. The study revealed that hydropower potential site can be effectively evaluated by analyzing the Digital Elevation Model (DEM), stream network and the SWAT model.

**Keywords:** DEM,GIS, RS, hydropower, Arc SWAT.

# TABLE OF CONTENTS

# LIST OF TABLE

# LIST OF FIGURES

# LIST OF SYMBOLS AND ABBREVIATIONS

$\mu_{mon}$ = Mean daily rainfall (mmH$_2$O)

aa = Exponent between 0 and 1 that varies with atmospheric stability and surface roughness

Alfa_Bf = Base flow alpha factors

ARS = Agricultural Research Service

AVSWATX = Lower version of SWAT hydrological model

$b_{mlt}$ = Melt factor for the day (mm H$_2$O/day °C)

CEA = Central Electrical Authority

CER = Carbon emission reduction

CO$_2$ = Carbon dioxide

d = Index of agreement

DEM = Digital Elevation Model

$E_a$ = Amount of evapotranspiration on day i (mm H$_2$O)

ESCO = Soil Evaporation compensation factor

ET = Evapotranspiration

FDC = Flow Duration Curve

$g_{mon}$ = Skew coefficient for daily precipitation in the month

GIS = Geographical Information System

GWQMN = Threshold depth of water in the shallow aquifer required for return flow to occur

$h_c$ = Canopy height (cm)

$H_{day}$ = Total solar radiation reaching the earth's surface on that day

HRU = Hydrologic Response Units

$I_a$ = Initial abstractions (mm) which includes surface storage interception and Infiltration prior to runoff.

$I_{frac}$ = Fraction of total daily radiation falling during that hour

$I_{hr}$ = Solar radiation reaching the earth's surface during a specific hour of the day (MJ m$^{-2}$ hr$^{-1}$)

IVF = Index of Volumetric Fit

kN/m3 = Kilo Newton per cubic meter

kWh/m$^2$ = Kilowatt hour per square meter

LH = Latin-Hypercube

m = Order number of the discharge (or class value)

m/s = Meter per second

MW = Megawatt

n = Manning's roughness coefficient

NADUF = National Long-term Monitoring of Swiss Rivers

NLCD = National Land Cover Data

NSE = Nash and Sutcliffe efficiency

OAT = One-factor-At-a-Time

PBIAS = Percent BIAS

PME = Persistence Model Efficiency

Pp = Percentage probability of the flow magnitude being exceeded,

Q = Discharge

Qavg = Average value of observed discharge

$Q_{gw}$ = Amount of return flow on day i (mm H$_2$O)

Qmod = Model discharge

Qobs = Observed discharge

$Q_{surf}$ = Amount of surface runoff on day i (mm H$_2$O)

R $_{hmon}$ = Average relative humidity for the month.

R$^2$ = Coefficient of determination

$R_{day}$ = Amount of precipitation on day i (mm H$_2$O)

RE $\qquad$ = Relative error of the stream flow volume

REVAPMN $\qquad$ = Threshold depth of water in the shallow aquifer for 'revap' or percolation to the deep aquifer to occur

$R_{hUmon}$ $\qquad$ = Largest relative humidity value that can be generated on a given day in the month

RS $\qquad$ = Remote Sensing

S $\qquad$ = Retention Parameter (mm)

$SDN_{day}$ $\qquad$ = Standard normal deviate calculated for the day

$sno_{cov}$ $\qquad$ = Fraction of the HRU area covered by snow

$SNO_{mlt}$ $\qquad$ = Amount of snow melt on a given day (mm H 2 O)

SOL_AWC $\qquad$ = Available water capacity of soil layer

SOTERSAF $\qquad$ = Soil and Terrain Database for Southern Africa

STN $\qquad$ = Meteorological station

$SW_0$ $\qquad$ = Initial soil water content on day i (mm $H_2O$)

SWAT $\qquad$ = Soil and Water Assessment Tool

$SW_t$ $\qquad$ = Final soil water content (mm $H_2O$)

t $\qquad$ = time (days)

$T_{av}$ $\qquad$ = Average temperature on the day ($^oC$)

$T_{hr}$ $\qquad$ = Air temperature during hour hr of the day ($^oC$)

$t_i$ $\qquad$ = Solar time at the midpoint of hour I

$T_{mlt}$ $\qquad$ = Base temperature above which snow melt is allowed ($^oC$)

$T_{mn}$ $\qquad$ = Daily minimum temperature ($^oC$)

$T_{mx}$ $\qquad$ = Maximum air temperature on a given day ($^oC$)

$T_{snow}$ $\qquad$ = Snow pack temperature on a given day ($^oC$)

UK $\qquad$ = United Kingdom

USDA $\qquad$ = United State Department of Agriculture

USGS LULC $\qquad$ = United State Geological Survey Landuse / Landcover

$u_{z1}$ = Wind speed (m s$^{-1}$) at height $z_1$ (cm)

$u_{z2}$ = Wind speed (m s$^{-1}$) at height $z_2$ (cm)

$W_{seep}$ = Amount of water entering the vadose zone from the soil profile on day i

$z_w$ = Height of the wind speed measurement (cm)

$\eta$ = Overall efficiency of the turbine, generator etc.

$\sigma$ = Solar declination in radians

$\sigma_{mon}$ = Standard deviation of daily rainfall for the month

$\varphi$ = Geographic latitude in radians

$\omega$ = Angular velocity of the earth's rotation (0.2618 rad h$^{-1}$ or 15$^\circ$h$^{-1}$)

$\omega t$ = Hour angle.

# CHAPTER I

# INTRODUCTION

## 1.1    General

Harnessing the water resources available greatly affects the stability of the economy of country. In recent times the depletion rate of non-renewable sources of energy has increased greatly with the fast growing of population and deployment of advance technologies. Also, the by-products from non-renewable sources are polluting the environment and pose a serious threat to the whole community (U.S. Department of Energy). Hydropower is an important alternate source of energy due to its renewability and cleanliness. Therefore, water resources development and its management play a vital role in sustainable development of a nation.

Hydropower has generated lot of interest because it is inexhaustible source of energy and its convenience of providing electricity to far flung areas in hilly regions. The running costs of the hydropower installation are very low as compared to the thermal stations or the nuclear power station (Dandekar, 2008).

Hydropower has immense benefits and has been brought forward as a preferred option for power generation over the last decade (Ramchandra et al., 2004). The reasons for these can be summed as follows:

- Abundant potential of hydropower development in India.

- With relative independence from international trade in commodities like oil, hydropower involves no extra foreign exchange outgo.

- Hydropower is a no-inflation power as water- the 'raw material' for power generation is free of inflation

- Environment friendly

- Hydropower projects support socio-economic development of remote areas as the project site is developed.

- Hydropower is cost effective and renewable form of energy.

- Hydropower projects can also provide additional benefits like irrigation, flood control, tourism etc. with small additional investment.

India has immense economically exploitable hydropower potential of over the country with the identified capacity of 1487401 MW out of which the developed capacity is only 32077.8 MW which is 22.07 % of the total available potential. The capacity of projects under development is 14278.0 MW which is 9.83% from the total available potential. The remaining 68.1% as on 28.2.2010 remains un-harnessed due to many issues and barriers to the large scale development of hydropower in India according to Central Electrical Authority (www.cea.nic.in). The river Brahmaputra is the one of the largest river in the world which originates from southwestern Tibet, and flows across southern Tibet, Arunachal Pradesh, Assam Valley, Bangladesh and it merges with the Ganges to form a vast delta. The river is about 2900 km and has a large possible capacity of hydropower in India of about 34,920 MW which constitute about 41.5 percent from the total basin in India (Singh et al., 2004).

India's power system is divided into five major regions namely, the Northern, Western, Southern, Eastern and North-Eastern, with each region facing separate issues. While the Eastern and North-Eastern regions are power abundant, the Northern and Western regions have greater power demands. The hydropower potential is largest in NE region with 93.16% of it still untapped. Northern, Southern, Eastern and Western regions have 59.4%, 37.55%, 50.67% and 26.8% untapped hydropower potential respectively (CEA, 2010).

North-East India comprises of seven states commonly known as the "Seven Sisters". They are Arunachal Pradesh, Assam, Manipur, Meghalaya, Mizoram, Nagaland and Tripura. The North East region occupies 27.22 Mha of land (Kusre et al., 2010). It is characterized by hills and valleys with 70% of the land falls under hilly terrain. Northeast India has a predominantly humid sub-tropical climate with hot, humid summers, severe monsoons and mild winters. This region has some of the Indian sub-continent's last remaining rain forests. The average rainfall varies from 2000 to 4000 mm annually in different parts of the region. Agriculture is the major activity in this region. Several unique characteristic features make this region distinguished form the remaining part of India. Existence of traditional cultivation practices (shifting cultivation), diverse cultural norms and fabrics in form of multiple tribes, community land holding pattern in the tribal areas and fragmented land holding in plain areas, high rainfall, inaccessible areas due to difficult terrain are some of the distinguishing

features of this region. The Jhuming system of cultivation involves clearing of a piece of land by setting fire or clear felling and using the area for growing crops of agriculture importance such as rice or fruits (after a few cycles, the land loses fertility and a new area is chosen). The North Easter region has been marked as the highest potential region for development of hydropower (Table.1.1).

**Table 1.1: Status of Hydropower development (above 25 MW) in North-Eastern Region (CEA, 2010)**

| Region | Total Available potential | Capacity developed above 25MW | | Capacity above 25 MW under construction | | Capacity above 25 MW yet to be developed | |
|---|---|---|---|---|---|---|---|
| | (MW) | (MW) | % | (MW) | % | (MW) | % |
| Meghalaya | 2394 | 156 | 6.79 | 166 | 7.22 | 1976 | 85.99 |
| Tripura | 15 | 0 | 0 | 0 | 0 | 0 | 0 |
| Manipur | 1784 | 105 | 5.96 | 0 | 0 | 1656 | 94.04 |
| Assam | 680 | 375 | 57.69 | 0 | 0 | 275 | 42.31 |
| Nagaland | 1574 | 75 | 5.17 | 0 | 0 | 1377 | 94.83 |
| Arunachal Pd | 50328 | 405 | 0.81 | 2710 | 5.41 | 46949 | 93.78 |
| Mizoram | 2196 | 0 | 0 | 0 | 0 | 2131 | 100 |
| **Total** | **58971** | **1116** | **1.91** | **2876** | **4.93** | **54364** | **93.16** |

## 1.2    Hydropower development in Mizoram

Mizoram is one of the seven states of North-Eastern region. A major part of Mizoram state is covered by Lushai hills running from North to South. The average height of the hills is about 900 m above Mean Sea Level (M.S.L.). The highest peak in the range is Phawngpui with a height of 2065 m above M.S.L. Mizoram has a population of 0.89 million as per census of 2001. The state is spread over an area of 2108 $km^2$. Density of population in the study area is very low. Agriculture is the mainstay of the local people. The state has a total potential of 2196 MW which are yet to be developed as per CEA (2010). The major rivers in Mizoram are the Tlawng (also known as Dhaleswari or Katakhal), Tut (Gutur), Tuirial (Sonai) and Tuivawl which flow through the northern territory and eventually join river Barak in Cachar. None of these major rivers have been utilized for hydropower generation. Mizoram is rated as

3

one of potential area for hydropower development. It is a hilly region with deep valleys which make it all the more suitable for hydropower development.

Hilly regions have high potential for hydropower development but at the same time there are more problems in accessing the remotely located areas. Hydropower development in a hilly terrain requires a thorough study of geology, topography, land use patterns, availability of resources, infrastructure, socio-economic activities (Kusre et al., 2010). The feasibility study and baseline survey for hydropower is very difficult, time consuming and costly. But recent advances in Remote Sensing (RS) and Geographical Information System (GIS) provide more realistic and useful information for assessment of hydro power potential (Sung et al., 2009). The satellite image provides rich and accurate geographical information which can be access and studied using various GIS software available today. Collection of accurate information of topography, land use pattern, river morphology, and geology is easier within lesser time in the GIS environment than the conventional way of field survey (Rojanamon et al., 2009). GIS can manage all variables with reference to location, and can provide a clear picture about the hydropower project area and its impact zone.

The main purpose of this study is to assess the hydropower potential of various sites using GIS. Further, this study identifies the possible location for hydropower projects along the Mat river by measuring the river bed elevation difference using GIS. The runoff at these potential hydropower project sites is modeled using the SWAT (Soil and Water Assessment Tool) hydrological model.

## 1.3   Objective

In the present study RS, GIS and validated SWAT model will be used to assess the temporal and spatial availability of the hydropower potential in Mat River basin of Mizoram state, Mizoram.

The specific objectives of the study are as follows:

(i)     Calibration, validation and sensitivity analysis of the SWAT model for the Mat river basin of Mizoram, India.

(ii)    Identification of suitable sites for hydropower generation using RS, GIS and the SWAT model.

(iii)   Estimation of hydropower potential at the identified sites.

This study has employed the Soil and Water Assessment Tool (SWAT) model as it has the capability to generate multiple outputs taking into consideration the spatial and temporal changes of the physical and climatic conditions. This chapter deals with the theoretical aspects of deferent parameters, mathematical relations their interrelationship for generation of flow in the hydrological model SWAT.

The SWAT model is a watershed scale model. It was developed by Dr. Jeff Arnold for the USDA Agricultural Research Service (ARS) (Neitsch et al., 2005). SWAT was developed to predict the impact of land management practices on water, sediment and agricultural chemical yields in large complex watersheds with varying soils, land use and management conditions over long periods of time.

SWAT is physically based model, rather than incorporating regression equations to describe the relationship between input and output variables, SWAT requires specific information about weather, soil properties, topography, vegetation, and land management practices occurring in the watershed (Neitsch et al., 2005). The physical processes associated with water movement, sediment movement, crop growth, nutrient cycling, etc. are directly modeled by the SWAT using this input data.

SWAT has capabilities of simulating surface runoff, percolation, return flow, erosion, nutrient loading, pesticide fate and transport, irrigation, ground water flow, channel transmission losses, pond and reservoir storage, channel routing, field drainage, plant water use and other supporting processes from small, medium and large watersheds. SWAT model divides a watershed into sub basins which allows accounting of land uses and soil properties and its impact on hydrology. Then, the model subdivides these sub basins into smaller homogenous units known as Hydrologic Response Units (HRU). The HRUs are lumped land areas within the sub basin comprising of unique features of land cover, soil and its management (Arnold et al., 1993).

SWAT allows a number of different physical processes to be simulated in a watershed. For modeling purposes, a watershed may be partitioned into a number of subwatersheds or subbasins. The use of subbasins in a simulation is particularly

beneficial when different areas of the watershed are dominated by land uses or soils dissimilar enough in properties to impact hydrology. By partitioning the watershed into subbasins, the user is able to reference different areas of the watershed to one another spatially.

Input information for each subbasin is grouped or organized into the following categories: climate; hydrologic response units or HRUs; ponds/wetlands; groundwater; and the main channel, or reach, draining the subbasin. Hydrologic response units are lumped land areas within the subbasin that are comprised of unique land cover, soil, and management combinations.

No matter what type of problem studied with the SWAT, water balance is the first thing that must be correctly simulated in the watershed. To accurately predict the movement of pesticides, sediments or nutrients, the hydrologic cycle simulated by the model must conform to what is happening in the watershed.

Simulation of the hydrology of a watershed can be separated into two major divisions:

(i)    The first division is the land phase of the hydrologic cycle (Fig. 2.1). The land phase of the hydrologic cycle controls the amount of water, sediment, nutrient. and pesticide loadings to the main channel in each subbasin.

(ii)    The second division is the water or routing phase of the hydrologic cycle which can be defined as the movement of water, sediments, etc. through the channel network of the watershed to the outlet.

### 2.1.1  Land phase of the hydrologic cycle

The hydrologic cycle simulated by the SWAT is based on the water balance equation:

$$SW_t = SW_o + \sum_{i=1}^{t}( R_{day,i} - Q_{surf,i} - E_{a,i} - W_{seep,i} - Q_{gw,i})$$

where,

    $SW_t$ is the final soil water content (mm $H_2O$),

    $SW_0$ is the initial soil water content on day $i$ (mm $H_2O$),

    $t$ is the time (days),

$R_{day}$ is the amount of precipitation on day $i$ (mm $H_2O$),

$Q_{surf}$ is the amount of surface runoff on day $i$ (mm $H_2O$),

$E_a$ is the amount of evapotranspiration on day $i$ (mm $H_2O$),

$W_{seep}$ is the amount of water entering the vadose zone from the soil profile on

day $i$ (mm $H_2O$),

$Q_{gw}$ is the amount of return flow on day $i$ (mm $H_2O$).

The subdivision of the watershed enables the model to reflect differences in evapotranspiration for various crops and soils. Runoff is predicted separately for each HRU and routed to obtain the total runoff for the watershed. This increases accuracy and gives a much better physical description of the water balance. Fig. 2.2 shows the general sequence of processes used by SWAT to model the land phase of the hydrologic cycle.
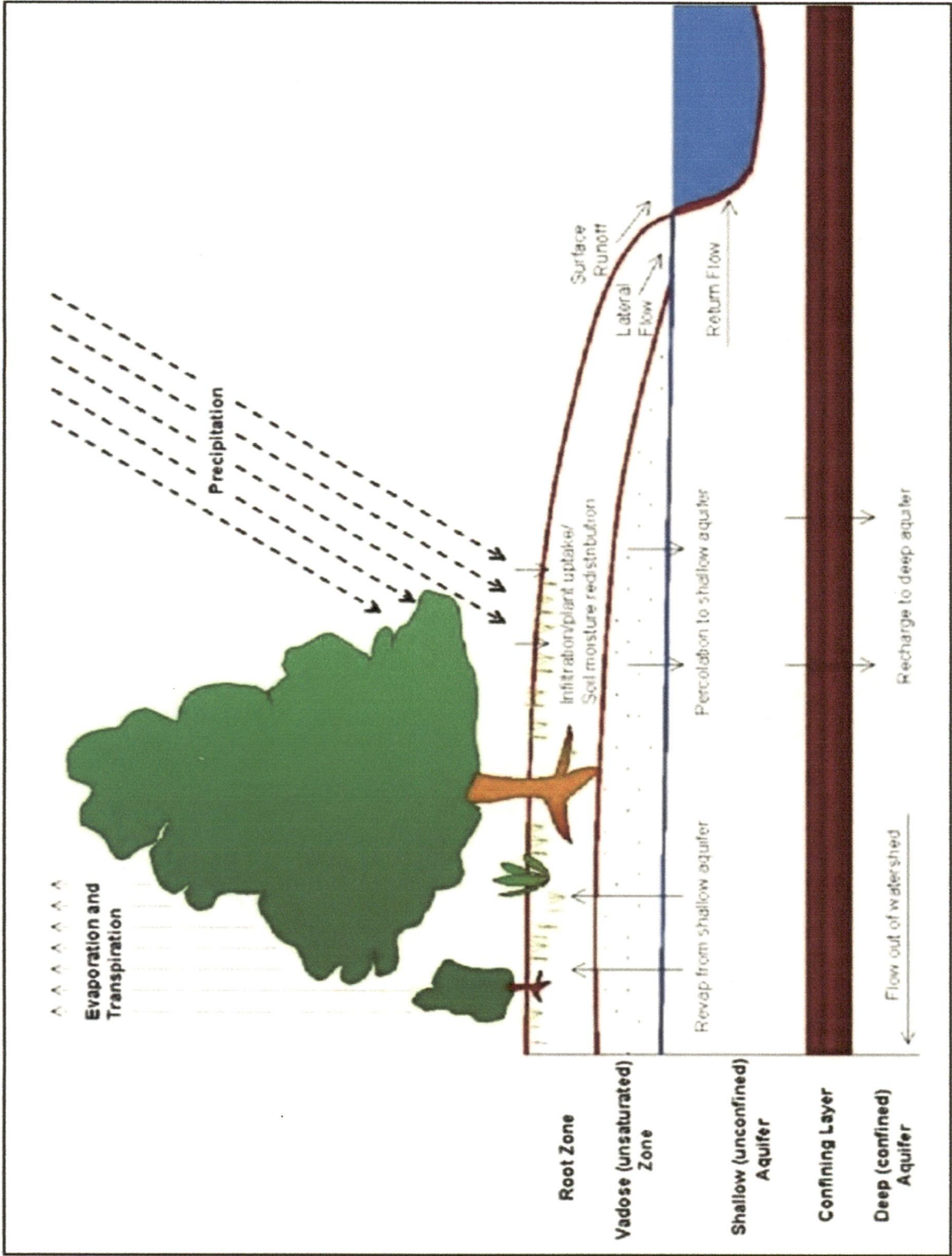
**Figure 2.1 Schematic presentation of hydrologic cycle.**
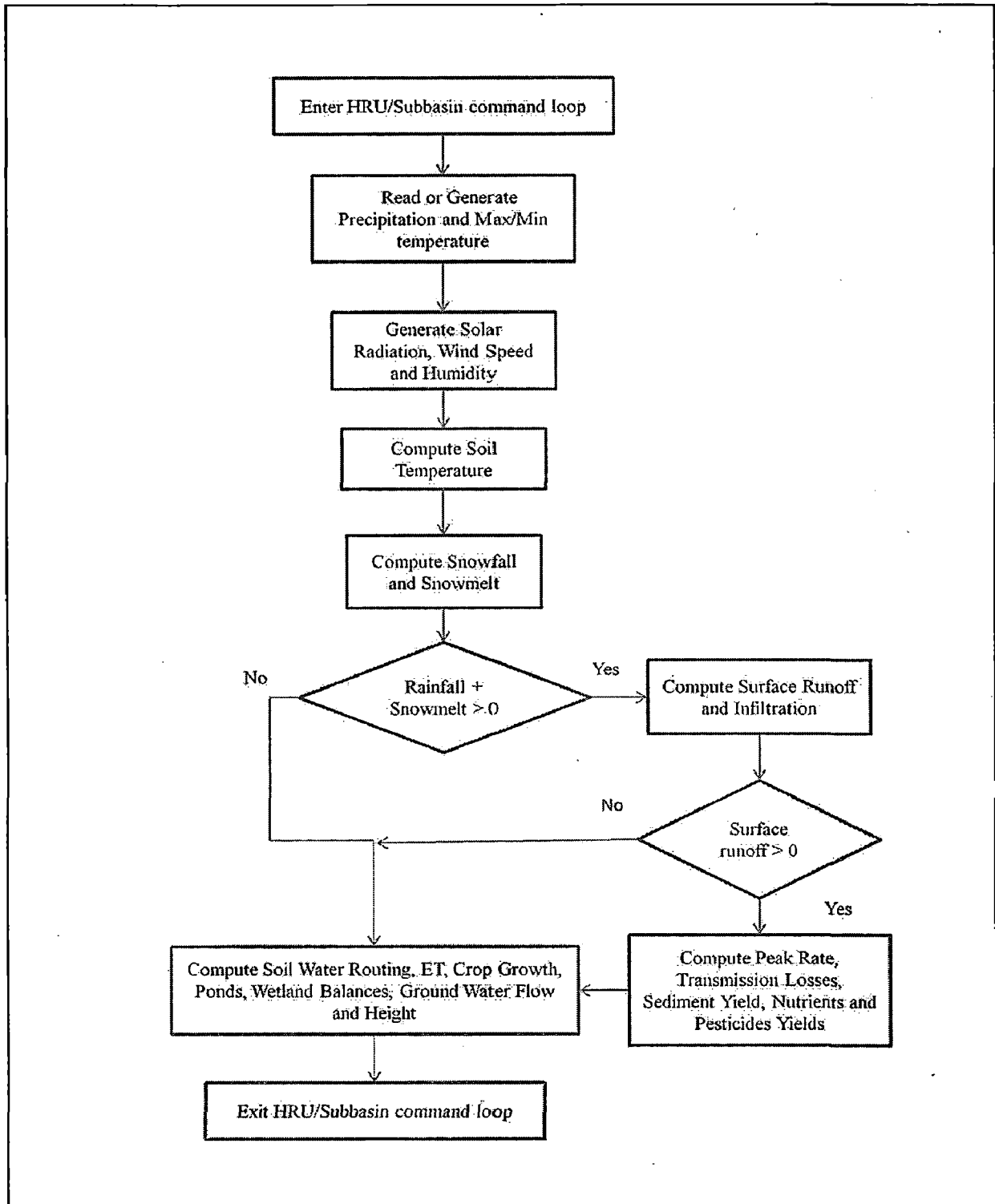
**Figure 2.2 HRU/Subbasin command Loop in SWAT (Neitsch et al., 2005)**

### 2.1.1.1 Generation of climatic parameters

The climate of a watershed provides the moisture and energy inputs that control the water balance and determine the relative importance of the different components of the hydrologic cycle. The climatic variables required by the SWAT consist of daily precipitation, maximum/minimum air temperature, solar radiation, wind speed and relative humidity. The model allows values for daily precipitation, maximum/minimum air temperatures, solar radiation, wind speed and relative humidity to be input from records of observed data or generated during the simulation.

### 2.1.1.2 Weather generator

The model generates a set of weather data for each subbasin. The values for any one subbasin will be generated independently and there will be no spatial correlation of generated values between the different subbasins.

### 2.1.1.3 Generated precipitation

SWAT uses a model developed by Nicks (1974) to generate daily precipitation for simulations which do not read in measured data. This precipitation model is also used to fill in missing data in the measured records. The precipitation generator uses a first-order Markov chain model to define a day as wet or dry by comparing a random number (0.0-1.0) generated by the model to monthly wet-dry probabilities input by the user. If the day is classified as wet, the amount of precipitation is generated from a skewed distribution or a modified exponential distribution.

The equation used to calculate the amount of precipitation on a wet day is:

$$R_{day} = \mu_{mon} + 2.\sigma_{mon} \left\{ \frac{\left[ \left( SDN_{day} - \frac{g_{mon}}{6} \right) \left( \frac{g_{mon}}{6} \right) + 1 \right]^3 - 1}{g_{mon}} \right\}$$

Where,

$R_{day}$ is the amount of rainfall on a given day (mmH$_2$O),

$\mu_{mon}$ is the mean daily rainfall (mmH$_2$O),

$\sigma_{mon}$ is the standard deviation of daily rainfall for the month,

$SDN_{day}$ is the standard normal deviate calculated for the day,

$g_{mon}$ is the skew coefficient for daily precipitation in the month.

### 2.1.1.4 Subdaily rainfall patterns

If subdaily precipitation values are needed, a double exponential function is used to represent the intensity patterns within a storm. With the double exponential distribution, rainfall intensity exponentially increases with time to a maximum, or peak, intensity. Once the peak intensity is reached, the rainfall intensity exponentially decreases with time until the end of the storm.

### 2.1.1.5 Generated air temperature and solar radiation

Maximum and minimum air temperatures and solar radiation are generated from a normal distribution. A continuity equation is incorporated into the generator to account for temperature and radiation variations caused by dry vs. rainy conditions. Maximum air temperature and solar radiation are adjusted downward when simulating rainy conditions and upwards when simulating dry conditions. The adjustments are made so that the long-term generated values for the average monthly maximum temperature and monthly solar radiation agree with the input averages.

Air temperature data are usually provided in the form of daily maximum and minimum temperature. A reasonable approximation for converting these to hourly temperatures is to assume a sinusoidal interpolation function between the minimum and maximum daily temperatures. The maximum daily temperature is assumed to occur at 1500 hours and the minimum daily temperature at 300 hours (Campbell, 1985). The temperature for the hour is then calculated with the following equation:

$$T_{hr} = T_{av}.\frac{(T_{mx}-T_{mn})}{2}.cos(0.2618(hr - 15))$$

Where, $T_{hr}$ is the air temperature during hour *hr* of the day ( °C),

$T_{av}$ is the average temperature on the day (°C),

$T_{mx}$ is the daily maximum temperature (°C), and

$T_{mn}$ is the daily minimum temperature (°C).

SWAT calculates hourly solar radiation at the earth's surface with the equation:

$$I_{hr} = I_{frac} \cdot H_{day}$$

Where, $I_{hr}$ is the solar radiation reaching the earth's surface during a specific hour of the day (MJ m -2 hr -1 ),

$I_{frac}$ is the fraction of total daily radiation falling during that hour, and

$H_{day}$ is the total solar radiation reaching the earth's surface on that day.

The fraction of total daily radiati on falling during an hour is calculated as:

$$I_{frac} = \frac{(sin\partial.sin\emptyset + cos\partial.cos\emptyset.cos\omega t_i)}{\sum_{t=SR}^{SS}(sin\partial.sin\emptyset + cos\partial.cos\emptyset.cos\omega t)}$$

Where, $t_i$ is the solar time at the midpoint of hour $I$,

σ is the solar declination in radians,

φ is the geographic latitude in radians,

ω is the angular velocity of the earth's rotation (0.2618 rad $h^{-1}$ or $15°h^{-1}$ ), and

$t$ is the solar hour. $t$ equals zero at solar noon, is a positive value in the morning and is a negative value in the evening.

The combined term $\omega t$ is referred to as the hour angle.

Sunrise, $T_{SR}$ , and sunset, $T_{SS}$ , occur at equal times before and after solar noon.

## 2.1.1.6 Generated wind speed

Wind speed is required by the SWAT if the Penman-Monteith equation is used to estimate potential evapotranspiration and transpiration. SWAT assumes wind speed information is collected from gages positioned 1.7 meters above the ground surface. When using the Penman-Monteith equation to estimate transpiration, the wind measurement used in the equation must be above the canopy. In SWAT, a minimum difference of 1 meter is specified for canopy height and wind speed measurements. When the canopy height exceeds 1 meter, the original wind measurements is adjusted to:

$$Z_w = h_c + 100$$

Where, $z_w$ is the height of the wind speed measurement (cm), and

$h_c$ is the canopy height (cm).

The variation of wind speed with elevation near the ground surface is estimated with the equation (Haltiner and Martin, 1957):

$$u_{z2} = u_{z1} \cdot \left[\frac{z_2}{z_1}\right]^{aa}$$

Where, $u_z 1$ is the wind speed (m s$^{-1}$) at height $z_1$ (cm),

$u_{z2}$ is the wind speed (m s$^{-1}$) at height $z_2$ (cm), and

$aa$ is an exponent between 0 and 1 that varies with atmospheric

stability and surface roughness.

Jensen (1974) recommended a value of 0.2 for $aa$ and this is the value used in SWAT.

### 2.1.1.7 Generated relative humidity

The relative humidity model uses a triangular distribution to simulate the daily average relative humidity from the monthly average. The triangular distribution used to generate daily relative humidity values requires four inputs: mean monthly relative humidity, maximum relative humidity value allowed in month, minimum relative humidity value allowed in month, and a random number between 0.0 and 1.0. The maximum relative humidity value, or upper limit of the triangular distribution, is calculated from the mean monthly relative humidity with the equation:

$$R_{hUmon} = R_{hmon} + (1 - R_{hmon}) \cdot exp(R_{hmon} - 1)$$

Where, $R_{hUmon}$ is the largest relative humidity value that can be generated on a

given day in the month, and

$R_{hmon}$ is the average relative humidity for the month.

### 2.1.1.8 Snow melt generation

SWAT classifies precipitation as rain or freezing rain/snow using the average daily temperature. The snow cover component of the SWAT has been updated from a simple, uniform snow cover model to a more complex model which allows non-uniform cover due to shading, drifting, topography and land cover. The user defines a threshold snow depth above which snow coverage will always extend over 100% of the area. As the snow depth in a subbasin decreases below this value, the snow coverage is allowed to decline non-linearly based on an area depletion curve.

Snow melt is controlled by the air and snow pack temperature, the melting rate, and the areal coverage of snow. If snow is present, it is melted on days when the maximum temperature exceeds 0°C using a linear function of the difference between the average snow pack maximum air temperature and the base or threshold temperature for snow melt. Melted snow is treated the same as rainfall for estimating runoff and percolation. For snow melt, rainfall energy is set to zero and the peak runoff rate is estimated assuming uniformly melted snow for 24 hour duration.

The snow melt in the SWAT is calculated as a linear function of the difference between the average snow pack-maximum air temperature and the base or threshold temperature for snow melt:

$$SNO_{mlt} = b_{mlt} \cdot sno_{cov} \cdot \left[ \frac{T_{snow} + T_{mx}}{2} - T_{mlt} \right]$$

where $SNO_{mlt}$ is the amount of snow melt on a given day (mm H 2 O),

$b_{mlt}$ is the melt factor for the day (mm $H_2O$/day- °C),

$sno_{cov}$ is the fraction of the HRU area covered by snow,

$T_{snow}$ is the snow pack temperature on a given day ( °C),

$T_{mx}$ is the maximum air temperature on a given day ( °C), and

$T_{mlt}$ is the base temperature above which snow melt is allowed ( °C).

## 2.1.1.9 Elevation bands

The model allows the subbasin to be split into a maximum of ten elevation bands. Snow cover and snow melt are simulated separately for each elevation band. By dividing the subbasin into elevation bands, the model is able to assess the differences in snow cover and snow melt caused by orographic variation in precipitation and temperature.

## 2.1.1.10 Soil temperature

Soil temperature impacts water movement and the decay rate of residue in the soil. Daily average soil temperature is calculated at the soil surface and the center of each soil layer. The temperature of the soil surface is a function of snow cover, plant cover and residue cover, the bare soil surface temperature, and the previous day's soil surface temperature. The temperature of a soil layer is a function of the surface temperature, mean annual air temperature and the depth in the soil at which variation

14

in temperature due to changes in climatic conditions no longer occurs. This depth, referred to as the damping depth, is dependent upon the bulk density and the soil water content.

## 2.1.2 Hydrology

As precipitation descends, it may be intercepted and held in the vegetation canopy or fall to the soil surface. Water on the soil surface will infiltrate into the soil profile or flow overland as runoff. Runoff moves relatively quickly toward a stream channel and contributes to short-term stream response. Infiltrated water may be held in the soil and later evapotranspired or it may slowly make its way to the surface-water system via underground paths. Fig. 2.3 illustrates the potential pathways of water movement simulated by the SWAT in the HRU.

### 2.1.2.1 Canopy storage

Canopy storage is the water intercepted by vegetative surfaces (the canopy) where it is held and made available for evaporation. When using the curve number (CN) method to compute surface runoff, canopy storage is taken into account in the surface runoff calculations. However, if methods such as Green &Ampt are used to model infiltration and runoff, canopy storage must be modeled separately. SWAT allows the user to input the maximum amount of water that can be stored in the canopy at the maximum leaf area index for the land cover. This value and the leaf area index are used by the model to compute the maximum storage at any time in the growth cycle of the land cover/crop. When evaporation is computed, water is first removed from canopy storage.

### 2.1.2.2 Infiltration

Infiltration refers to the entry of water into a soil profile from the soil surface. As infiltration continues, the soil becomes increasingly wet, causing the rate of infiltration to decrease with time until it reaches a steady value. The initial rate of infiltration depends on the moisture content of the soil prior to the introduction of water at the soil surface. The final rate of infiltration is equivalent to the saturated hydraulic conductivity of the soil. Because the CN method used to calculate surface runoff operates on a daily time-step, it is unable to directly model infiltration. The amount of water entering the soil profile is calculated as the difference between the amount of rainfall and the amount of surface runoff.

15
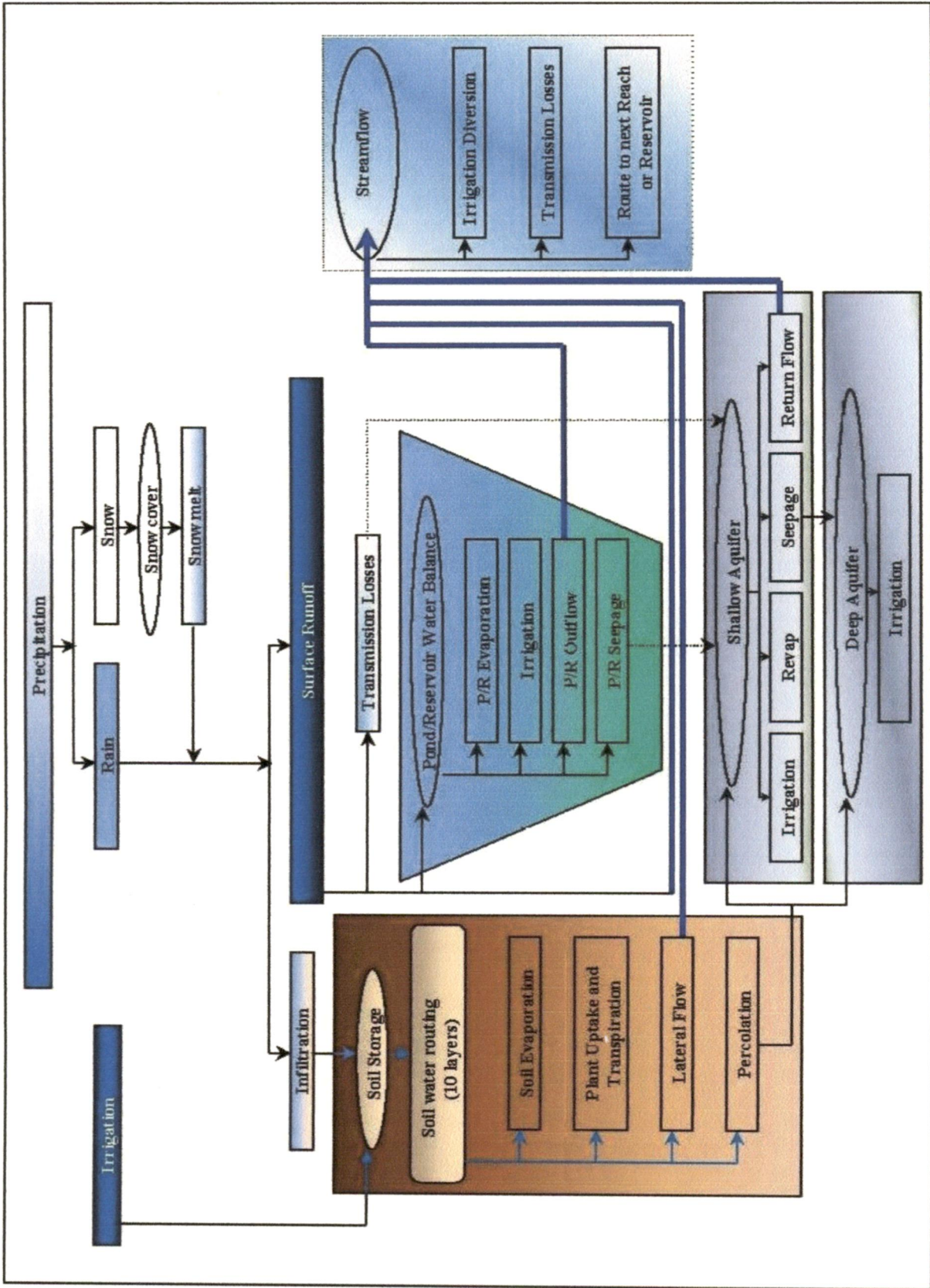
**Figure 2.3 Schematics of pathways available for water movement in SWAT**

16

The Green & Ampt infiltration method does directly model infiltration, but it requires precipitation data in smaller time increments.

## 2.1.2.3 Redistribution

Redistribution refers to the continued movement of water through a soil profile after input of water (via precipitation or irrigation) has ceased at the soil surface. Redistribution is caused by differences in water content in the profile. Once the water content throughout the entire profile is uniform, redistribution will cease. The redistribution component of the SWAT uses a storage routing technique to predict flow through each soil layer in the root zone. Downward flow, or percolation, occurs when field capacity of a soil layer is exceeded and the layer below is not saturated. The flow rate is governed by the saturated conductivity of the soil layer. Redistribution is affected by soil temperature. If the temperature in a particular layer is 0°C or below, no redistribution is allowed from that layer.

## 2.1.2.4 Evapotranspiration

Evapotranspiration is a collective term for all processes by which water in the liquid or solid phase at or near the earth's surface becomes atmospheric water vapor. Evapotranspiration includes evaporation from rivers and lakes, bare soil, and vegetative surfaces; evaporation from within the leaves of plants (transpiration); and sublimation from ice and snow surfaces. The model computes evaporation from soils and plants separately as described by Ritchie (1972). Potential soil water evaporation is estimated as a function of potential evapotranspiration and leaf area index (area of plant leaves relative to the area of the HRU). Actual soil water evaporation is estimated by using exponential functions of soil depth and water content. Plant transpiration is simulated as a linear function of potential evapotranspiration and leaf area index.

## 2.1.2.5 Potential evapotranspiration

Potential evapotranspiration is the rate at which evapotranspiration would occur from a large area completely and uniformly covered with growing vegetation that has access to an unlimited supply of soil water. This rate is assumed to be unaffected by microclimatic processes such as advection or heat-storage effects. The model offers three options for estimating potential evapotranspiration: Hargreaves (Hargreaves et

17

al., 1985), Priestley-Taylor (Priestley and Taylor, 1972), and Penman-Monteith (Monteith, 1965).

### 2.1.2.6 Lateral subsurface flow

Lateral subsurface flow, or interflow, is streamflow contribution that originates below the surface but above the zone where rocks are saturated with water. Lateral subsurface flow in the soil profile (0-2 m) is calculated simultaneously with redistribution. A kinematic storage model is used to predict lateral flow in each soil layer. The model accounts for variation in conductivity, slope and soil water content.

### 2.1.2.7 Surface runoff

Surface runoff, or overland flow, is the flow that occurs along a sloping surface. Using daily or subdaily rainfall amounts, SWAT simulates surface runoff volumes and peak runoff rates for each HRU.

Surface runoff volume is computed using a modification of the SCS curve number method (USDA Soil Conservation Service, 1972) or the Green & Ampt infiltration method (Green and Ampt, 1911). In the curve number method, the curve number varies non-linearly with the moisture content of the soil. The curve number drops as the soil approaches the wilting point and increases to near 100 as the soil approaches saturation. The Green & Ampt method requires subdaily precipitation data and calculates infiltration as a function of the wetting front matric potential and effective hydraulic conductivity. The SCS curve number equation is ( SCS, 1972):

$$Q_{surf} = \frac{(R_{day} - I_a)^2}{(R_{day} - I_a + S)}$$

Where,

$Q_{surf}$ is the accumulated runoff or rainfall excess (mm).

$R_{day}$ is the rainfall depth for the day (mm),

$S$ is the Retention Parameter (mm),

$I_a$ is the initial abstractions (mm) which includes surface storage, interception and Infiltration prior to runoff.

## 2.1.2.8 Peak runoff rate

Predictions are made with a modification of the rational method. In brief, the rational method is based on the idea that if a rainfall of intensity $i$ begins instantaneously and continues indefinitely, the rate of runoff will increase until the time of concentration, $tc$, when all of the subbasin is contributing to flow at the outlet. In the modified Rational Formula, the peak runoff rate is a function of the proportion of daily precipitation that falls during the subbasin $tc$, the daily surface runoff volume, and the subbasin time of concentration. The proportion of rainfall occurring during the subbasin $tc$ is estimated as a function of total daily rainfall using a stochastic technique. The subbasin time of concentration is estimated using Manning's Formula considering both overland and channel flow.

## 2.1.2.9 Ponds

Ponds are water storage structures located within a subbasin which intercept surface runoff. The catchment area of a pond is defined as a fraction of the total area of the subbasin. Ponds are assumed to be located off the main channel in a subbasin and will never receive water from upstream subbasins. Pond water storage is a function of pond capacity, daily inflows and outflows, seepage and evaporation. Required inputs are the storage capacity and surface area of the pond when filled to capacity. Surface area below capacity is estimated as a non-linear function of storage.

## 2.1.2.10 Tributary channels

Two types of channels are defined within a subbasin: the main channel and tributary channels. Tributary channels are minor or lower order channels branching off the main channel within the subbasin. Each tributary channel within a subbasin drains only a portion of the subbasin and does not receive groundwater contribution to its flow. All flow in the tributary channels is released and routed through the main channel of the subbasin. SWAT uses the attributes of tributary channels to determine the time of concentration for the subbasin.

## 2.1.2.11 Transmission losses

Transmission losses are losses of surface flow via leaching through the streambed. This type of loss occurs in ephemeral or intermittent streams where groundwater contribution occurs only at certain times of the year, or not at all. SWAT uses Lane's method described in Chapter 19 of the SCS Hydrology Handbook (USDA Soil

Conservation Service, 1983) to estimate transmission losses. Water losses from the channel are a function of channel width and length and flow duration. Both runoff volume and peak rate are adjusted when transmission losses occur in tributary channels.

### 2.1.2.12 Return flow

Return flow, or base flow, is the volume of stream flow originating from groundwater. SWAT partitions groundwater into two aquifer systems: a shallow, unconfined aquifer that contributes return flow to streams within the watershed and a deep, confined aquifer that contributes return flow to streams outside the watershed (Arnold et al., 1993). Water percolating past the bottom of the root zone is partitioned into two fractions - each fraction becomes recharge for one of the aquifers. In addition to return flow, water stored in the shallow aquifer may replenish moisture in the soil profile in very dry conditions or be directly removed by plant. Water in the shallow or deep aquifer may be removed by pumping.

### 2.1.3   Land cover/plant growth

SWAT utilizes a single plant growth model to simulate all types of land covers. The model is able to differentiate between annual and perennial plants. Annual plants grow from the planting date to the harvest date or until the accumulated heat units equal the potential heat units for the plant. Perennial plants maintain their root systems throughout the year, becoming dormant in the winter months. They resume growth when the average daily air temperature exceeds the minimum, or base, temperature required. The plant growth model is used to assess removal of water and nutrients from the root zone, transpiration, and biomass/yield production.

### 2.1.3.1 Potential growth

The potential increase in plant biomass on a given day is defined as the increase in biomass under ideal growing conditions. The potential increase in biomass for a day is a function of intercepted energy and the plant's efficiency in converting energy to biomass. Energy interception is estimated as a function of solar radiation and the plant's leaf area index.

### 2.1.3.2 Nutrient uptake

Plant use of nitrogen and phosphorus are estimated with a supply and demand approach where the daily plant nitrogen and phosphorus demands are calculated as the difference between the actual concentration of the element in the plant and the optimal concentration. The optimal concentration of the elements varies with growth stage as described by Jones (1983).
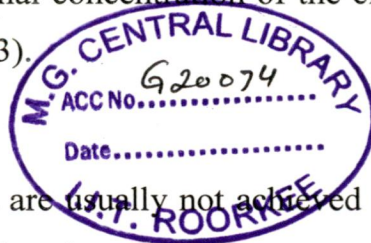
### 2.1.3.3 Growth constraints

Potential plant growth and yield are usually not achieved due to constraints imposed by the environment. The model estimates stresses caused by water, nutrients and temperature.

### 2.1.3.4 Erosion

Erosion and sediment yield are estimated for each HRU with the Modified Universal Soil Loss Equation (MUSLE) (Williams, 1975). While the USLE uses rainfall as an indicator of erosive energy, MUSLE uses the amount of runoff to simulate erosion and sediment yield. The substitution results in a number of benefits: the prediction accuracy of the model is increased, the need for a delivery ratio is eliminated, and single storm estimates of sediment yields can be calculated. The hydrology model supplies estimates of runoff volume and peak runoff rate which, with the subbasin area, are used to calculate the runoff erosive energy variable. The crop management factor is recalculated every day that runoff occurs. It is a function of aboveground biomass, residue on the soil surface, and the minimum C factor for the plant. Other factors of the erosion equation are evaluated as described by Wischmeier and Smith (1978).

### 2.1.4   Nutrients

SWAT tracks the movement and transformation of several forms of nitrogen and phosphorus in the watershed. In the soil, transformation of nitrogen from one form to another is governed by the nitrogen cycle. The transformation of phosphorus in the soil is controlled by the phosphorus cycle. Nutrients may be introduced to the main channel and transported downstream through surface runoff and lateral subsurface flow.

## 2.1.4.1 Nitrogen

The different processes modeled by SWAT in the HRUs and the various pools of nitrogen in the soil are depicted in Fig. 2.4. Plant use of nitrogen is estimated using the supply and demand approach described in the section on plant growth. In addition to plant use, nitrate and organic N may be removed from the soil via mass flow of water. Amounts of NO3-N contained in runoff, lateral flow and percolation are estimated as products of the volume of water and the average concentration of nitrate in the layer. Organic N transport with sediment is calculated with a loading function developed by McElroy et al. (1976) and modified by Williams and Hann (1978) for application to individual runoff events. The loading function estimates the daily organic N runoff loss based on the concentration of organic N in the top soil layer, the sediment yield, and the enrichment ratio. The enrichment ratio is the concentration of organic N in the sediment divided by that in the soil.

## 2.1.4.2 Phosphorus

Plant use of phosphorus is estimated using the supply and demand approach described in the section on plant growth. In addition to plant use, soluble phosphorus and organic P may be removed from the soil via mass flow of water (Fig. 2.5). Phosphorus is not a mobile nutrient and interaction between surface runoff with solution P in the top mm of soil will not be complete. The amount of soluble P removed in runoff is predicted using solution P concentration in the top 10 mm of soil, the runoff volume and a partitioning factor. Sediment transport of P is simulated with a loading function as described in organic N transport.

## 2.1.4.3 Pesticides

Although SWAT does not simulate stress on the growth of a plant due to the presence of weeds, damaging insects, and other pests, pesticides may be applied to an HRU to study the movement of the chemical in the watershed (Fig. 2.6). SWAT simulates pesticide movement into the stream network via surface runoff (in solution and sorbed to sediment transported by the runoff), and into the soil profile and aquifer by percolation (in solution). The equations used to model the movement of pesticide in the land phase of the hydrologic cycle were adopted from GLEAMS (Leonard et al., 1987). The movement of the pesticide is controlled by its solubility, degradation half-life, and soil organic carbon adsorption coefficient.
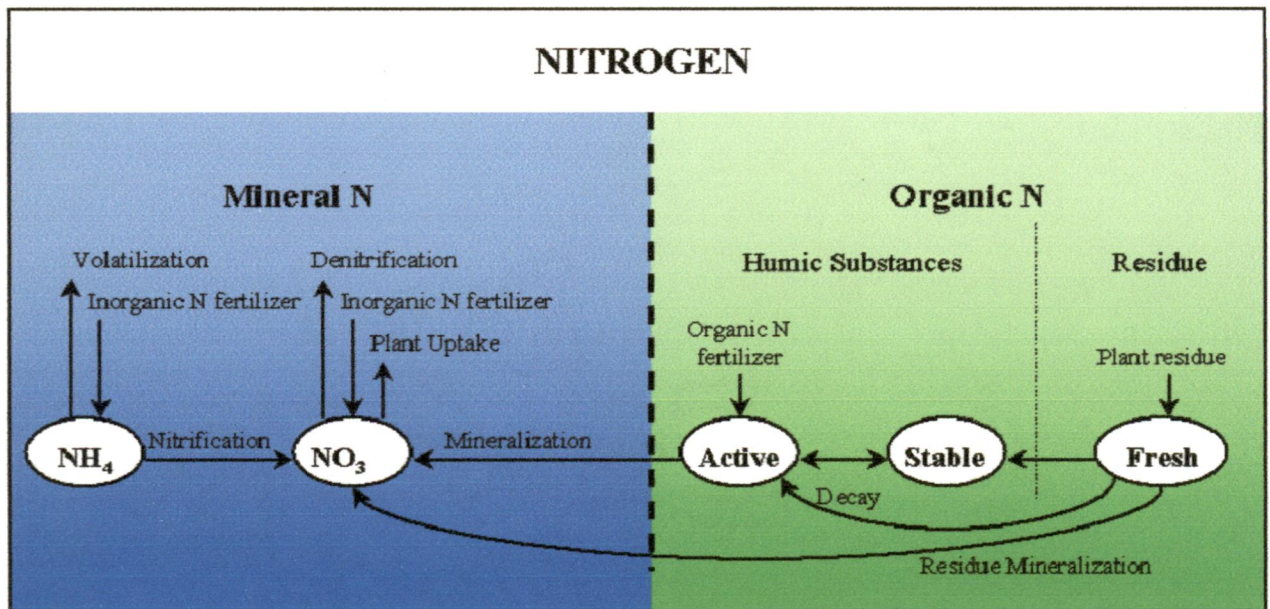
**Figure 2.4  Partitioning of ntrogen in SWAT.**
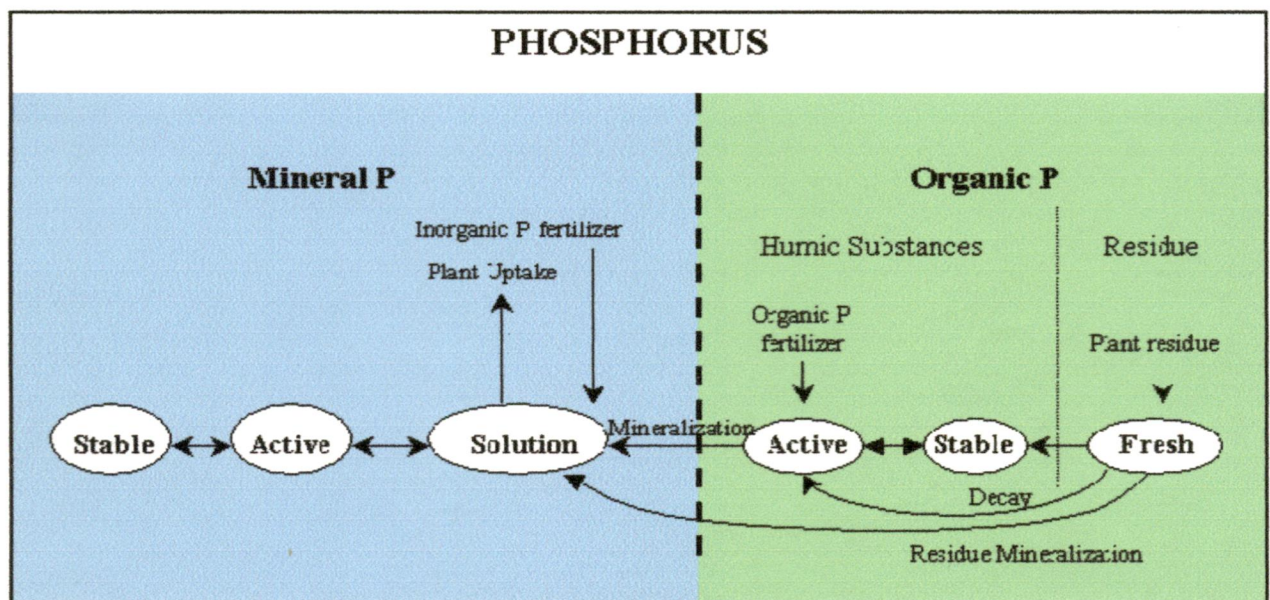


**Figure 2.5  Partitioning of phosphorus in SWAT.**
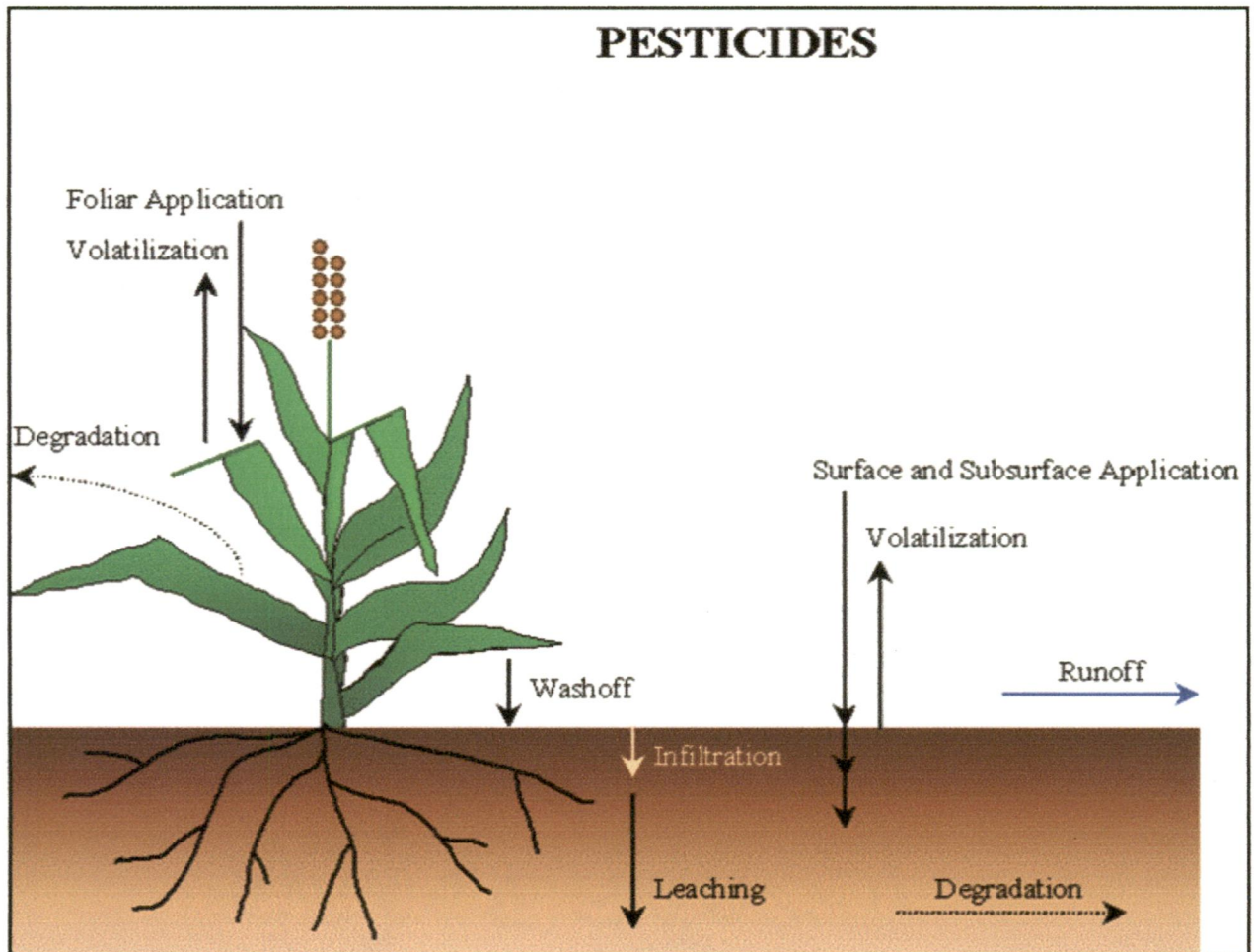
**Figure 2.6  Pesticide fate and transport in SWAT.**

Pesticide on plant foliage and the soil degrades exponentially according to the appropriate half-life. Pesticide transport by water and sediment is calculated for each runoff event and pesticide leaching is estimated for each soil layer when percolation occurs.

## 2.1.5.0 Management

SWAT allows the user to define management practices taking place in every HRU. The user may define the beginning and the ending of the growing season, specify timing and amounts of fertilizer, pesticide and irrigation applications as well as timing of tillage operations. At the end of the growing season, the biomass may be removed from the HRU as yield or placed on the surface as residue. In addition to these basic management practices, operations such as grazing, automated fertilizer and water applications, and incorporation of every conceivable management option for water use are available. The latest improvement to land management is the incorporation of routines to calculate sediment and nutrient loadings from urban areas.

## 2.1.5.1 Rotations

The dictionary defines a rotation as the growing of different crops in succession in one field, usually in a regular sequence. A rotation in SWAT refers to a change in management practices from one year to the next. There is no limit to the number of years of different management operations specified in a rotation. SWAT also does not limit the number of land cover/crops grown within one year in the HRU. However, only one land cover can be growing at any one time.

## 2.1.5.2 Water use

The two most typical uses of water are for application to agricultural lands or use as a town's water supply. SWAT allows water to be applied on an HRU from any water source within or outside the watershed. Water may also be transferred between reservoirs, reaches and subbasins as well as exported from the watershed.

## 2.2    Routing phase of the hydrologic cycle

Once SWAT determines the loadings of water, sediment, nutrients and pesticides to the main channel, the loadings are routed through the stream network of the watershed using a command structure similar to that of HYMO (Williams and Hann, 1972). In addition to keeping track of mass flow in the channel, SWAT models the

transformation of chemicals in the stream and streambed. Fig. 2.7 illustrates the different in-stream processes modeled by SWAT.

### 2.2.1 Routing in the main channel or reach

Routing in the main channel can be divided into four components: water, sediment, nutrients and organic chemicals.

### 2.2.1.1 Flood routing

As water flows downstream, a portion may be lost due to evaporation and transmission through the bed of the channel. Another potential loss is removal of water from the channel for agricultural or human use. Flow may be supplemented by the fall of rain directly on the channel and/or addition of water from point source discharges. Flow is routed through the channel using a variable storage coefficient method developed by Williams (1969) or the Muskingum routing method.

### 2.2.1.2 Sediment routing

The transport of sediment in the channel is controlled by the simultaneous operation of two processes, deposition and degradation. Previous versions of SWAT used stream power to estimate deposition/degradation in the channels (Arnold et al., 1995). Bagnold (1977) defined stream power as the product of water density, flow rate and water surface slope. Williams (1980) used Bagnold's definition of stream power to develop a method for determining degradation as a function of channel slope and velocity. In this version of SWAT, the equations have been simplified and the maximum amount of sediment that can be transported from a reach segment is a function of the peak channel velocity. Available stream power is used to re-entrain loose and deposited material until all of the material is removed. Excess stream power causes bed degradation. Bed degradation is adjusted for stream bed erodibility and cover.

### 2.2.1.3 Nutrient routing

Nutrient transformations in the stream are controlled by the instream water quality component of the model. The in-stream kinetics used in SWAT for nutrient routing are adapted from QUAL2E (Brown and Barnwell, 1987). The model tracks nutrients dissolved in the stream and nutrients adsorbed to the sediment. Dissolved nutrients are

transported with the water while those sorbed to sediments are allowed to be deposited with the sediment on the bed of the channel.

### 2.2.1.4 Channel pesticide routing

While an unlimited number of pesticides may be applied to the HRUs, only one pesticide may be routed through the channel network of the watershed due to the complexity of the processes simulated. As with the nutrients, the total pesticide load in the channel is partitioned into dissolved and sediment-attached components. While the dissolved pesticide is transported with water, the pesticide attached to sediment is affected by sediment transport and deposition processes. Pesticide transformations in the dissolved and sorbed phases are governed by first-order decay relationships. The major in-stream processes simulated by the model are settling, burial, re-suspension, volatilization, diffusion and transformation.

### 2.2.2    Routing in the reservoir

The water balance for reservoirs includes inflow, outflow, rainfall on the surface, evaporation, seepage from the reservoir bottom and diversions.

### 2.2.2.1 Reservoir outflow

The model offers three alternatives for estimating outflow from the reservoir. The first option allows the user to input measured outflow. The second option, designed for small, uncontrolled reservoirs, requires the users to specify a water release rate. When the reservoir volume exceeds the principal storage, the extra water is released at the specified rate. Volume exceeding the emergency spillway is released within one day. The third option, designed for larger, managed reservoirs, has the user specify monthly target volumes for the reservoir.

### 2.2.2.2 Sediment routing

Sediment inflow may originate from transport through the upstream reaches or from surface runoff within the subbasin. The concentration of sediment in the reservoir is estimated using a simple continuity equation based on volume and concentration of inflow, outflow, and water retained in the reservoir. Settling of sediment in the reservoir is governed by an equilibrium sediment concentration and the median sediment particle size. The amount of sediment in the reservoir outflow is the product

of the volume of water flowing out of the reservoir and the suspended sediment concentration in the reservoir at the time of release.

## 2.2.2.3 Reservoir nutrients

A simple model for nitrogen and phosphorus mass balance was taken from Chapra (1997). The model assumes: 1) the lake is completely mixed; 2) phosphorus is the limiting nutrient; and, 3) total phosphorus is a measure of the lake trophic status. The first assumption ignores lake stratification and intensification of phytoplankton in the epilimnon. The second assumption is generally valid when non-point sources dominate and the third assumption implies that a relationship exists between total phosphorus and biomass. The phosphorus mass balance equation includes the concentration in the lake, inflow, outflow and overall loss rate.

## 2.2.2.4 Reservoir pesticides

The lake pesticide balance model is taken from Chapra (1997) and assumes well mixed conditions. The system is partitioned into a well mixed surface water layer underlain by a well mixed sediment layer. The pesticide is partitioned into dissolved and particulate phases in both the water and sediment layers. The major processes simulated by the model are loading, outflow, transformation, volatilization, settling, diffusion, re-suspension and burial.
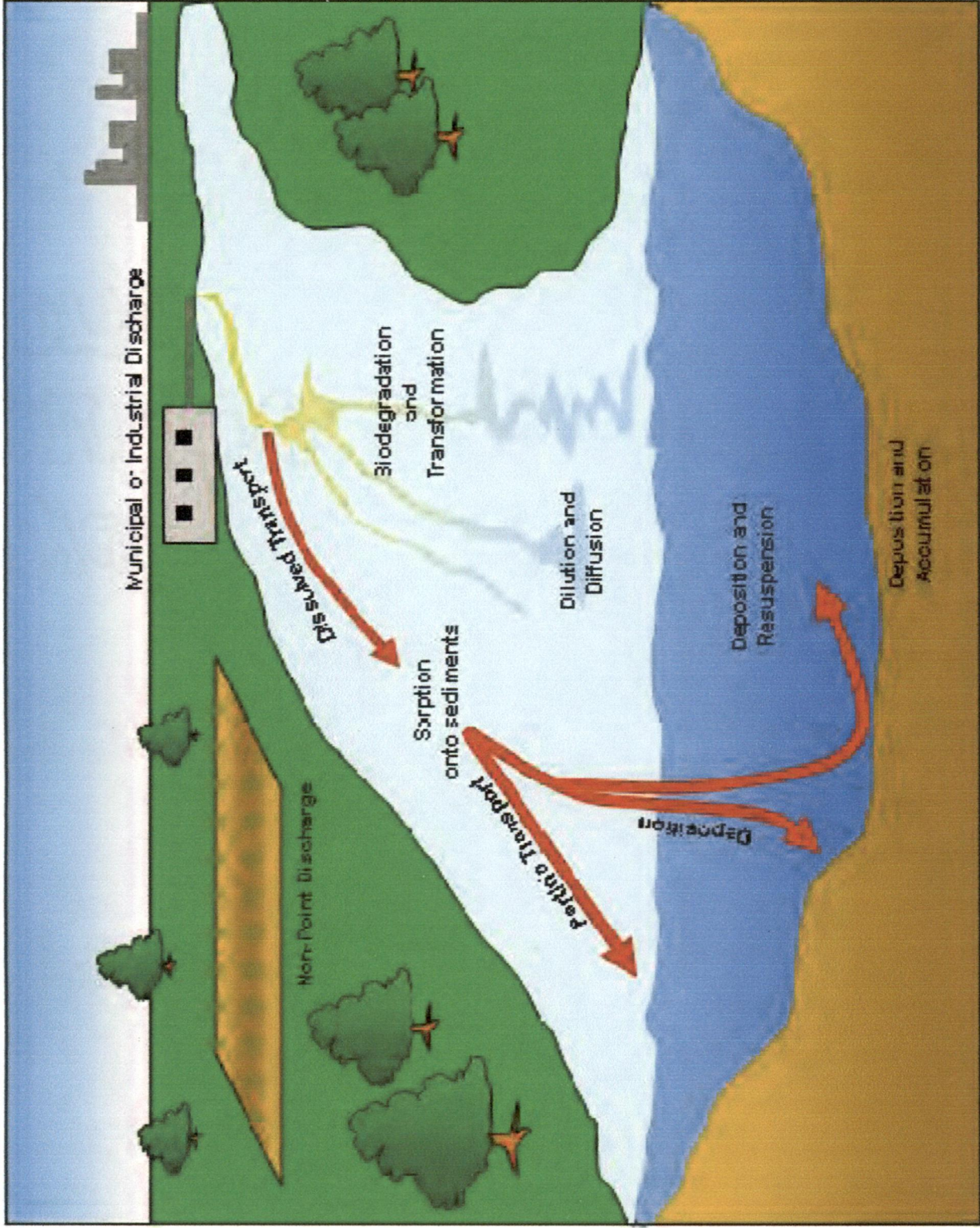
**Figure 2.7 Instream processes modeled by SWAT**

29

This chapter presents a brief review of the available literature on calibration, validation and sensitivity analysis for hydrological model (SWAT) and assessment of hydropower potential using Remote Sensing (RS) and Geographical Information System (GIS).

## 3.1    Catchment modeling using SWAT

*Pisinaras et al. (2010)* applied SWAT to Kosynthos River watershed located in Northeastern Greece. The 440 km$^2$ drainage basin was discretized into 32 sub-basins using an automated delineation routine. The multiple hydrologic response unit (HRU) approach was used and the basin was discretized into 135 HRUs. The model was calibrated and verified using continuous meteorological data from three stations, and runoff and nutrient concentrations measured at four monitoring sites located within the main tributaries of the watershed, for the time period from November 2003 to November 2006. Calibration and verification results showed good agreement between simulated and measured data. Model performance was evaluated using several statistical parameters, such as the Nash–Sutcliffe coefficient and the normalized objective function. The study showed that SWAT model, if properly validated, can be used effectively in testing management scenarios in Mediterranean watersheds. The SWAT model application, supported by GIS technology, proved to be a very flexible and reliable tool for water decision making.

*Jie et al. (2010)* applied the SWAT model in the Fenhe irrigation district. The information on hydrology, weather and water use from 1996 to 2001 in the Fenhe irrigation district was used to simulate and analyze the water balance. The sensitive parameters were estimated by Nash-Sutcliffe efficiency (NSE), relative error (RE) and coefficient of correlation (R$^2$). The model was further validated with the monthly flow data from 2002 to 2006. The results showed that the simulated results of two monitoring points meet the estimated requirements. The RE value of the average annual runoff at the Erba Station varied from -7.34% to 19.13% except a low RE value (-30.70%) in 2006. The RE of the average annual runoff at the Yitang station was from-17.21% to 9.86% with an exceptional RE value (-21.13%) in 2003. From

the monthly simulated results, the $R^2$ of the monthly runoff at the Erba and Yitang stations was 0.81 and 0.77, respectively. The NSE of the monthly runoff was 0.72 and 0.65, respectively. A modified SWAT model was applicable for water balance simulation at the Fenhe irrigation district.

*Vale et al. (2009)* applied SWAT to improve the understanding of the hydrological functioning of the Bosherston Lakes in west Wales which are an internationally important set of linked freshwater lowland lakes. It was created by damming tidal creeks in the 18th and 19th centuries. The lakes have an average water depth of 1–3 m, and receive surface water inflows but have an uncertain interaction with the underlying karstic Carboniferous Limestone. The temporally variable and limited observational data were used within a two-step calibration process. The simulated surface water inflows and groundwater levels were calibrated, followed by the lake volumes (Nash–Sutcliffe (NSE) coefficient ranging from 0.67 to 0.74). Finally the simulated lake volumes were validated (NSE ranging from 0.56 to 0.74) and the simulated lake outflows demonstrated to be plausible. Simulations reveal that three of the four linked water bodies lose significant water to the underlying aquifer. The simulated water balance demonstrates that the catchment outputs are dominated by evapotranspiration, surface outflow from the lake system to the sea and coastal groundwater discharge, with abstraction and lake evaporation being of lesser importance. The coastal groundwater discharge originates from both leakage from the lakes and previously unrecognised larger scale groundwater flow paths in the limestone aquifer. The study has provided an improved basis for the future hydrological management of the catchment and lakes and has demonstrated the wider utility of SWAT in simulating karstic systems.

*Kannan et al. (2006)* evaluated the performance of the SWAT-2000 model using stream flow at the outlet of the 142 ha Colworth catchment (Bedfordshire, UK). This catchment has been monitored since October 1999. The soil type consists of clay loam soil over stony calcareous clay and a rotation of wheat, oil seed rape, grass, beans and peas is grown. Much of the catchment is tile drained. Acceptable performance in hydrological modeling, along with correct simulation of the processes driving the water balance was essential first requirements for predicting contaminant transport. The results shows that hydrological simulation, crop growth and evapotranspiration

31

(ET) patterns were realistic when compared with empirical data. Acceptable model performance (based on a number of error measures) was obtained in final model runs, with reasonable runoff partitioning into overland flow, tile drainage and base flow.

*Wu et al. (2007)* conducted a case study for a 901 km$^2$ watershed of northern Michigan to compare the effects of calibrating SWAT watershed model with different climatic datasets representing drought (1948–1949) versus average (1969–1970) conditions. The effects of the different climatic conditions on parameter response and sensitivity were evaluated, and performance of the two calibration versions was compared using a common validation period, 1950–1965. For the drought and average calibration periods, models were well calibrated, as indicated by high Nash-Sutcliffe efficiency coefficients (NSE = 0.8 and 0.9), and low deviation of discharge values (D = 2.9% and 3.4%). Evapotranspiration parameters differed under the two sets of climatic conditions. The plant water uptake compensation factor (EPCO), appropriately reflected plant water uptake patterns in varied climatic conditions. Snow melting parameters differed between the two scenarios. A comparison of baseflow values simulated by SWAT versus those computed by a hydrograph separation method showed that the SWAT method treated most snowmelt as surface runoff, whereas the latter method treated much of it as baseflow. The drought-calibrated version of the model performed much better during the validation period (1950–1965) (NSE = 0.8, D = 2.6%) than did the average-calibrated version (E = 0.4, D = 41.4%).

*Ficklin et al. (2009)* modeled the hydrological responses to variations of atmospheric $CO_2$ (550 and 970 ppm), temperature (+1.1 and +6.4 °C), and precipitation (0%, ±10%, and ±20%) based on Intergovernmental Panel on Climate Change projections. The SWAT was used to model the hydrology and impact of climate change in the highly agricultural San Joaquin watershed in California. This watershed has an area of 14,983 km$^2$ with a Mediterranean climate, resulting in a strong dependence on irrigation. Model calibration (1992–1997) and validation (1998–2005) resulted in Nash–Sutcliffe coefficients of 0.95 and 0.94, respectively, for monthly stream flow. The results of this study suggest that atmospheric $CO_2$, temperature and precipitation change have significant effects on water yield, evapotranspiration, irrigation water use, and stream flow. Increasing $CO_2$ concentration to 970 ppm and temperature by 6.4 °C caused watershed-wide average evapotranspiration, averaged over 50

simulated years, to decrease by 37.5%, resulting in increases of water yield by 36.5%, and stream flow by 23.5% compared to the present-day climate.

Increasing temperature caused a temporal shift in plant growth patterns and redistributed evapotranspiration and irrigation water demand earlier in the year. This caused an increase in stream flow during the summer months due to decreased irrigation demand. Water yield, however, decreased with an increase in temperature. Increase of precipitation by ±10% and ±20% generally changed water yield and stream flow proportionally, and had negligible effects on predicted evapotranspiration and irrigation water use. Overall, the results indicate that the San Joaquin watershed hydrology is very sensitive to potential future climate changes. Agricultural implications include changes to plant growth rates, irrigation timing and runoff, all of which may affect future water resources and water quality.

*Green et al. (2007)* evaluate the effectiveness of the autocalibration-sensitivity analysis procedures at small-scale watersheds to six small-scale watersheds (subwatersheds) in the central Texas Blackland Prairie. Model simulations are completed using two data scenarios: (1) 1 year used for parameter calibration; (2) 5 years used for parameter calibration. The impact of manual parameter calibration versus auto calibration with manual adjustment on model simulation results is tested. The combination of auto calibration tool parameter values and manually adjusted parameters for the 2000-2004 simulation period resulted in the highest NSE and $R^2$ values for discharge; however, the same 5-year period yielded better overall NSE, $R^2$ and P-values for the simulation values that were manually adjusted. The disparity is most likely due to the limited number of parameters that are included in this version of the autocalibration tool (i.e. Nperco, Pperco, and nitrate). It was found out that autocallibration gives a better results as compared with the manual calibration.

*Kang et al. (2005)* applied SWAT to develop total maximum daily load (TMDL) programs for a small watershed containing rice paddy fields in the Republic of Korea. The total maximum daily load system (TOLOS) was incorporated with the SWAT model to simulate water balance and water quality from irrigated paddy fields. Model parameters related to hydrology and water quality were calibrated and validated by comparing model predictions with the field data collected for 4 years. The results indicated that the simulated runoff and water quality values were acceptably close to

the observed data. Water quality parameters also appeared to be reasonably comparable to the field data.

*Xu et al. (2010)* compare the impact of different climate datasets (station vs. gridded) on the parameterization of a hydrological model (developed using SWAT2005) of the River Xiangxi. Climate data used in this study derive from two sources: point daily observations from the Xingshan meteorological station (STN) and gridded ($0.5° \times 0.5°$) monthly observations of the CRU TS3.0 global dataset (CRU) downscaled to daily data using a weather generator. Data from 1970 to 1974 were applied for sensitivity analyses and autocalibration and subsequently validate hindcasts over the period 1976–1986. Despite there being only slight differences in mean annual precipitation (1003 mm vs. 1052 mm) between STN and CRU, the data differ more in their estimates of the number of rain days (136 vs. 112) and wet days standard deviation (11.75 mm vs. 18.49 mm).

The mean, maximum and minimum temperatures from CRU are all lower than those from STN. SWAT parameter sensitivity analysis results show slight differences in the relative rank of the most sensitive parameters, with the differences mainly caused by the lower temperature and more intensive rainfall in CRU relative to STN. Auto calibrated parameters showed very similar values, except for the surface runoff lag coefficient which is higher for the CRU dataset compared to that derived from the STN dataset. Statistic results for discharge simulated based on CRU compared rather well with that based on STN CRU as evaluated using the standard statistics of the Nash–Sutcliffe efficiency, coefficient of determination, and percent error. The sensitivity analysis and auto calibration tool embedded in SWAT2005 is a powerful utility in hydrological modeling of the River Xiangxi.

*Mulungu et al. (2007)* have done the hydrologic modeling of the Simiyu River catchment using SWAT. In this study, the SWAT model set-up and subsequent application to the catchment was based on high-resolution data such as land use from 30 m LandSat TM Satellite, 90 m DEM and soil data from Soil and Terrain Database for Southern Africa (SOTERSAF). The land use data were reclassified based on some ground truth maps using IDRISI Kilimanjaro software. The soil data were also reclassified manually to represent different soil hydrologic groups, which are important for the SWAT model set-up and simulations.

The SWAT application first involved analysis of parameter sensitivity, which was then used for model auto-calibration that followed hierarchy of sensitive model parameters. The analysis of sensitive parameters and auto-calibration was achieved by sensitivity analysis and auto-calibration options. The river discharge estimates from this and a previous study were compared so as to evaluate performances of the recent hydrologic simulations in the catchment. Results showed that surface water model parameters are the most sensitive and have more physical meaning especially CN2 (the most sensitive) and SOL_K. Simulation results showed more or less same estimate of river flow at Ndagalu gauging station. The model efficiencies (coefficient of correlation $R^2$ %) during calibration and validation periods were, respectively, 13.73, 14.22 and 40.54, 36.17. The lower value of model performance achieved in these studies showed that other factors than the spatial land data are greatly important for improvement of flow estimation by SWAT in Simiyu.

***Tolson and Shoemaker (1994)*** applied SWAT model to Canonsville watershed in USA for prediction of flow, sediment and phosphorus on spatial and temporal basis. The Nash–Suttcliffe coefficient of efficiency (NSE) for daily flows at the main flow station in the watershed was at least 0.80 in both the seven-year calibration period and the one year and four year validation periods.

***Abbaspour et al. (2007)*** applied SWAT model to the Thur catchment in Switzerland. In a national effort, since 1972, the Swiss Government started the "National Long-term Monitoring of Swiss Rivers" (NADUF) program aimed at evaluating the chemical and physical states of major rivers leaving Swiss political boundaries. The established monitoring network of 19 sampling stations included locations on all major rivers of Switzerland. This study complements the monitoring program and aims to model one of the program's catchments – Thur River basin (area 1700 km$^2$), which is located in the north-east of Switzerland and is a direct tributary to the Rhine. The program SWAT was used to simulate all related processes affecting water quantity, sediment, and nutrient loads in the catchment. The main objectives were to test the performance of SWAT and the feasibility of using this model as a simulator of flow and transport processes at a watershed scale. They concluded that simulation of hydrology, sediment and nutrient loads were of reasonable accuracy and such integrated models can be used for scenario analysis.

Kannan *et al.* (2007) applied the SWAT model in Colworth watershed (UK) and stated that SWAT model can be reliably used to simulate stream flow. Model performance was evaluated using a range of different error measures: Percent BIAS (PBIAS), Persistence Model Efficiency (PME), Nash and Sutcliffe Efficiency (NSE), and Daily Root Mean Square (DRMS) error criteria. Data from the period September 1, 1999 to June 29, 2001 were used as the simulation period for calibration and validation. Because of their simplicity and limited data requirements, the NRCS-curve number method for rainfall-runoff modeling and the Hargreaves method for estimation of evapotranspiration were used for initial model runs. In accordance with the hydrological behaviour of the study area, surface runoff is considered as the quick response component and base flow as the slow response component of runoff. Base flow is separated from the observed flow using an automated digital filter technique (Nathan and McMahon, 1990) proposed by Arnold et al. (1995). The filter has three passes and pass 3 gave acceptable base flow values for the hydrograph (Kannan, 2003). Calibration of stream flow was carried out in accordance with SWAT user manual and other published literature from SWAT users (e.g. Santhi et al., 2001; Lenhart et al., 2002; Moriasi et al., in press). From the perspective of PME (65.85%) and NSE (67.87%), the model performance is acceptable with regard to the target values of the model performance evaluation criteria considered. In addition, the DRMS estimation criterion (0.78 mm) is low which also indicates good model performance. In the case of PBIAS, the value obtained (11.95) is above the optimum value of zero indicating under estimation of stream flow in general. In summary, according to the performance evaluation criteria, the overall model performance is good, indicating the suitability of SWAT for hydrological modeling of this catchment.

*Ndomba et al. (2008)* demonstrated the validation SWAT model in data scarce environment in a complex tropical catchment in the Pangani River Basin located in northeast Tanzania. The validation process involved the model initialization, calibration, verification and sensitivity analysis. Both manual and auto-calibration procedures were used to facilitate the comparison of the results with past studies in the same catchment. For this study, some model parameters including soil depth and saturated hydraulic conductivity were assumed uniform within the study catchment and were therefore lumped comprising the huge computation resource requirement of the SWAT model. Results indicated that the same set of important parameters was

identified with or without the use of observed flows data. Some of the parameters had physical interpretation and could therefore relate directly to hydrological controlling factors within the catchment. Despite swapping ranking importance of parameters, these results suggest the suitability of the SWAT model for identifying hydrological controlling factors/parameters in ungauged catchments. Results of calibration and validation at the daily timescale gave moderately satisfactory Nash–Sutcliffe Coef-fi-cient of Efficiency (NSE) of 54.6% for calibration and 68% for validation while simulated and observed mean annual flow discharges gave an Index of Volumetric Fit (IVF) of 100%. The study further indicated the improvement of model estimation when more reliable spatial representation of rainfall was used.

*Taddese et al. (2005)* used the SWAT model to delineate the Tana sub basin in Blue Nile River Basin. The tool has demonstrated that it is robust to delineate sub-basins, watersheds, stream networks, outlet and inlet of the streams. The land use and soil options in AVSWATX define the land use and soil properly, which then are used to define the hydrological response units (HRU) distribution in each sub watershed. The HRU are the basic unit for environmental, crop/livestock production, water resources studies and their impact on the main water resources systems. In addition to it is important to develop user table for non-US users as DBF from Excel spread sheet. Finally the first part of this study showed that the SWAT can be used at Watershed scale level.

*Ullrich et al. (2009)* run the sensitivity analysis for conservation management parameters (specifically tillage depth, mechanical soil mixing efficiency, biological soil mixing efficiency, curve number, Manning's roughness coefficient for overland flow, USLE support practice factor, and filter strip width) in SWAT. This analysis was aimed to improve model parameterization and calibration efficiency. In contrast to less sensitive parameters such as tillage depth and mixing efficiency we parameterized sensitive parameters such as curve number values in detail. In the second step the analysis consisted of varying management practices (conventional tillage, conservation tillage, and no-tillage) for different crops (spring barley, winter barley, and sugar beet) and varying operation dates. Results showed that the model is very sensitive to applied crop rotations and in some cases even to small variations of management practices. But the different settings do not have the same sensitivity.

Duration of vegetation period and soil cover over time was most sensitive followed by soil cover characteristics of applied crops.

**Schmalz and Fohrer (2009)** investigated mesoscale catchments located in Northern Germany within lowland areas using the SWAT model. The basin covers areas from 50 to 517 km². These rural catchments have sandy, loamy and peaty soils and are drained in high fraction by open ditches and tile drainage. Using the river basin model SWAT, sensitivity analyses were carried out through an automatic routine that is based on the Latin-Hypercube (LH) and a One-factor-At-a-Time (OAT) sampling. The objective of this study is to investigate how specific landscape features influence the model behaviour. The results show that groundwater and soil parameters were found to be most sensitive in the studied lowland catchments and they turned out to be the most influential factors on simulated water discharge. The most sensitive parameter was the threshold water level in shallow aquifer for baseflow (GWQMN). In contrast, many studies of mountainous or low mountain range catchments show that the most sensitive parameters were the surface runoff parameters.

## 3.2 Application of GIS for assessment of water resources

**Kusre et al. (2010)** assessed the Kopili River basin in Assam (India) for hydropower potential using GIS and hydrological model (SWAT2000). The prediction accuracy of the model was confirmed through three well known efficiency criteria viz., coefficient of determination ($R^2 = 0.70$), Nash–Sutcliffe efficiency (NSE = 0.64) and Index of agreement (d = 0.91). A total of 107 sites on 9 streams could be identified as potential location for hydropower generation in the study watershed using the model outputs. Distributed power availability through micro units (<0.5 MW) has been the characteristic feature of the watershed. Estimated potential carbon emission reduction (CER) within the watershed might be up to 125 thousand t $CO_2$, even 50% of the potential hydropower of the 1204 sq km watershed could be implemented.

**Belmonte et al. (2008)** applied GIS in the territorial planning of Lerma Valley (Salta, Argentina) for mapping of potential energy resources taking into account the environmental diversity and site conditions (topographic, natural resource, infrastructure and service availability, social and economical). Solar radiation is spatialized through the application of statistical regressions between altitude, latitude,

precise incident solar radiation records, and radiation data estimated with the Geosol V.2.0.TM software. The Argentina Map program was used for the wind potential resource modeling. Digital Elevation Model, a land use and cover map (to determine roughness), and measured and/or estimated wind speed and frequency data are the required inputs.

The hydroelectric potential for microturbine applications is calculated from the topographic drop and the annual mean flow in cumulative models, through the application of the Idrisi KilimanjaroTM's runoff tool; while the power densities are compared at the watershed. Biomass potential (at this exploratory stage), is interpreted from the available biomass type (land use and cover map), its energy application availability, and some quantitative indicators associated with the biomass types identified as priority. It was concluded that the renewable energy potential in Lerma Valley is very high and diverse, and its close connection with social-environmental conditions is basic for the creation of energy resource-related territorial plans. And that GIS tools can make a quick and efficient assessment of the natural resource potential.

*Jia et al. (2008)* developed A Web GIS-based system designed to predict rainfall-runoff and assess real-time water resources for Beijing to provide support for scientific decision making regarding solving water shortages while effectively reducing urban flood threats in the city. The system adopts Browse Server (B/S) structure and combines the distributed hydrologic modeling and Web GIS techniques. For this system, a distributed hydrologic model of Beijing that adopts a grid cell-size of 1km by 1km and covers the city's entire area of 16,400 $km^2$ was developed and validated. This model employs a simple, yet practical rainfall-runoff correlation curve method to predict runoff, as well as prediction approaches for rainfall, evaporation, sub-surface runoff and recharge to ground water. In addition, a framework for the assessment of real-time water resources assessment based on hydrologic monitoring stations and the distributed model was established. Finally, a Web GIS-based system for rainfall-runoff prediction and real-time water resources assessment for Beijing was developed by integrating a data platform, the professional models and the Web GIS techniques. This system was successfully integrated into the hydrologic prediction

practices of the General Station of Hydrology, Bureau of Beijing Water Affairs in 2005,

*Ramachandra et al. (2005)* applied GIS to map the renewable energy potential talukwise in Karnataka State, India. GIS also aids as a Decision Support System while implementing location-specific renewable energy technologies. Regions suitable for tapping solar energy are mapped based on global solar radiation data, which provides a picture of the potential. Coastal taluks in Uttara Kannada have higher global solar radiation during summer (6.31 kWh/m$^2$), monsoon (4.16 kWh/m$^2$) and winter (5.48 kWh/m$^2$). Mapping of regions suitable for tapping wind energy has been done based on wind velocity data, and it shows that Chikkodi taluk, Belgaum district, has higher potential during summer (6.06 m/s), monsoon (8.27 m/s) and winter (5.19 m/s). It was found that Mysore district has the maximum number of small hydropower plants with a capacity of 36 MW.

*Pokharel (2000)* performed spatial analysis using GIS to develop location specific energy resource and consumption profile in rural area of Nepal. The study employs three levels of spatial analysis. First at the watershed level forest areas were disaggregated from major landuse patterns. Second, the energy situation such as fuel wood supply demand in each VDC was studied. Third, at the local level, potential sites for biogas and solar PV installations were identified. Although the area considered here is very small, it is expected that the spatial analysis methodology can be seamlessly transferred to larger areas. This study shows that a spatial energy information system is one of the better ways to develop a location specific energy resource and consumption profile. A spatial analysis helps in locating potential sites for energy generation such as hydropower, biogas and solar.

*Ramchandra et al. (2004)* developed a spatial decision support system for assessing micro, mini and small hydro project. The decision support system integrates spatial information generated through GIS and water resources using through direct and indirect methods incorporated in the system. The study explores the possibility of harnessing hydro potential in an ecologically sound way (by having run-of-river plants with no storage options) to suit the requirements of the region. The Sirsi, Siddapur and Yellapur taluks in hilly terrain amidst evergreen forests with a large number of streams are ideally suitable for micro, mini or small hydro power plants.

The stream at Muregar is perennial, with a flow of about 0.26 m$^3$ during summer and power of the order of 10-20 kW could be generated, while during the monsoon power of 300-400 kW could be harnessed.

***Das and Paul (2006)*** used GIS tools for identifying suitable location and estimated discharge based on observed data of base flow at accessible point in Himalayan region of India. The GIS technology was used to identify sites, which suit the head requirement for setting small hydropower plant. GIS has also been used to arrive at the best location within the identified sites. SCS CN method has been used to calculate the average monthly runoff for the identified site. The distributed curve number technique has been used in calculating the runoff. The base flow has been measured at an accessible point in different watersheds/sub-watersheds having similar characteristics in the same area. The streams are all ungauged and so regression analysis has been done to arrive at an equation for calculation of the base flow on the basis of number of pixels draining at the point of measurement and the average slope of the watershed/sub watershed. The base flow at the site in the sub watershed has been ascertained on relational basis. Knowing the total flow and the head the power generating capacity at the site was ascertained.

***Dudhani et al. (2005)*** demonstrated a systematic and comprehensive computational approach to extract information for identification and assessment of water resources and its associates such as inhabitation and settlement pattern, forest and vegetation coverage, snow coverage and selection of probable sites for small hydropower projects, etc. from satellite image in a scientific manner for Ganga and Alakananda rivers in India. Although cost comparisons of the proposed methodology with conventional methods of surveying is not actually worked out, it is expected that saving of manpower and time required for surveying and updating the information of the potential sites will have significant impact on the cost. Manual surveys and site selection for pre-feasibility report are not only time consuming but also requires large man-power due to the undulating topography, dense forest cover and bad climatic conditions. Work can be further extended for development of regional flow duration model.

***Yi et al. (2009)*** demonstrated on establishing the criteria and methodology for searching for alternative locations rather than selecting the most suitable site among

41

the alternatives. By applying the newly developed methodology, a large area can be precisely surveyed within a short period of time and expect to be able to use the method in policy making for SHP development by improving the convenience for the user. The newly developed methodology was applied to the upper part of Geum River Basin, in Korea, and found six potential SHP sites.

*Rojanamon et al. (2009)* proposes a new method to select feasible sites of small run-of-river hydropower projects by using GIS technology. A combination of engineering, economic, and environmental criteria, as well as social impact is employed in this study. The selected study area is the upper Nan river basin situated in the north of Thailand. For the engineering criteria, the project locations are found by GIS in visual basic platform, and then economic evaluations of the selected projects are performed. The environmental parameters are used to rank the projects by total weighted scores. Finally, a social impact study at the potential sites is conducted based on the public participation process, i.e. questionnaire survey and focus group discussions. The applicability of the proposed method is verified by the results of site selection of the small hydropower projects located on the Nan river basin in Thailand.

*Winnaar et al. (2007)* utilized GIS to manage spatial information and linked to hydrological response models. The catchment level identification was provided as a rational means to facilitate decision making, planning and assessment of runoff harvesting sites and gives illustration at the Potshini catchment, a small sub-catchment in the Thukela River basin, South Africa. Through the linked GIS, potential runoff harvesting sites are identified relative to areas that concentrate runoff and where the stored water will be appropriately distributed. Based on GIS analysis it was found that 17% percent of the Potshini catchment area has a high potential for generating surface runoff, whereas an analysis of all factors which influence the location of such systems, shows that 18% is highly suitable for runoff harvesting. It is concluded that providing an accurate spatial representation of the runoff generation potential within a catchment is an important step in developing a strategic runoff harvesting plan for any catchment.

## 3.3    Critiques on review of literature

The Arc SWAT model is a physically based hydrological model which requires specific information of topography, soil type, vegetation, land use practice and detailed meteorological data for modelling the discharge of a watershed. Therefore, the SWAT hydrological model which has been developed for one catchment could not be used for another catchment due to different topographical settings, climatic condition, soil and land use practices, etc. The physical parameters and meteorological data governing the hydrological processes must be changed according to the watershed.

GIS provides a Platform for Simulation of the hydrological model. Remote sensing provides Earth's surface information of an area and temporal period with different scales, and the derived data can be used as input data for the SWAT hydrological model. The SWAT also has several inbuilt parameters affecting the discharge of the watershed regarding the ground water variability, water holding capacity of the soil etc. which can be adjusted to suite the watershed.

The DEM (Digital Elevation Model) can give the information of the catchment regarding the longitude, latitude and elevation within the catchment. Together with the stream network it is possible to have elevation information of any point along the river. Therefore, the advance in GIS and Remote Sensing makes it possible to study the character of the stream and investigate hydrological behavior of watershed.

From the above review of the literature it is understood that the advancement of Hydrological model and GIS makes it possible to assess river basin and have feasibility knowledge of the hydropower potential with high accuracy where the sites are inaccessible.

This chapter describes the study area, data acquisition and the generation of various thematic maps (drainage, soil, land use/land cover, contour, basin) using GIS and Remote Sensing. The SWAT hydrological model is used for simulation of discharge in this study, and input requirements, calibration, validation and sensitivity analysis of the SWAT parameters are also discussed. Further, the methodology for assessment of the potential sites of hydro power project for the runoff-river scheme and the estimation of power capacity has been described.

## 4.1 Study area

The catchment of Mat river lies within 92°30 ' E to 93°00' E and 22°30 ' to 23°45'N and covers an area of 147.325 km². The river Mat originates from the hills near Baktawng at an altitude of 1423 m above M.S.L in Aizawl district, Mizoram, India. The altitude of the outlet which is consider for this study is 497 m above M.S.L. The river is joined by numerous small streams, locally known as 'Luis', from the hills on both banks. Mawngping Lui and Mangang Lui are the main tributaries which join the Mat river from the right bank and left bank respectively (Fig. 4.1). The Mat river is a perennial river and is flashy and effluent. Water of this river is an important natural resource for the economic development of the people of this region. The river has a length of 127 km in south direction flowing through Lunglei District and finally joins River Tuipui also known as Kolodyne River.

The geological properties at the considered outlet of the river belong to Lower Bhuban Formation consisting of banded sandstone, pebble conglomeratic sandstone, interbanded and sandstone (Central Water Commission, report 1997).

## 4.1.1 Hydrology

The rainfall in the state varies from 2000 mm to 4200 mm and about 78% of the annual rainfall takes place during the monsoon season from May to September. Data of Discharge observations are available for the period from June 1988 to December 1989, January to December 1991 and 1994.

India

Mizoram

Outlet
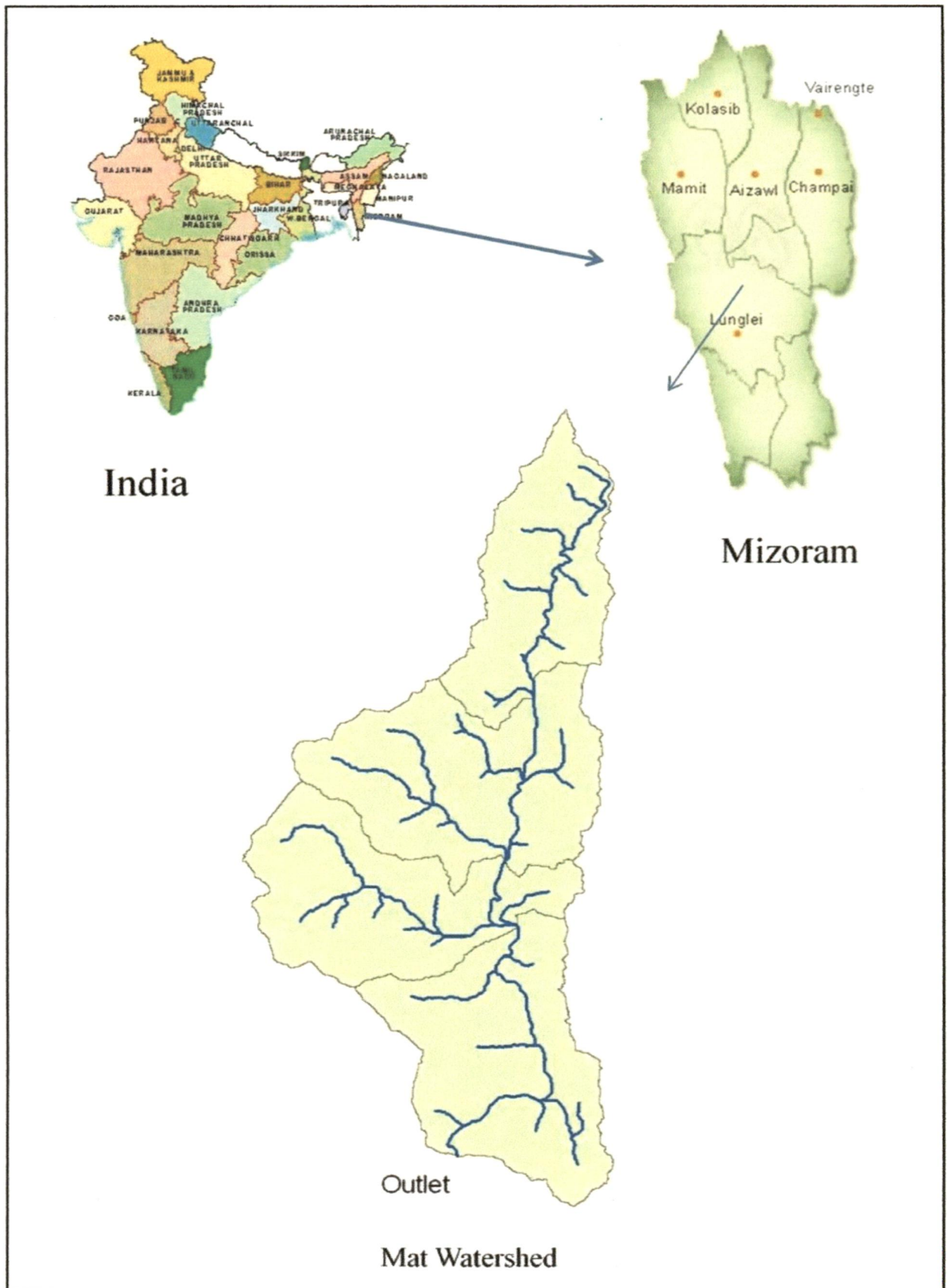
Mat Watershed

**Figure 4.1 Location Map of Mat watershed**

from the origin of the river Mat. The rainfalls data are collected from the office of Agricultural Department, Government of Mizoram. The meteorological data are collected from the office of Indian Council of Agricultural Research, Kolasib, and from Mizoram Science Centre, Zemabawk.

## 4.1.2 Climate

Mizoram enjoys a very pleasant climate. Summers are generally cool to warm and winters are not very cold. During winter the temperature varies from 8°C to 21°C and in summer it varies between 20°C to 32°C respectively. Mean daily maximum temperature is highest in the month of April being 26.5°C and mean daily minimum temperature is lowest in the month of January being 11.3°C.

The relative humidity in monsoon months varies from 79% to 94%. The river Mat has remained untapped for any kind of hydropower and irrigation purpose.

## 4.2 Data acquisition

The details of collection of metrological data, satellite data and the other data and information used in this study are briefly discussed below:

### 4.2.1 Meteorological data

Daily rainfall data for 14 years (1988 -2001) were collected from the Office of Agriculture Department Government of Mizoram. Relative humidity and Temperature recorded data were collected from the office of Mizoram Remote Sensing Application Centre, Chaltlang, Aizawl, Mizoram. Wind speed data was collected from the office of Zoram Energy Development Agency.

### 4.2.2 Hydrological data

Daily discharge data were collected from the office of Central Water Commission, Mizoram. The daily discharge data were available for the year 1988 to 1989, 1991 and 1994. The daily discharge data from the year of 1988 was used for calibration and the discharge data for the year 1989, 1991 and 1994 were used for validation of the SWAT hydrological model.

### 4.2.3 Digital Elevation Model (DEM)

Digital Elevation Models are data files that contain the elevation of the terrain over a specified area, usually at a fixed grid interval over the surface of the earth. The intervals between each of the grid points will always be referenced to some geographical coordinate system. This is usually either latitude-longitude or Universal Transverse Mercator (UTM) coordinate systems. The closer together the grid points are located, the more detailed the information will be in the file. The details of the peaks and valleys in the terrain will be better modeled with small grid spacing than when the grid intervals are very large. Elevations other than at the specific grid point locations are not contained in the file. As a result, peak points and valley points not coincident with the grid will not be recorded in the file.

The files can be in either American Standard Code for Information Interchange (ASCII) or binary. In order to read the files directly one must know the exact format of the entire file layout. Usually the name of the file gives the reference location to some map corner point in the file. The files usually contain only the z value (elevation value) and do not contain the actual geographical location that is associated with that point. The actual location associated with that elevation data is calculated by software reading the actual DEM file, knowing the precise location of the data value inside the DEM file. In addition, there will be some needed reference information in the header (first part) of the file. When an elevation is calculated at locations other than the actual grid points, some method of interpolation from the known grid points is used. Again, this is done in software that is external to the actual DEM file.

The DEM file also does not contain civil information such as roads or buildings. It is not a scanned image of the paper map (graphic). It is not a bitmap. The DEM does not contain elevation contours, only the specific elevation values at specific grid point locations.

The Digital Elevation Map (DEM) was collected from the office of Mizoram Remote Sensing Application Centre, Chaltlang, Aizawl, Mizoram. The resolution of the DEM is 10m x 10m (Fig. 4.2).

#### 4.2.4 Soil Map

Soil map was collected from The Department of Agriculture, Mizoram. Georeferencing has been done using ERDAS and digitalization is done with Arc GIS software (Fig 4.3).

The soil within the study area consists of two types of soils:-

a) Humic Hapludult and Typic Distrochrepts:- Dark brown ( surface ) and dark reddish brown (sub-surface) very deep, well drained, fine loamy soils on moderately steep to very steep hills slopes with severe erosion. This is the predominant soil in the study area (89.06 %).

b) Typic Hspludult and Umbric Distrochrepts:- Dark brown( surface ) and yellowish brown (sub-surface) very deep, well drained, fine loamy soils on moderately steep to very steep hills with severe erosion. It covers 10.94 % of the total watershed.

#### 4.2.5 Land Use Map

Forest area covers more than 50% of the Mat watershed, the different type of forest mainly are Dense/closed and open forest. As the practice of Jhuming system of cultivation is prevalent there, frequently forest areas are cut down and burned up for cultivation which destroys the watershed to a large extent. The Jhuming cultivated areas are grouped into two zones, current shifting cultivation and Abandoned shifting cultivation. 42 percent the total watershed is covered by Jhuming cultivated area. The residential area only made up 1.6 percent of the total watershed area. The rest of the class are minor occupying only a small portion of the watershed. The Land Use Land Cover map for the year 2008 was collected from the office of Mizoram Remote Sensing Application centre, Chaltlang, Aizawl, Mizoram. The various Land use/Land cover classes within the study area are presented in Table 4.1 and Fig. 4.4 respectively.

**Table 4.1: Area (%) under different Land Use/ Land cover of Mat watershed**

| Sl. No. | Land use / Land cover | Area (km²) | % (area) |
|---------|----------------------|-----------|----------|
| 1 | Dense/Closed Forest | 61.215 | 41.731 |
| 2 | Abandoned Shifting Cultivation | 39.875 | 27.066 |
| 3 | Villages(Rural) | 1.006 | 0.683 |
| 4 | Open Forest | 20.991 | 14.248 |
| 5 | Current Shifting Cultivation | 22.312 | 15.145 |
| 6 | Forest Plantations (Rubber) | 0.022 | 0.015 |
| 7 | Residential | 1.522 | 1.033 |
| 8 | Rice | 0.331 | 0.225 |
| 9 | Water Body | 0.016 | 0.011 |
| 10 | Land with scrub | 0.037 | 0.025 |

### 4.2.6 Hardware and Software

The hardware includes the input device, the output device and the system on which it is operated. The computer forms the backbone of the hardware, where data are input through the Scanner or a digitizer board. Scanner converts a picture into a digital image for further processing. The output of scanner can be stored in many formats e.g. TIFF, BMP, JPG etc. A digitizer board is flat board used for vectorisation of a given map objects. Printers and plotters are the most common output devices for a GIS hardware setup. The GIS software provides the functions and tools needed to store, analyze, and display geographic information. GIS softwares in use are MapInfo, ARC/Info, AutoCAD Map, etc. Geographic data and related tabular data can be collected in-house or purchased from a commercial data provider.

Personal computer equipped with ERDAS IMAGINE 9.1, ARC GIS and ARC VIEW 9.3, ARC SWAT 2005 and Auto CAD softwares were used for this study.

### 4.2.7 Scanning and Geometric registration of topographic maps

The scanned topographic maps were geometrically corrected with ERDAS IMAGINE 9.1 using 5 control points as the graticule intersections. The scanned maps were displayed and rectangular coordinates were entered in place of spherical coordinates.

49

Then these were geometrically transformed and transferred to the appropriate location on the blank raster database to finally provide a geometrically rectified map in the digital mode. The geometric precision was tested, by comparing the Root Mean Square Error (RMSE) of the corresponding graticule intersections with their theoretical coordinates kept within one pixel.

### 4.2.8 Generation of thematic map

Thematic map is a map that displays the spatial distribution of an attribute that relates to a single topic, theme, or subject of discourse. Usually, a thematic map displays a single attribute such as soil type, vegetation, geology, land use, or landownership. For attributes such as soil type or land use, shaded maps that highlight regions by employing different colors or patterns is generally wanted. For other attributes, a shaded map in which each shade corresponds to a range of population densities is generally wanted. Thematic maps are used to display geographical concepts such as density, distribution, relative magnitudes, gradients, spatial relationships and movements.

The generated thematic map includes the delineation of boundary of watershed and sub watersheds (Fig 4.5), establishment of digital contour, digitization of soil map and Land use / Land cover map.
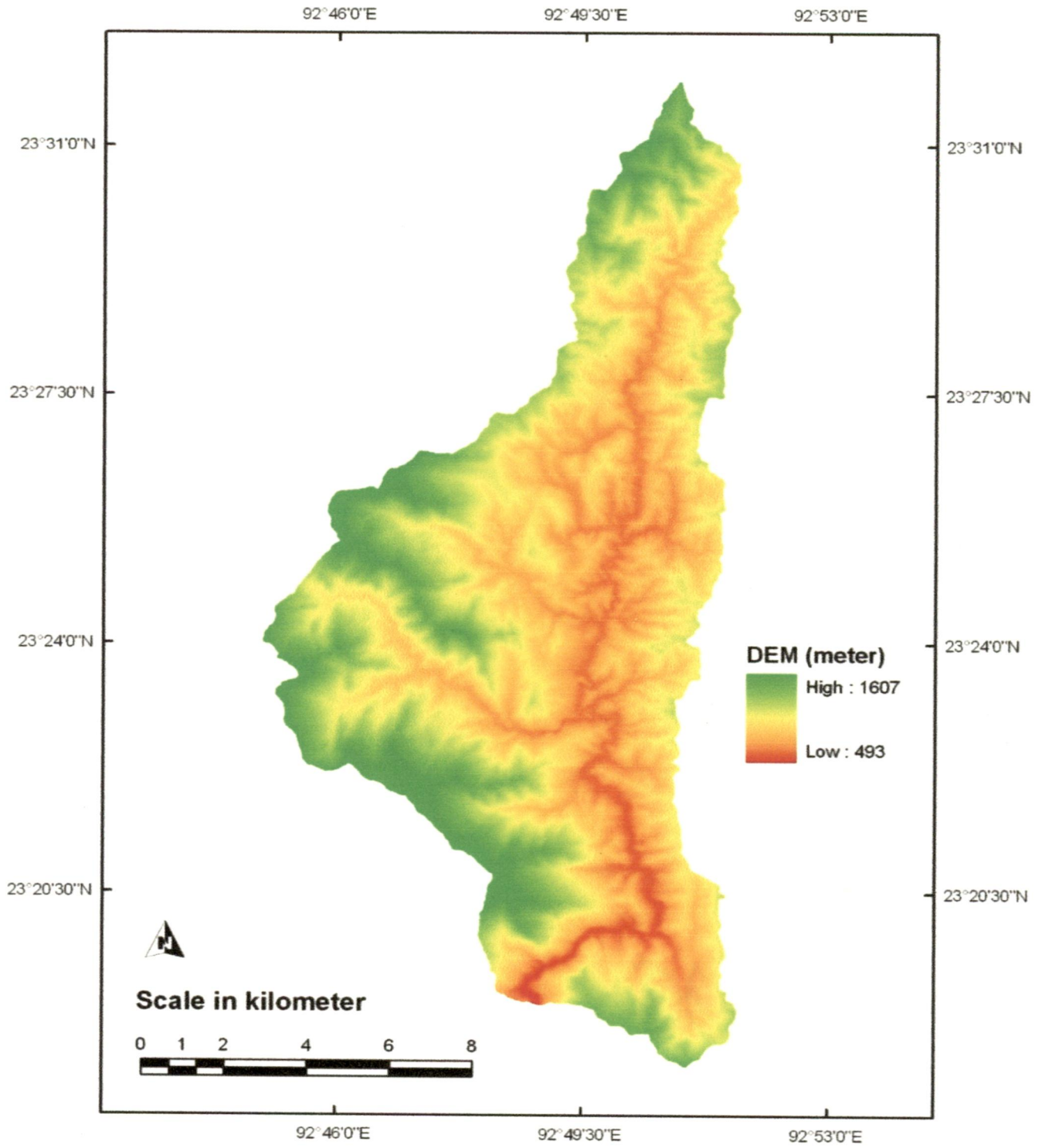
**Figure 4.2 Digital Elevation Model (DEM) of Mat watershed**
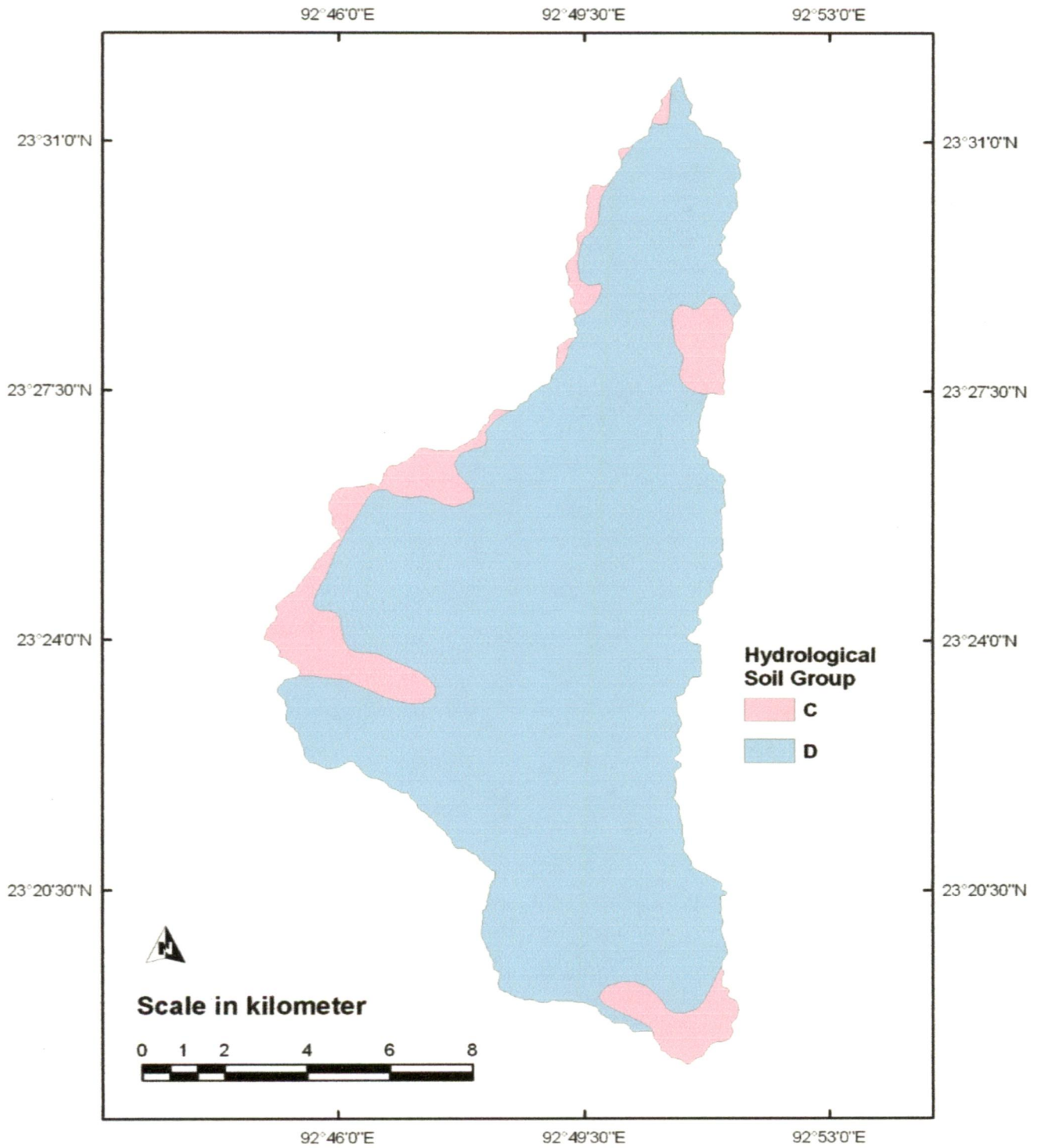
Figure 4.3 Soil map of Mat watershed

**Legend: Landuse / Landcover Classes**

- Abandoned Shifting Cultivation
- Current Shifting Cultivation
- Dense/Closed Forest
- Forest Plantations
- Rice
- Land with scrub
- Open Forest
- Residential
- Villages(Rural)
- Water Body

**Scale in Kilometer**

0  1  2  4  6  8
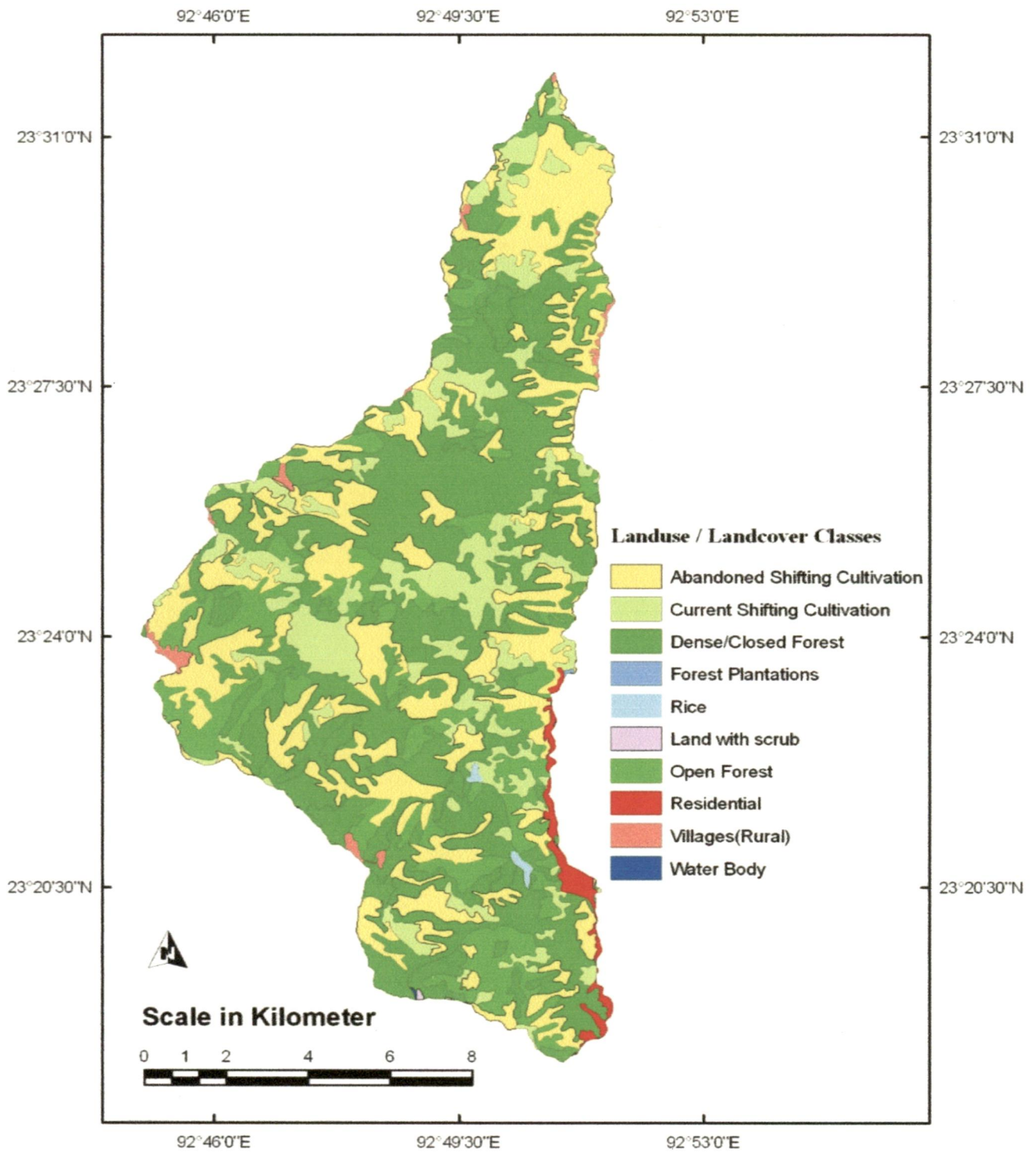
**Figure 4.4 Land use / Land cover map of Mat watershed**
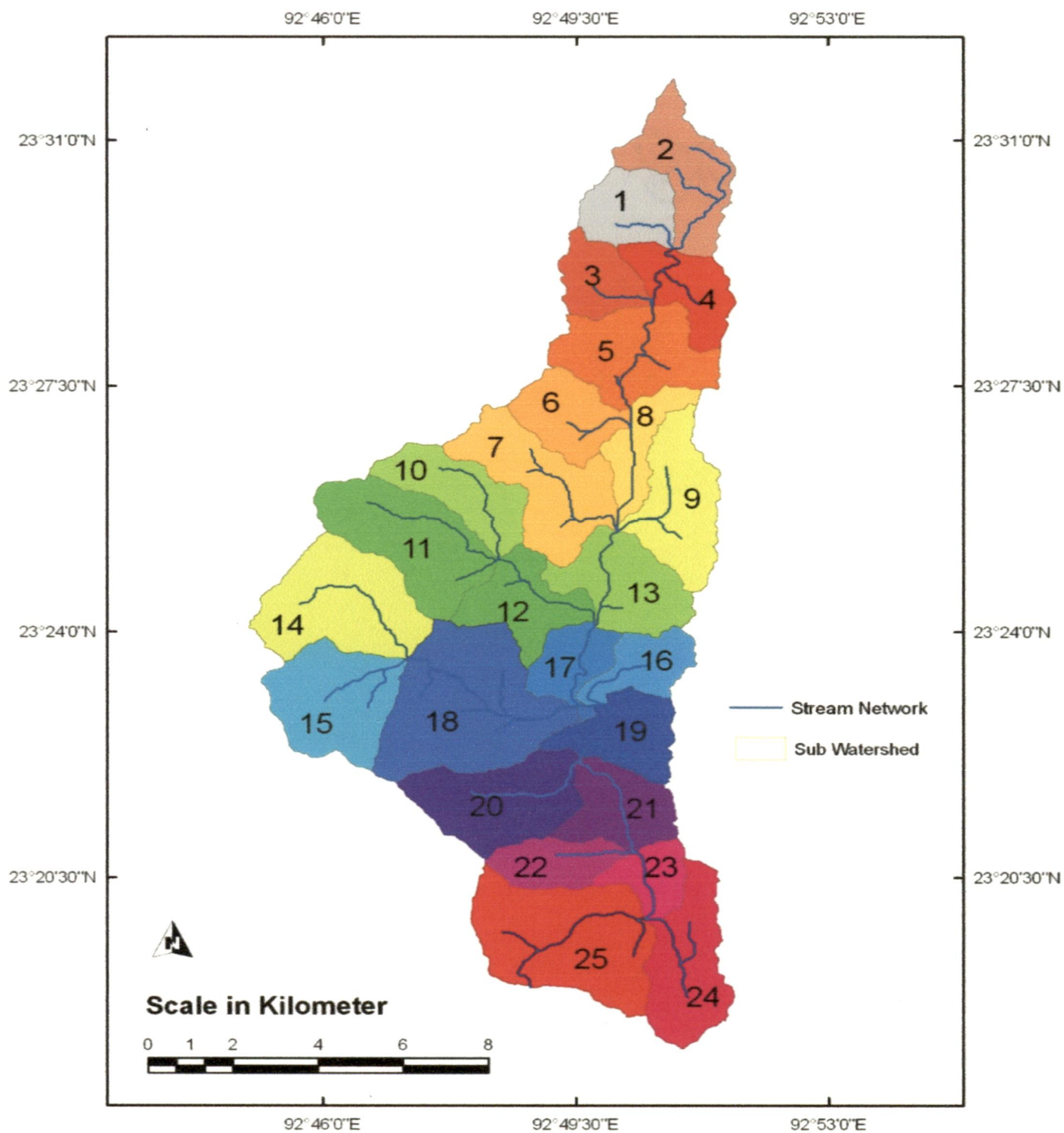
**Figure 4.5 Subwatershed map of Mat watershed**

## 4.3 Generation of discharge using the SWAT model

The ArcSWAT ArcGIS extension is a graphical user interface for the SWAT model (Arnold et al., 1998). Basically, Arc-swat is a long term, physically based, continuous simulation watershed model developed to quantify the impact of land management practices in large, complex catchments. A large number of inputs are required for running the model to obtain modeled discharge. DEM, Landuse/Landcover map and Soil map of the study watershed are three spatial inputs required for the model. Other inputs required for the model are long term weather data, soil properties and discharge data.

Finally, the SWAT model required discharge data at representative outlets of the streams for calibration and validation of the model. Discharge data recorded at the outlet of the study watershed during 1988 to 1989, 1991 and 1994 have been taken for these purposes.

### 4.3.1 Preparation of Arc SWAT input data set

To create a SWAT dataset, the interface will need to access ArcGIS compatible raster (GRIDs) and vector datasets (shapefiles and feature classes) and database files which provide certain types of information about the watershed. The necessary spatial datasets and database files need to be prepared prior to running the interface.

### 4.3.1.1 Digital Elevation Model (DEM): ESRI GRID Format

The SWAT interface allows the DEM to use integer or real numbers for elevation values. The units used to define the GRID resolution and the elevation is not required to be identical. The GRID resolution can be defined in one of the following units: meters, kilometers, feet, yards, miles, decimal degrees. The elevation can be defined in one of the following units: meters, centimeters, yards, and feet.

The ArcGIS compatible raster (GRIDS) was extracted from the DEM image file. The GRID resolution and the elevation for this study were both defined in meters.

### 4.3.1.2 Landuse/Landcover map: ESRI GRID Format

The categories specified in the landcover/land use map needed to be reclassified into SWAT land cover/plant types. There are three options for reclassifying the categories. The first option is to use a landcover/landuse lookup table that is built into the ArcSWAT interface. The interface contains the USGS LULC and NLCD 1992 lookup

tables in the SWAT2005.mdb database that identifies the different SWAT land cover/plant types used to model the various USGS LULC or NLCD 1992 land uses. The second option is to type in the 4-letter SWAT land cover/plant type code for each category when the land cover/land use map theme is loaded in the interface. The third option is to create a user look up table that identifies the 4-letter SWAT code for the different categories of land cover/land use on the map.

The third option is used for this study; the user look up table that identifies the 4-letter SWAT code for each category was created. The ArcGIS compatible raster (GRIDS) image was extracted from the vector files.

### 4.3.1.3 Soil map: ESRI GRID Format

The categories specified in the soil map needed to be linked to the soil database (U.S. soils data only) included with the interface or to the User Soils database, a custom soil database designed to hold data for soils not included with the United State soil database. There are four options for linking the map to the soil database.

(i) The STATSGO polygon (MUID) number method.

(ii) The STMUID method.

(iii) Linking the soils map to the database via Soils 5ID number.

(iv) Linking the soils data from the User Soils database are to be utilized.

The fourth option was used to reclassify the map categories, by linking the soil data from the user soils database. A look up table was loaded which has this information listed. The ArcSWAT spatial datasets were created in the same projection as the DEM and Landuse/Landcover projection.

### 4.3.1.4 Weather Station set up

The user Weather Station set up was done by entering the climatic variables required by the SWAT model to the model database. The climatic variables input (**Table 4.2**) to set up the weather station database are as follows:

(i)     Longitude and Latitude of the user weather station.

(ii)    Elevation of the weather station.

(iii)   Average or mean maximum air temperature for month (°C).

(iv)    Average or mean minimum air temperature for month (°C).

(v)     Standard deviation for daily maximum air temperature in month (°C).

Table 4.2 Input hydrological statistic of Mat watershed for weather station in SWAT

| Climatic parameters | Statistical parameters | Jan | Feb | Mar | Apr | May | Jun | Jul | Aug | Sep | Oct | Nov | Dec |
|---|---|---|---|---|---|---|---|---|---|---|---|---|---|
| Maximum temperature | Mean | 22.98 | 25.28 | 30.22 | 32.20 | 30.94 | 31.32 | 30.26 | 28.48 | 29.92 | 29.30 | 27.18 | 23.92 |
| | Std. dev. | 1.40 | 1.64 | 1.37 | 2.30 | 1.71 | 1.41 | 0.86 | 3.47 | 0.82 | 0.69 | 1.68 | 1.14 |
| Minimum temperature | Mean | 8.24 | 10.82 | 13.82 | 15.04 | 16.98 | 18.64 | 18.90 | 17.86 | 18.76 | 17.00 | 13.68 | 9.26 |
| | Std. dev. | 1.38 | 1.02 | 1.74 | 1.42 | 1.11 | 0.76 | 0.32 | 2.09 | 0.94 | 0.98 | 1.05 | 1.85 |
| Rainfall | Mean | 7.72 | 45.39 | 111.23 | 164.65 | 355.92 | 465.81 | 490.69 | 487.35 | 399.72 | 183.23 | 46.92 | 11.87 |
| | Std. dev. | 0.52 | 3.36 | 7.24 | 13.80 | 16.55 | 22.23 | 19.83 | 16.95 | 18.57 | 14.17 | 7.60 | 2.81 |
| | Skewness | 1.11 | 3.47 | 4.16 | 2.73 | 2.02 | 2.76 | 1.89 | 1.64 | 2.28 | 2.50 | 4.48 | 3.90 |
| | Average rainfall day | 0.40 | 5.80 | 6.40 | 10.80 | 18.80 | 24.40 | 29.60 | 28.40 | 25.20 | 12.80 | 4.20 | 1.80 |
| Probability of wet day following dry day | | 0.01 | 0.18 | 0.13 | 0.22 | 0.47 | 0.69 | 0.73 | 0.55 | 0.65 | 0.25 | 0.07 | 0.03 |
| Probability of wet day following dry day | | 0.10 | 0.32 | 0.37 | 0.55 | 0.64 | 0.84 | 0.91 | 0.91 | 0.85 | 0.58 | 0.53 | 0.27 |
| Relative humidity | | 68.33 | 64.49 | 63.45 | 70.28 | 79.56 | 85.16 | 88.00 | 89.77 | 87.98 | 82.59 | 72.45 | 67.02 |
| wind velocity (m/sec) | | 0.62 | 0.90 | 0.96 | 1.15 | 1.59 | 1.25 | 1.52 | 1.75 | 1.52 | 0.81 | 0.61 | 1.69 |
| Solar Radiation ($MJ/m^2/day$) | | 24.64 | 28.71 | 33.11 | 36.94 | 38.72 | 39.28 | 38.88 | 37.50 | 34.58 | 30.34 | 25.78 | 23.33 |

(vi) Standard deviation for daily minimum air temperature in month (°C).

(vii) Average or mean total monthly precipitation (mm).

(viii) Standard deviation for daily precipitation in month (mm/day).

(ix) Skew coefficient for daily precipitation in month.

(x) Probability of a wet day following a dry day in the month.

(xi) Probability of a wet day following a wet day in the month.

(xii) Average number of days of precipitation in a month.

(xiii) Maximum 0.50 hour rainfall in the entire record period for month (mm).

(xiv) Average daily Solar radiation for month (MJ/m$^2$/day).

(xv) Average daily Dew point temperature in month (°C).

(xvi) Average daily wind speed in month (m/s).

### 4.3.2 Delineation of Stream network

Stream networks are delineated from a DEM using the output from the ARC INFO grid flow direction and flow accumulation functions. Flow direction uses a DEM to determine the direction of flow from every cell in the raster. Flow accumulation, in its simplest form, is the number of upslope cells that flow into each cell. By applying a threshold value to the results of flow accumulation, stream networks are delineated.

### 4.3.2.1 Flow direction

Water flows in the direction of the steepest downhill gradient. Every pixel is potentially surrounded by eight neighboring pixels. The slope in each of these eight directions may be calculated by taking the difference in elevation indicated by the DEM value at each of these eight neighboring locations and the value at the pixel being examined. This difference in elevation is then divided by the center-to-center distance between these pixels (this distance will be the cell size in the cardinal directions and the cellsize.√2 in each of the diagonal directions. The direction that yields the steepest downhill slope is the inferred direction of water flow. In this study the flow direction was calculated by the SWAT model from the input DEM.

### 4.3.2.2 Flow Accumulation

It is the number of cells, or area, which contribute to runoff of a given cell. Accumulation, once it reaches a threshold appropriate to a region, forms a drainage channel. Water accumulates along the flow paths dictated by the topography and defined earlier as the flow direction. Adjusted to proper units, the flow accumulation

is synonymous with drainage area. Flow accumulation once adjusted from a count of pixels to units of area is synonymous with drainage area. Calculating it as a spatially distributed quantity allows us to determine drainage area not at just one point, but at any point within the domain of the original DEM field. For this study the flow accumulation was calculated by the SWAT model for a threshold value of 12000 to ensure the flow (Fig. 4.6). The flow accumulation value for Mat watershed ranges from 0 to 1474532.

### 4.3.2.3 Establishment of Stream network

After the threshold value 12000 have been selected for the flow accumulation, the stream network having the threshold value or greater was generated by the SWAT model. This method is arbitrary, because it is based on the threshold selected by the user. The model generates the stream network in shape file format (Fig. 4.7).

The drainage network was also extracted and digitized from the topographic map for comparison with the stream network generated by the model. It was found that the stream network generated by the model closely follows the stream network extracted from the topographic map (Fig.4.8). The order of the stream at a threshold value of 12000 flow accumulation was found to be 3$^{rd}$ order and above.

### 4.3.3   Delineation of watershed and subwatersheds boundary

It is the process of delineating an area that contributes to drainage or flow to the considered outlet. The watershed boundary was delineated from the topographic map in the GIS environment with the ERDAS imagine 9.1 software. This boundary was used as a mask in the SWAT environment to finalize the watershed boundary.

In the SWAT model each single stream are assigned to one catchment and have a separate outlet. This was achieved by manually minimizing the numbers of the sub-watershed outlet from the automatic watershed delineator in SWAT.

### 4.3.4   Map overlay and Hydrological Response Unit (HRU) analysis

The SWAT model subdivides the sub basins into smaller homogenous units known as hydrologic Response Units (HRU). The HRUs are lumped land areas within the sub basin comprising of unique features of land cover, soil and its management (Arnold et.al. 1993 and Neitsch et.al. 2001). The land use and soil datasets were imported and linked to the SWAT databases and reclassified.
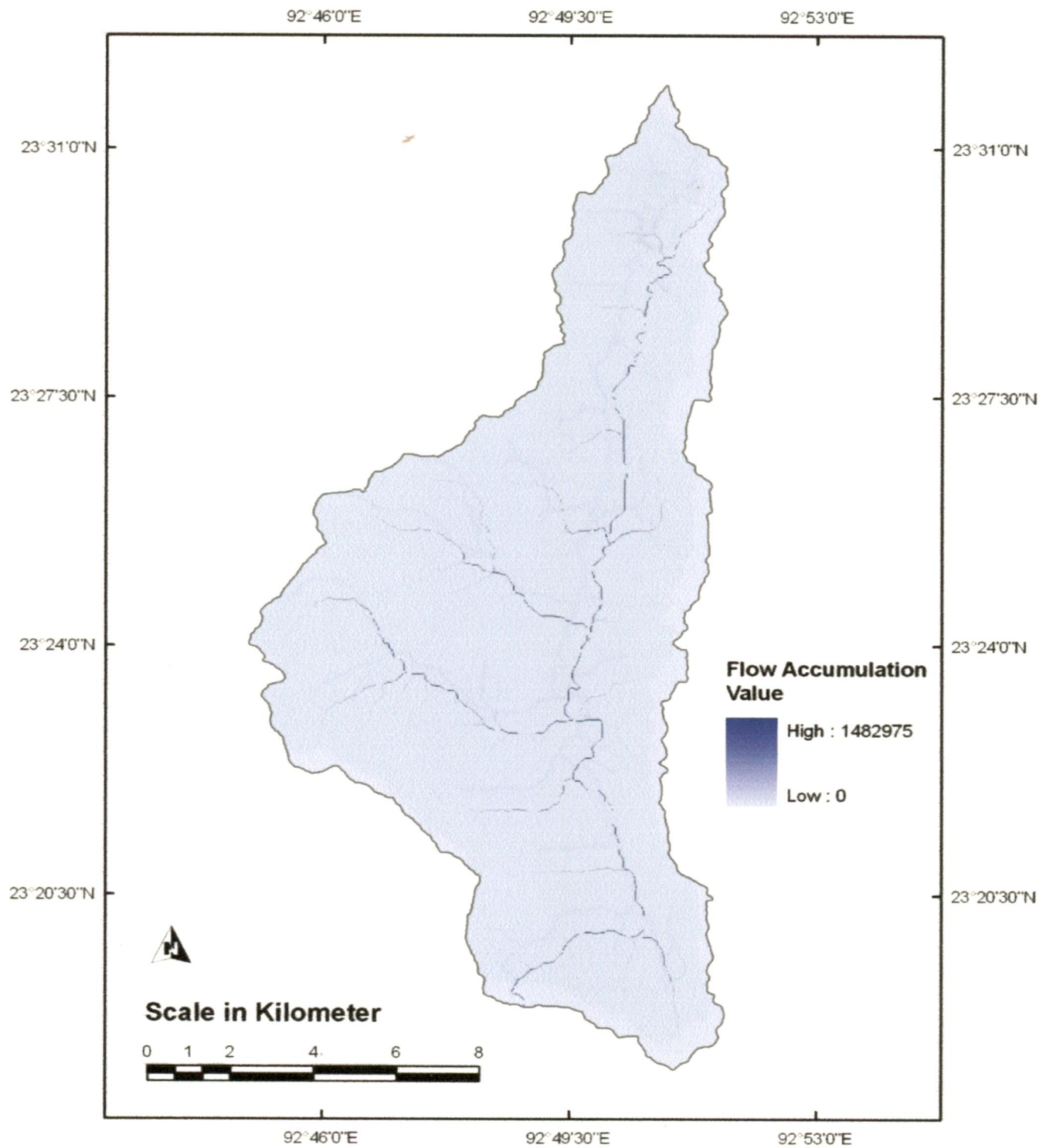
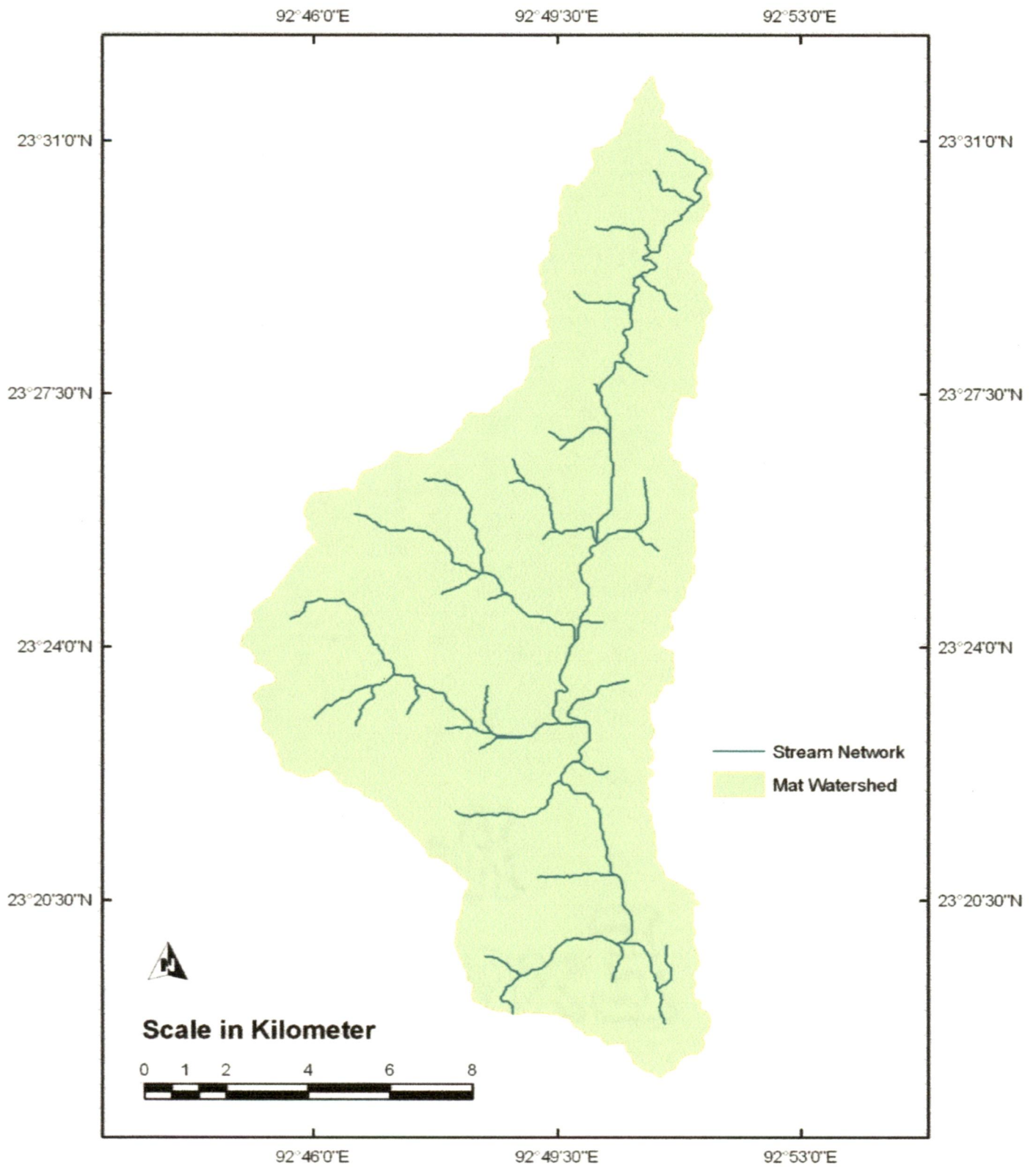**Figure 4.6 Flow Accumulation map of Mat watershed**

**Figure 4.7 Stream network of 12000 Flow accumulation and above at Mat watershed**
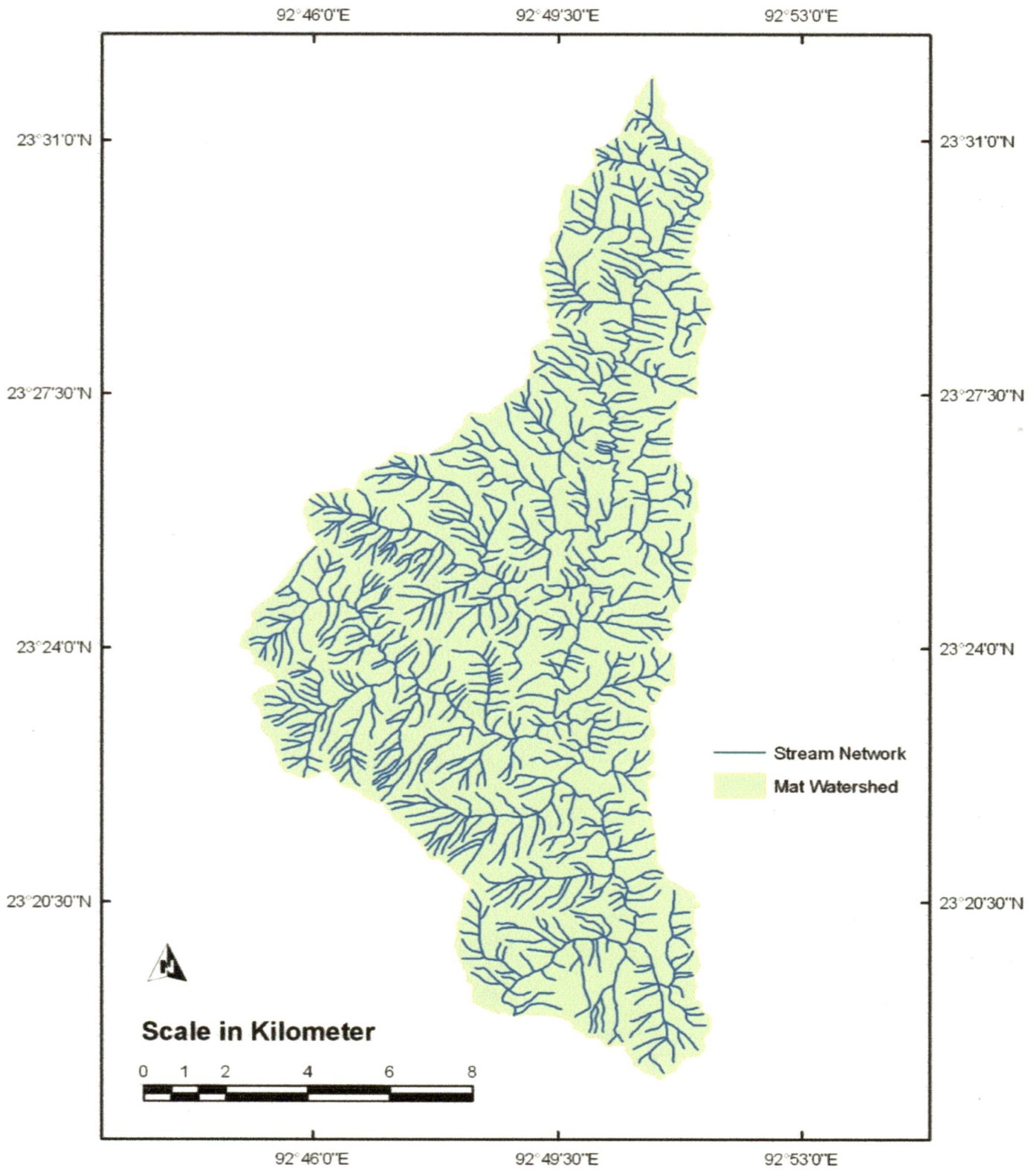
**Figure 4.8 Stream network of Mat waterhed from Topographic Map**

HRU analysis in Arc SWAT includes division of HRUs by slope classes in addition to land use and soils. This is particularly important if subbasins are known to have a wide range of slopes occurring within them. The slope classification was made for multiple slopes with 5 classes as the elevation difference was 405 meter. Finally, the slope map was also overlaid to create a unique landuse/soil/slope combination (hydrologic response units or HRUs) for each subbasin.

Subdividing the watershed into areas having unique land use and soil combinations enables the model to reflect differences in evapotranspiration and other hydrologic conditions for different land covers/crops and soils. Runoff is predicted separately for each HRU and routed to obtain the total runoff for the watershed. This increases the accuracy of load predictions and provides a much better physical description of the water balance. Multiple HRUs are created for this study keeping the sensitivities for the land use, soil, and slope data are fixed at 20 %, 10% and 20 % respectively.

### 4.3.6 Import weather data

Weather data to be used in a watershed simulation is imported once the HRU distribution has been defined. The weather data were formulated in dbf file conforming to the SWAT format. Weather data is loaded using the first command in the Write Input Tables menu item on the ArcSWAT toolbar. This tool allows users to load weather station locations into the current project and assign weather data to the sub-watersheds. For each type of weather data loaded, each sub-watershed is linked to one stream gage.

### 4.3.7 Creation of Inputs

The database files containing the information needed to generate default input for SWAT was build using the Write Input command. This command is enabled after weather data is successfully loaded. These commands are enabled in sequence (the next command is enabled only after the steps associated with the previous command are completed) and need to be processed only once for a project. Before SWAT can be run, the initial watershed input values must be defined. These values are set automatically based on the watershed delineation and landuse/soil/slope characterization.

### 4.3.8 Model Output

A number of outputs are created in every SWAT simulation. These files are: summary input files (input.std), the summary output file (output.std), the HRU output file (output.hru), the subbasin output file (output.sub), and the main channel or reach output file (output.rch).

The details of the data printed out in each file are controlled by the print code in the master watershed file. Average daily values are always printed in the HRU, subbasin and reach files, but the time period they are summarized over will vary. Depending upon the print code selected, the output file can include all daily values, daily amounts averaged over the month, and daily amounts averaged over the year.

## 4.4    Model calibration

Model calibration is the modification or adjustment of model parameters, within recommended ranges, to optimize the model output so that it matches with the observed set of data. The calibration tool of Arc-SWAT provided several different parameters for adjustment through user intervention. These parameters can be adjusted manually or automatically until the model output best matches with the observed data. The discharge data recorded during the year 1988-1989 was used for the calibration of the model. The model calibration was done manually by changing the various SWAT parameters one by one until the simulated model output matches the observed discharge data.

## 4.5    Model validation

Validation is the process of determining the degree to which a model or simulation is an accurate representation of the observed set of data from the perspective of the intended uses of the model. The values of simulated discharge at specified location will be compared with the observed discharge for validation of the model (Gassman et. al., 2007). The model performance can be evaluated using established indices like (i) coefficient of determination (R2), (ii) Index of agreement (d), (iii) Nash and Sutcliffe efficiency, and (iv) Relative Error (RE) etc.

(i)     Coefficient of determination is given by:

$$R^2 = \left\{ \frac{n(\sum Q_{mod} \cdot Q_{obs}) - (\sum Q_{mod}) \cdot (Q_{obs})}{\sqrt{[n(Q_{mod}^2) - (\sum Q_{mod})^2] \cdot [n(Q_{obs}^2) - (\sum Q_{obs})^2]}} \right\}^2$$

was generated using the input DEM. The SWAT model gives the length of each streams and their outlet along with the stream maximum and minimum elevation.

The model also, by default, gives all the outlets of the Subwatershed at every confluence point of the rivers. Subwatershed outlets are the points in the drainage network of a subwatershed where stream flow exits the sub-watershed area. The SWAT model has a provision for editing the outlet of a sub-watershed either removing or adding a new outlet through user intervention.

The ability of the SWAT model to generate detailed information of the stream is utilized for identification of the hydropower sites along the stream network and estimation of flow in each selected potential sites.

### 4.7.1 Identification of Hydropower sites

The SWAT model is run without editing subbasin outlet to have a knowledge on the characteristics of the stream as the model by default gives subbasin outlet for each single stream. Once the characters of the stream are known, the search for potential site is started. The DEM input is first analyzed to find position of the required elevation in the upstream of the main outlet by clicking on each pixel to know the elevation. The search for the required elevation is carried out along the stream network generated by the SWAT model. After locating the pixel having the required elevation, the stream length is measured from the outlet to check for the distance criteria. The subbasin outlet is than added manually in the stream network and the subwatershed is delineated again. The detailed information generated by the model is checked for the height and distance criteria. When both the criteria are met the site is selected as potential hydropower site. The next site is assessed in the same manner starting from the last selected site till the stream ends.

### 4.7.1.1 Criteria for identification of sites

For selection of sites the following three criteria have been considered:

(i) *Availability of flow:* This availability of adequate flow is checked by:
   a) Considering only the stream which has the flow accumulation of 12000 cells or more from the flow accumulation map.

b) The flow accumulation map was also compared with the order of the stream (Strahler, 1958) from the digitized drainage map to make sure the stream order is above 3$^{rd}$ order or more.

(ii) *Site interval* : Sites are selected observing the following two criteria:

a) Minimum distance between the consecutive sites should not be less than 500 meters. The distance between the tail race of one potential site and the diversion arrangement of the next potential site should be atleast 500 meters.

b) The maximum length of river considered to find the head should not be more than 3000 meters (1:150 slope). From the economic view point, the distance between the tail race of one potential site and the diversion arrangement of the next site should be restricted to a maximum distance of 3000 meters.

(iii) *Head availability*:

a) The head availability should be assessed starting from the main outlet of the watershed.

b) The head available along the river is assessed with an initial search of 20 meter rise in the river bed.

c) When criteria 500 meter distance requirement is not met, the search height (20 m) may be increased to have a minimum length requirement. At the same time the maximum distance criteria must be checked.

### 4.7.2 Estimation of flow

The discharge is generated using a validated SWAT model for each of the selected potential hydropower sites. Since the subbasin outlets are added to each potential site at the time of head assessment, the discharge at each sites are obtained. This gives a more realistic discharge for power estimation as the discharge at each site is simulated separately. The model estimates the discharge on daily basis from which 10 daily or monthly discharge can be obtained as per the requirement.

## 4.8    Hydropower generation

Hydropower is produced from generator driven by water turbines that convert the energy of fast-flowing water to mechanical energy. Water at a higher elevation flows downward through large pipes or tunnels (penstocks). The falling water rotates turbines, which drive the generators. The generator in turn converts the turbines mechanical energy into electricity. The quantity of water as well as the head availability determines the production of the hydropower. Therefore, the amount of power generated when Q cumecs of water is allowed to fall through a head of H meters is given by:

$$Power = 9.81 \times Q \times H \times \eta \quad \text{(in kw)}$$

Where,

> 9.81 is the unit weight of water in $kN/m^3$
>
> $\eta$ is the overall efficiency of the turbine, generator etc.

The working mechanism of hydropower generation can be understood from the schematic diagram of hydro power plant (Fig. 4.9).
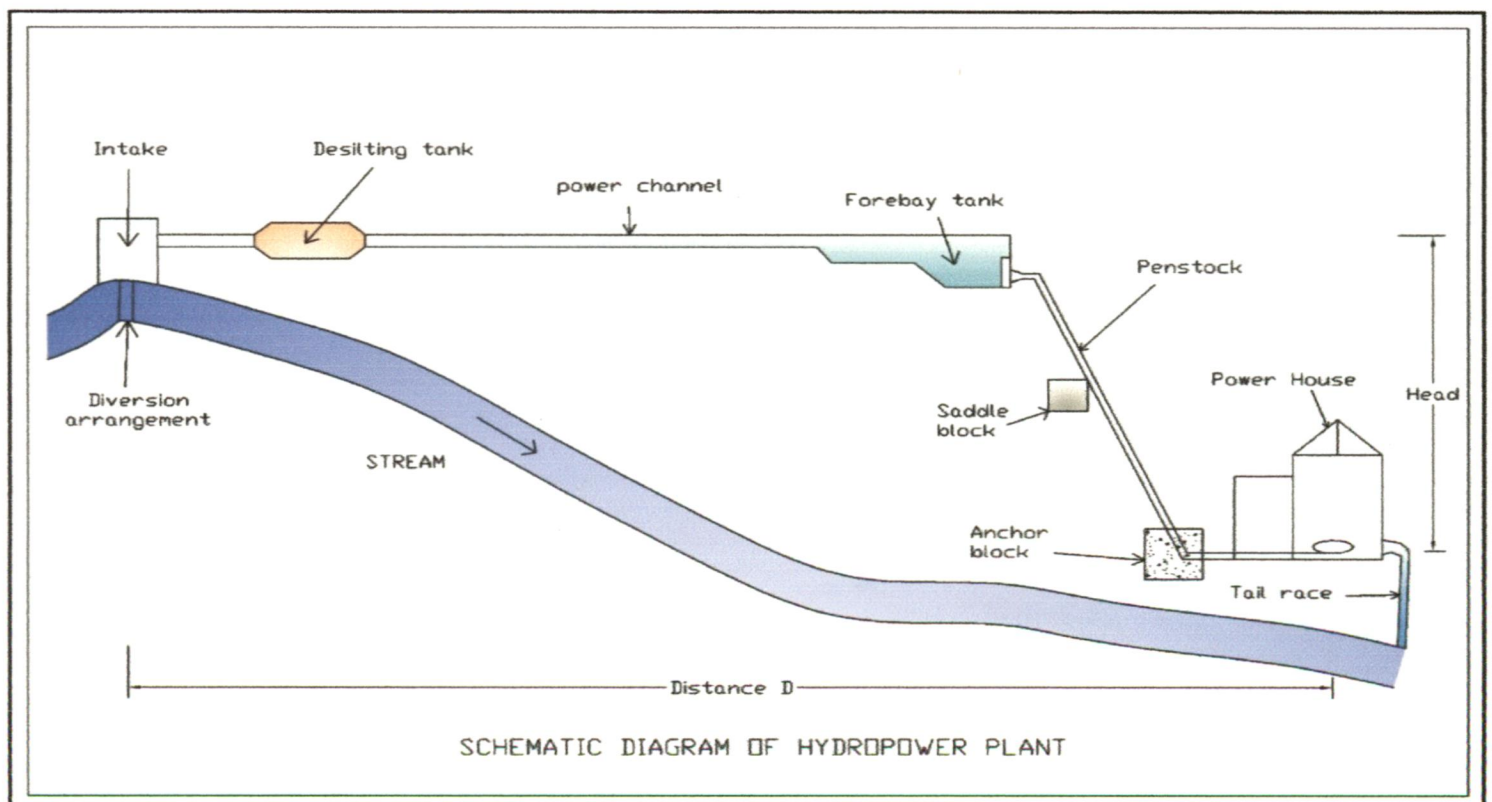


**Figure 4.9 Schematic diagram of a hydropower plant**

## 4.9  Estimation of hydropower potential using flow duration curve (FDC)

The discharge availability at the project site can be estimated with the help of flow duration curve. Flow duration curve of a stream is a plot of discharge against the percent of time the flow was equaled or exceeded. A flow-duration curve provides the percentage of time the stream flow is exceeded over a historical period for a particular river basin (Vogel *et.al.* 1994). Construction of FDC is a pre-requisite of hydropower planning besides other uses (Castellarin *et. al.* 2004).

The 90% dependable year was found out by arranging in descending order, the available annual runoffs and using Weilbuls' formula (MNES/AHEC, 2008).

$$P_p = \frac{m}{N+1} X 100\%$$

Where,

$m$ is the order number of the discharge (or class value),

$P_p$ is the percentage probability of the flow magnitude being exceeded,

The plot of the discharge $Q$ against $P_p$ is the flow duration curve. This gives the percentage of time a discharge is available for power production (Ministry of New and Renewable Energy, 2008).

Normally for power estimation 50%, 75% and 90% dependability discharge values are considered and for this study these three levels of flows dependability were considered. Only the possible run-of-the-river sites, where power could be generated without constructing reservoir, were identified. The work organization diagram for assessment of hydropower potential is given in Fig. 4.10.

After finding out the head and discharge available at each selected site, the available hydropower potential at the identified sites were estimated using established power equation (CEA, 1997).
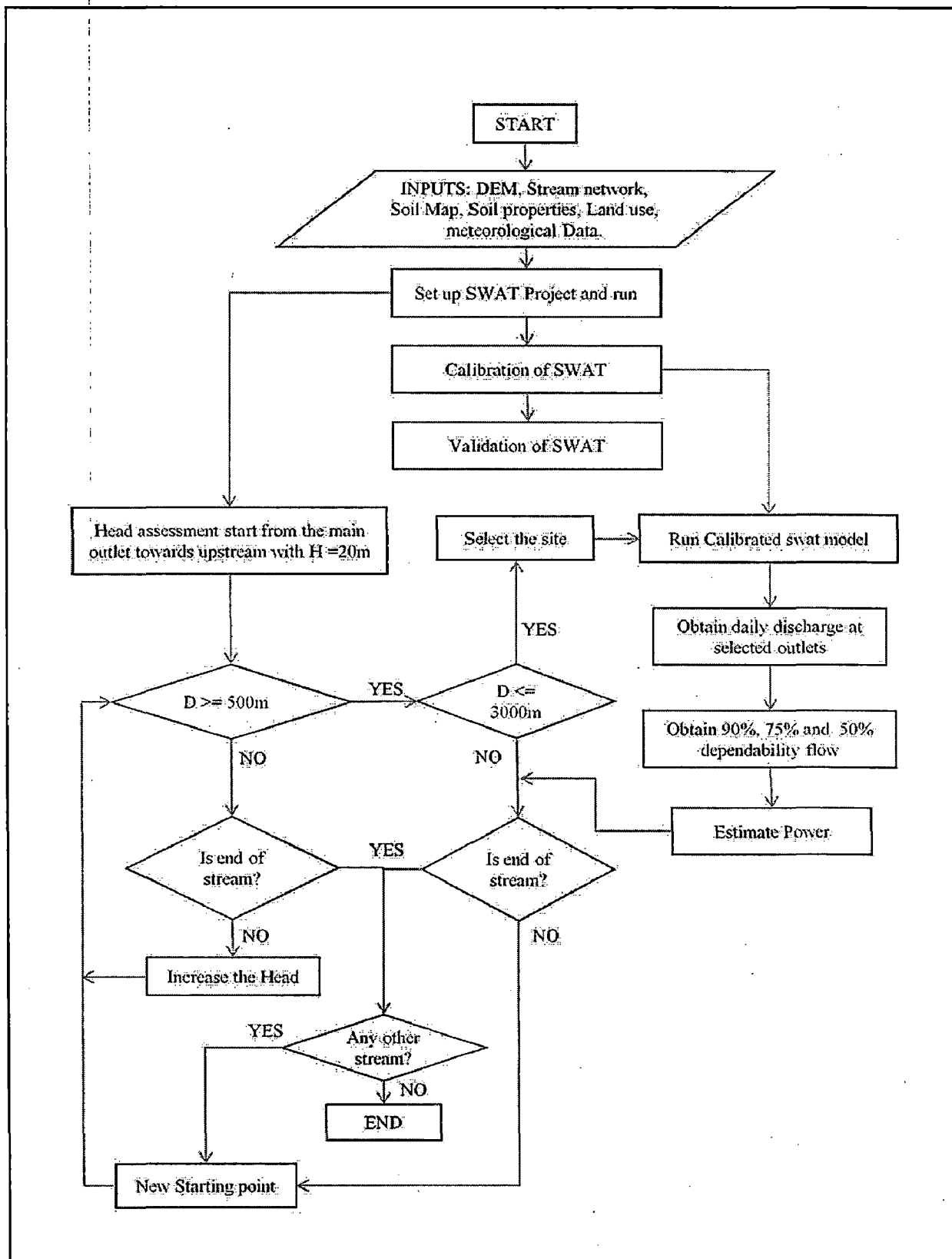
**Figure 4.10  Work organization loop for assessment of hydropower**

71

This chapter presents the results of calibration, validation, sensitivity analysis of the SWAT parameters of Mat watershed. The results of assessment of hydropower potential site and its selection of site using SWAT model by searching head rise along the river is also discussed. Further, the study estimates the potential of hydropower generation at each selected site.

## 5.1    Model calibration

Calibration of SWAT model was done by adjusting the inbuilt parameters affecting the flow generation (Table 5.1). The calibrated parameters for the Mat watershed and their individual effects in the runoff generation during calibration are discussed below.

*(i)*    ***Base flow alpha factors (Alfa_Bf)***

The base flow recession constant, $\alpha_{gw}$, is a direct index of ground water flow response to changes in recharge (Smedema and Rycroft, 1983). The base flow alpha range between $0 - 1.0$. The value may vary from 0.1 to 0.3 for catchment with slow response to recharge, and from 0.9 to 1.0 for catchment with rapid response. The calibrated base flow alpha factor is 0.56.

However, during calibration of the model, it is observed that with the increase in base flow alpha factor there is an increase in the runoff particularly during peak flow. But, at the same time it has reduced the base flow considerably during the dry season as the recharge is rapid and cause the base flow soon after the rain.

*(ii)*    ***Threshold depth of water in the shallow aquifer required for return flow to occur (GWQMN)***

Ground water flow towards the reach is allowed only if the depth of water in the shallow aquifer is equal to or greater than GWQMN. The value ranges from 0 to 5000. The final adjusted value for the catchment is 1.0.

It was observed that by increasing the value of GWGMN there is decrease in both runoff and base as a greater depth of water is required to make the base flow, consequently, there will be delay in base flow as a result of this.

*(iii)*    ***Threshold depth of water in the shallow aquifer for 'revap' or percolation to the deep aquifer to occur (REVAPMN).***

This parameter controls the movement of water from the shallow aquifer to the unsaturated zone of soil. The seepage takes place only when the volume of water in the aquifer is greater than or equal to REVAPMN. The value ranges from 0 to 500, and the calibrated value is 1.

It was observed that the runoff is affected by this parameter in such a way that when the rainfall depth exceeds or equals the value of REVAPMN, there is a decrease in runoff due to seepage to the unsaturated zone. Therefore, when the value of this parameter is more, the seepage to the unsaturated zone will take place later as more depth of water is required to cause the seepage resulting in more runoff until REVAPMN value is reached.

*(iv)*    ***Soil Evaporation compensation factor (ESCO).***

This coefficient has been incorporated to allow the user to modify the distribution used to meet the soil evaporated demand to account for the effect of capillary action, crusting and cracks. The value of ESCO is between 0.01 to 1.0. The model is able to extract more of the evaporative demand from the lower level when the value of ESCO is reduced. The calibrated value of ESCO is 0.8.

It was observed that higher the value of ESCO, lesser is the evaporation which results in more runoff. However, while lowering the value there was a significant drop in the peak as well as the base flow. The evaporation loss in the runoff is very high at the beginning of the rainy season rather than the end of the rainy season.

*(v)*    ***Available water capacity of soil layer (SOL_AWC)***

Available water capacity is the amount of water that a soil can store that is available for use by plants. The value ranges from 0.1 to 1.0.

It was observed that higher the value of SOL_AWC, higher is the runoff during rainy season, but base flow was observed to be decreasing during the lean season at higher value. The calibrated value of SOL_AWC is 0.25.

*(vi)* *Manning's coefficient of roughness 'n' for channel*

The value of CH_N2 ranges for natural stream with heavy timber and brush between 0.050 to 0.150 (chow, 1959). The calibrated value is 0.10. It has been observed that there is a small decrease in runoff rate with the increase in the Manning's coefficient.

**Table 5.1Parameters used for calibration for Mat watershed and their values.**

| Sl. No. | Parameters | Calibrated value | Range |
|---|---|---|---|
| 1 | Base flow recession alpha ( days ) | 0.56 | 0 - 1 |
| 2 | Threshold depth of water in shallow aquifer required for return flow to occur (mm $H_2O$) | 2 | 0 - 5000 |
| 3 | Threshold depth of water in shallow aquifer for percolation to the deep aquifer to occur | 1 | 0 - 500 |
| 4 | Soil evaporation compensation factor | 0.8 | 0.01 - 1.0 |
| 5 | Available water capacity of soil layer | 0.25 | 0 - 1 . |
| 6 | Manning's coefficient 'n' for channel | 0.1 | 0.01 - 0.12 |

Model calibration was performed for the year 1988 (Fig. 5.1) and graphically compared the model output with observed discharge data recorded during these years. It is observed that the model discharge closely matched the observed discharge consistently in both the calibrated years. The calibration was done with the average daily discharge in a month for the whole year.

The regression analysis was performed between the observed and simulated discharge and the best fit line is also shown for the calibrated year 1988. It is observed that the model slightly underpredicted the high value of discharge during monsoon (Fig. 5.2). The coefficient of correlation ($R^2$) is 0.907 and which shows a close relationship between the observed and simulated discharge.

Further, the efficiency of the model for simulating the runoff was also tested using established index (Table. 5.2). It is observed from the overall standard deviation and mean that the model underpredict during the year 1988. A high value of Nash–Sutcliffe efficiency and index of agreement shows that there is a good agreement between the model and observed discharge during the calibration.

**Table 5.2 Statistical analysis of model and observed daily discharge during calibration.**

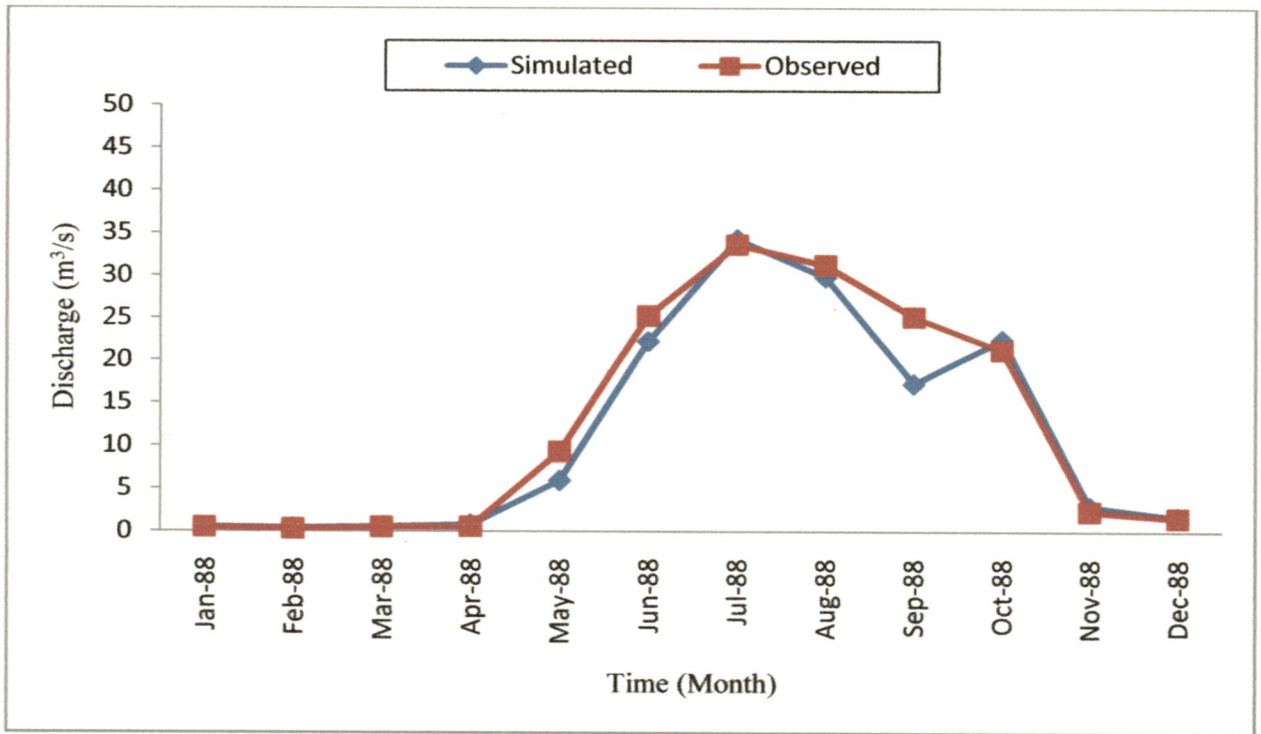| *Parametes* | *Runoff* | |
|---|---|---|
| | *Model* | *Observed* |
| Mean | 11.69 | 12.72 |
| Standard deviation | 17.61 | 19.27 |
| Maximum | 72.39 | 61.76 |
| Total | 420.80 | 457.84 |
| Coefficient of corelation ($R^2$) | 0.907 | |
| Nash-sutcliffe efficiency (NSE) | 0.903 | |
| Relative Error (RE) | -0.081 | |
| Index of Agreement (d) | 0.973 | |
| % Deviation | -8.089 | |

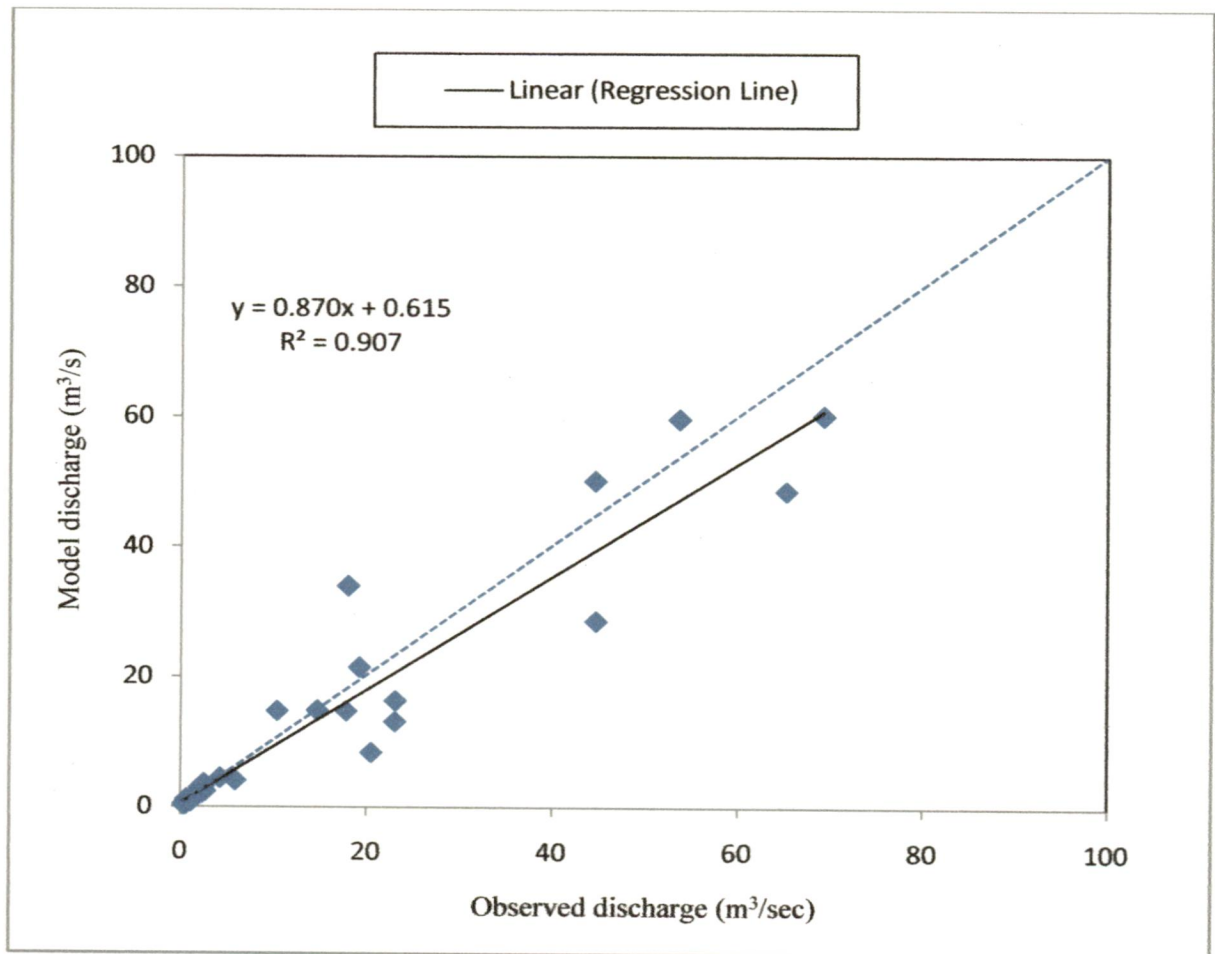**Figure 5.1 Simulated and observed discharge for the year 1988 for calibration**



**Figure 5.2 Comparison between Simulated and Observed discharge for the year 1988 for model calibration**

## 5.2 Model validation

Validation of a model is required to evaluate the performance of the model and is achieved by running the model without changing any parameter and with a different set of input data. Calibrated model was validated using the discharge data recorded. For this purpose the model was continuously run from 1987 to 1977 and for evaluation, results of 1988, 1989, 1994 were used as the observed discharge data is available for these years. The validation was also tested for the total year of 1988, 1989, 1991 and 1994 together and separately for the dry and rainy period for the whole four years.

### 5.2.1 Validation with 1989 discharge data

Model validation was performed for the year 1989 (Fig. 5.3) and graphically compared the model output with observed discharge data recorded. It is observed that the model discharge closely matched the observed discharge consistently. The regression analysis was performed between the observed and simulated discharge and the best fit line is also shown. The model slightly overpredicted the high value of discharge during monsoon (Fig. 5.4). The coefficient of correlation $(R^2)$ is 0.896 shows a close relationship between the observed and simulated discharge.

Further, the efficiency of the model for simulating the runoff was also tested using the efficiency index (Table. 5.3). A few high value of discharge during the monsoon were slightly over predicted. A high value of Nash – Sutcliffe efficiency and index of agreement shows that there is a good agreement between the model and observed discharge during the calibration.

**Table 5.3 Statistical analysis of model and observed daily discharge, 1989**

| Parametes | Discharge | |
|---|---|---|
| | *Model* | *Observed* |
| Mean | 9.87 | 9.91 |
| Standard deviation | 16.42 | 13.80 |
| Maximum | 72.39 | 61.76 |
| Total | 355.20 | 356.63 |
| Coeffient of corelation $(R^2)$ | 0.896 | |
| Nash-Sutcliffe efficiency (NSE) | 0.840 | |
| Relative Error (RE) | -0.004 | |
| Index of Agreement (d) | 0.966 | |
| % Deviation | -0.399 | |
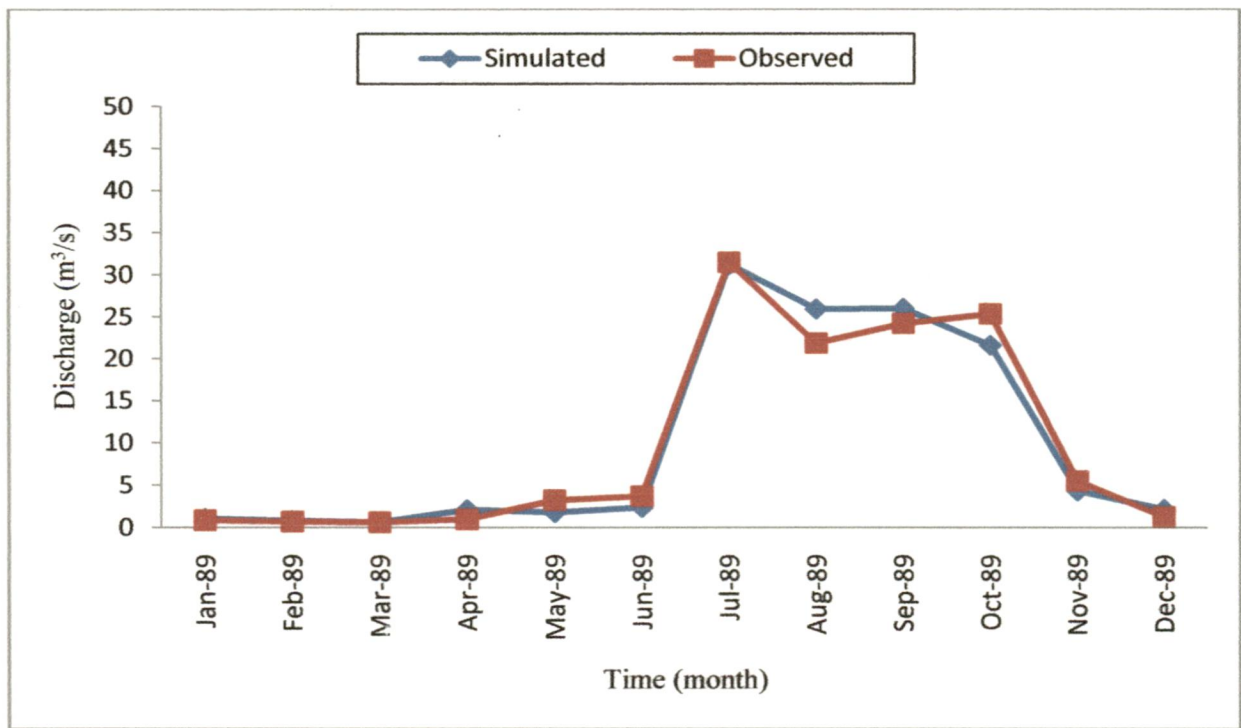
**Figure 5.3 Simulated and observed discharge for the year 1989 for model validation**



**Figure 5.4 Comparison between Simulated and Observed discharge for the year 1989 for model validation**

### 5.2.2 Validation with 1991 discharge data

The daily values of observed discharge for the year 1991 were compare graphically with the simulate discharge (Fig. 5.5). The model discharge closely matches the observed discharge data but at high value during monsoon the model underpredict the flow. However, during dry season the model discharge closely match the observed discharge.

The statistical analysis of the model was performed using statistical established parameters which give satisfactory results (Table. 5.4). A value of coefficient of determination (0.734) indicates a close relationship between the observed and model discharge data (Fig. 5.6). A close relationship between the means and standard deviation of the observed and model data shows that the frequency distribution is similar. A value of Nash-Sutcliffe value (0.72) and index of agreement (0.92) indicate that there is a reasonable agreement between the observed and simulated discharge. Moderate values of standard deviation (17.31) indicate that the overall predicted discharge by the model is within the acceptable limit.

**Table 5.4 Statistical analysis of model and observed daily discharge, 1991**

| Parametes | Discharge | |
|---|---|---|
| | Model | Observed |
| Mean | 13.48 | 16.30 |
| Standard deviation | 14.96 | 15.79 |
| Maximum | 59.08 | 47.62 |
| Total | 485.23 | 586.82 |
| Coeffient of corelation ($R^2$) | 0.734 | |
| Nash-Sutcliffe efficiency (NSE) | 0.720 | |
| Relative Error (RE) | -0.173 | |
| Index of Agreement (d) | 0.919 | |
| % Deviation | -17.311 | |
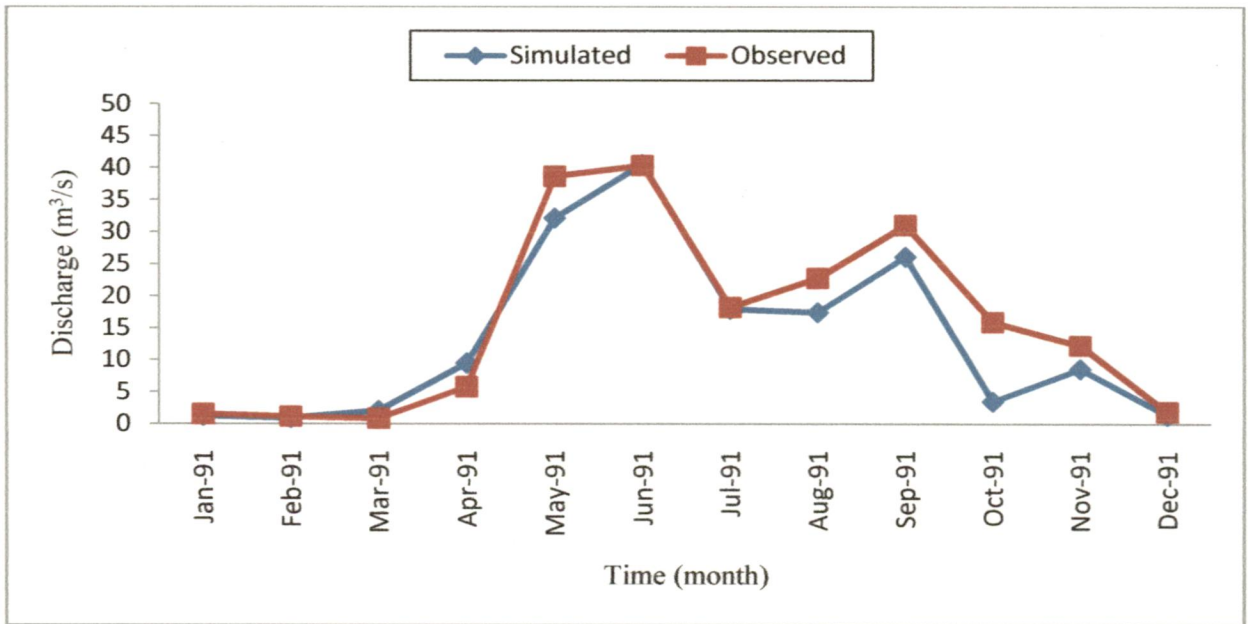
**Figure 5.5 Simulated and observed discharge for the year 1991 for model validation**
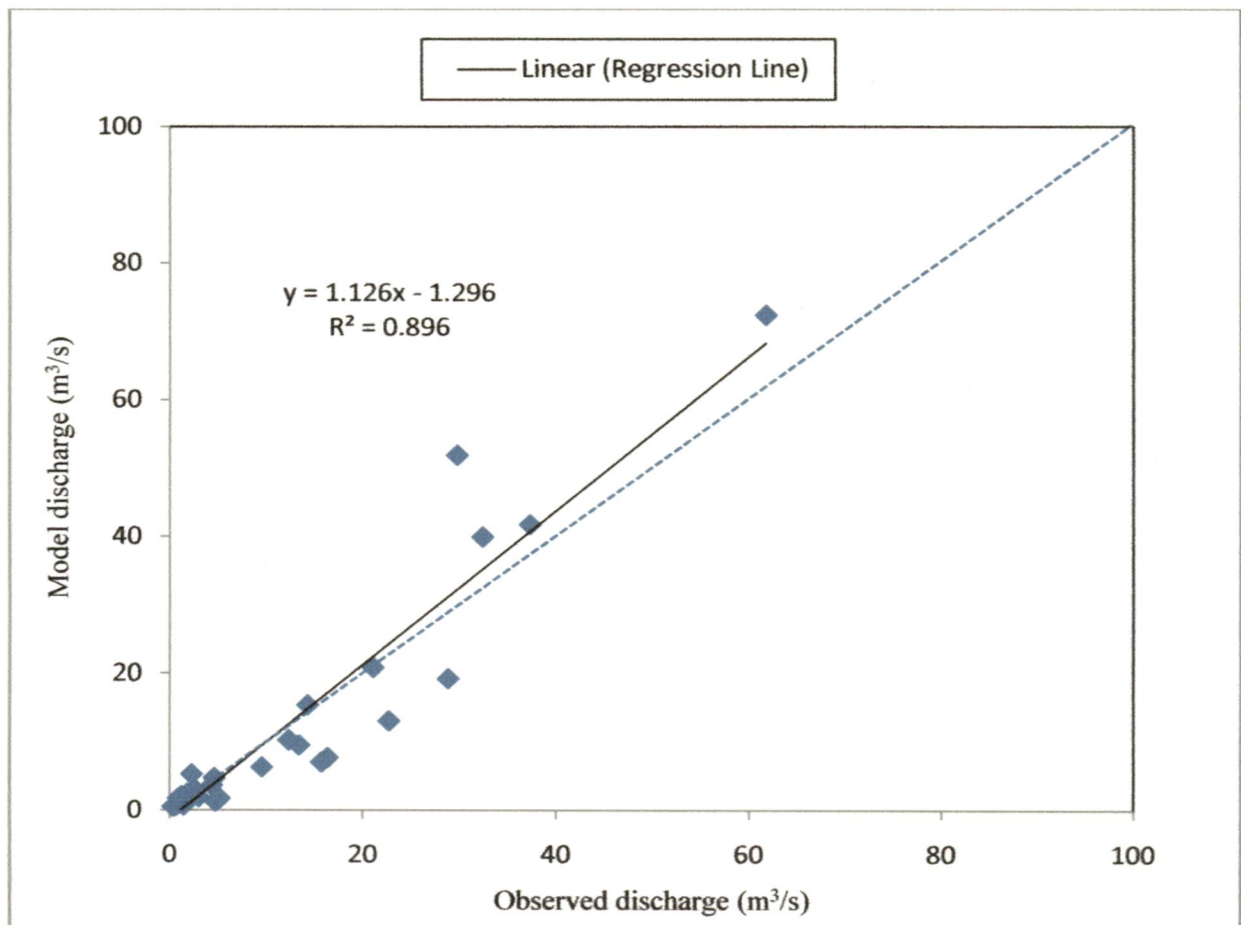


**Figure 5.6 Comparison between simulated and observed discharge for the year 1991 for model validation**

80

### 5.2.3 Validation with 1994 discharge data

The daily values of observed discharge for the year 1994 were compared graphically with the simulated discharge (Fig. 5.7). The model discharge closely matches the observed discharge data at high value in most of the cases during monsoon as well as during dry period of the year.

The performance of the model was also checked by statistical analysis (Table. 5.5). A regression analysis was performed between the observed and simulated discharge and the best fit line is also shown (Fig. 5.8). It is observed that the model discharge data are distributed uniformly along the 1:1 line. A high value of coefficient of determination (0.876) indicates a close relationship between the observed and model discharge data exist. A close relationship between the means and standard deviation of the observed and model data shows that the frequency distribution is similar. A high value of Nash-Sutcliffe value (0.892) and index of agreement (0.973) indicate that there is a reasonable agreement between the observed and simulated discharge. A low value of standard deviation (9.55) indicates that the overall predicted discharge by the model is well within the acceptable limit.

**Table 5.5 Statistical analysis of model and observed daily discharge, 1994**

| Parametes | Discharge | |
|---|---|---|
| | Model | Observed |
| Mean | 6.36 | 7.03 |
| Standard deviation | 9.50 | 9.55 |
| Maximum | 32.69 | 39.52 |
| Total | 229.01 | 253.19 |
| Coeffient of corelation ($R^2$) | 0.876 | |
| Nash-Sutcliffe efficiency (NSE) | 0.892 | |
| Relative Error (RE) | -0.096 | |
| Index of Agreement (d) | 0.973 | |
| % Deviation | -9.551 | |

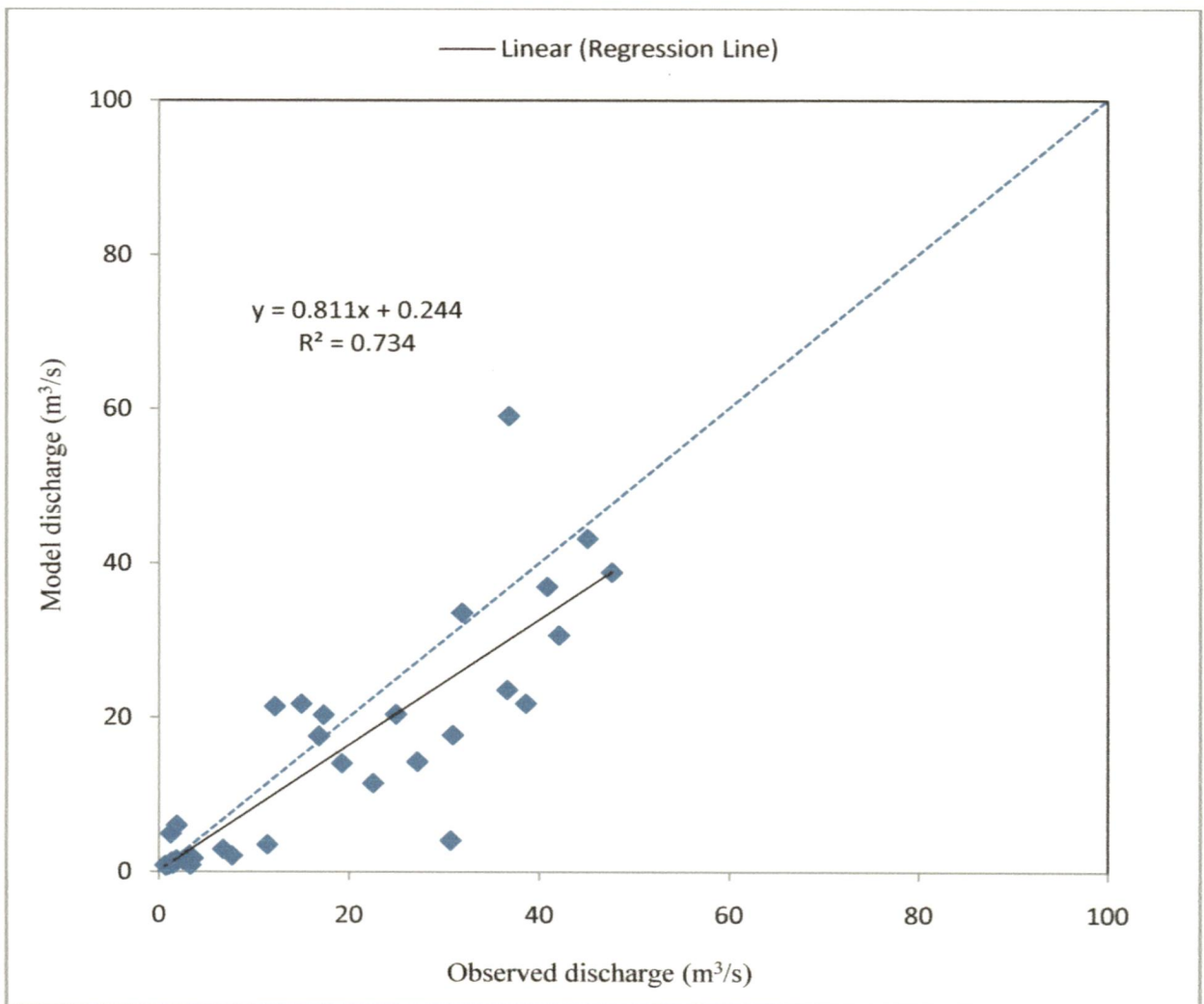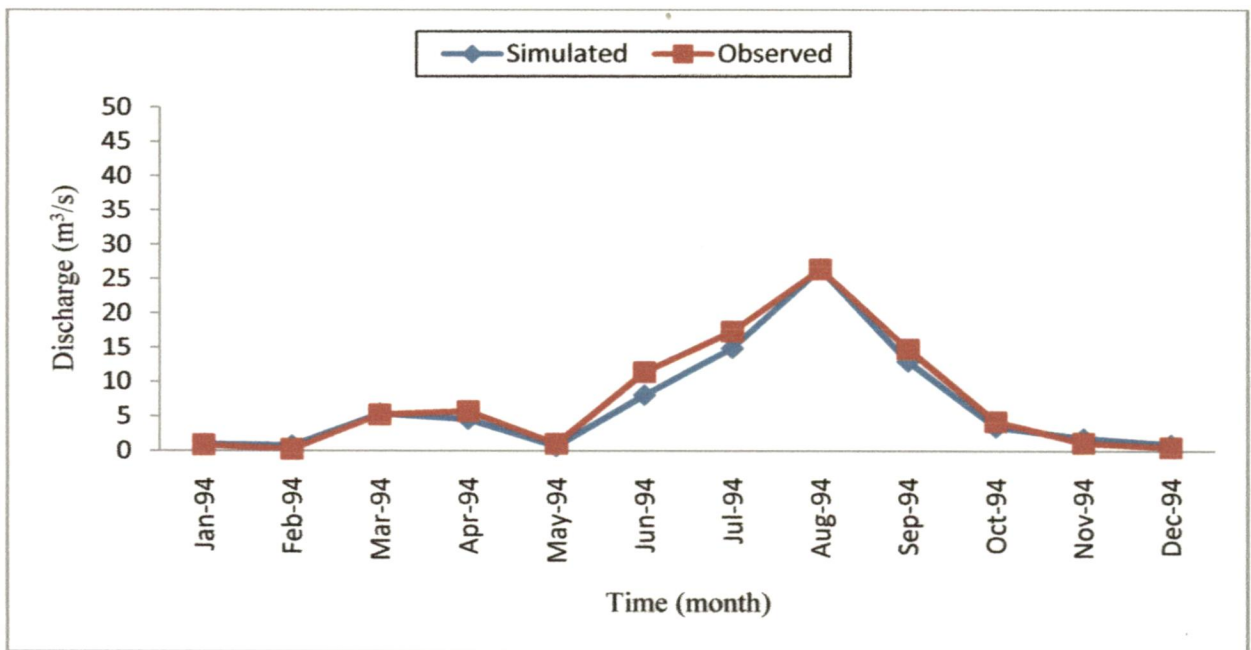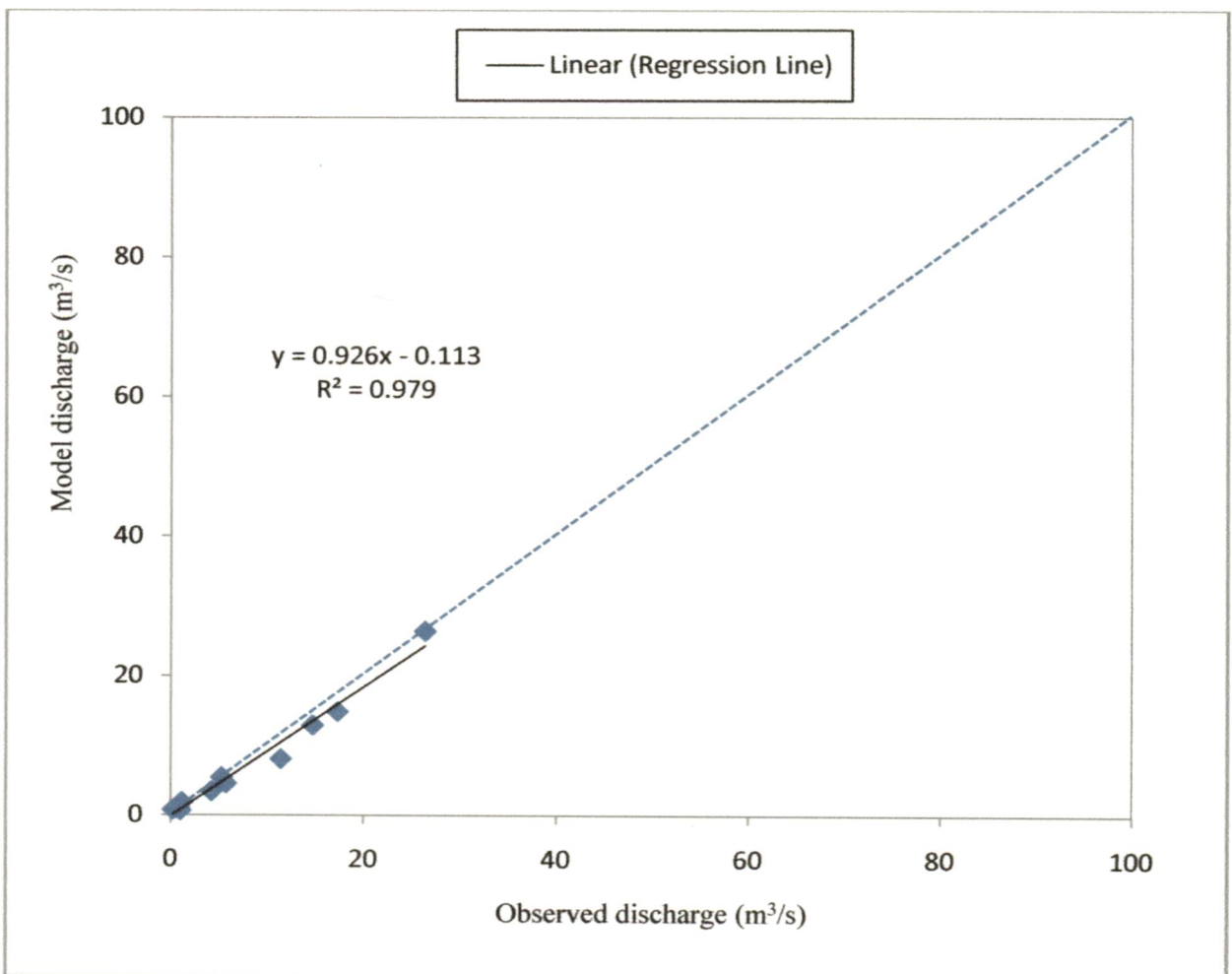**Figure 5.7 Simulated and observed discharge for the year 1994 for model validation**



**Figure 5.8 Comparison between simulated and observed discharge for the year 1994 for model validation**

### 5.2.4 Validation with discharge data of 1988, 1989, 1991 and 1994 combined

The performance of the model was checked by statistical analysis (Table. 5.6). A regression analysis was performed between the observed and simulated discharge and the best fit line is also shown (Fig. 5.9). It is observed that the model discharge data are distributed uniformly along the 1:1 line. A high value of coefficient of determination (0.846) indicates a close relationship between the observed and model discharge data exist. A close relationship between the means and standard deviation of the observed and model data shows that the frequency distribution is similar. A value of Nash-Sutcliffe value (0.836) indicates that there is a reasonable agreement between the observed and simulated discharge. A low value of standard deviation (9.926) indicates that the overall predicted discharge by the model is well within the acceptable limit.

**Table 5.6 Statistical analysis of model and observed daily discharge for all year**

| Parametes | Discharge | |
|---|---|---|
| | Model | Observed |
| Mean | 10.35 | 11.49 |
| Standard deviation | 15.03 | 15.25 |
| Coeffient of corelation ($R^2$) | 0.846 | |
| Nash-Sutcliffe efficiency (NSE) | 0.836 | |
| Relative Error (RE) | -0.099 | |
| % Deviation | -9.926 | |

### 5.2.4.1 Validation with discharge data during dry period of 1988, 1989, 1991 and 1994

The performance of the model was checked by statistical analysis (Table. 5.7). A regression analysis performed between the observed and simulated discharge shows the best fit line (Fig. 5.10). A value of coefficient of determination (0.877) indicates a close relationship between the observed and model discharge data exist. A value of Nash-Sutcliffe value (0.897) indicates that there is a reasonable agreement between the observed and simulated discharge. A low value of standard deviation (10.631) indicates that the overall predicted discharge by the model is well within the acceptable limit. The study shows that the model efficiency is higher during the dry period.

**Table 5.7 Statistical analysis of model and observed daily discharge for dry period**

| Parametes | Discharge | |
|---|---|---|
| | Model | Observed |
| Mean | 5.18 | 5.80 |
| Standard deviation | 11.32 | 12.32 |
| Coeffient of corelation ($R^2$) | 0.877 | |
| Nash-Sutcliffe efficiency (NSE) | 0.897 | |
| Relative Error (RE) | -0.106 | |
| % Deviation | -10.631 | |

**5.2.4.2 Validation with discharge data during rainy period of 1988, 1989, 1991, 1994**

The model performance was checked by statistical analysis (Table. 5.8). A regression analysis was performed between the observed and simulated discharge and the best fit line is also shown (Fig. 5.11). A value of coefficient of determination (0.726) indicates that a relationship between the observed and model discharge data exists. A value of Nash-Sutcliffe value (0.769) indicates that there is a reasonable agreement between the observed and simulated discharge.

A low value of standard deviation (9.569) indicates that the overall predicted discharge by the model is well within the acceptable limit. It is observed that the model is less efficient during the high discharge period (monsoon).

**Table 5.8 Statistical analysis of model and observed daily discharge for rainy period**

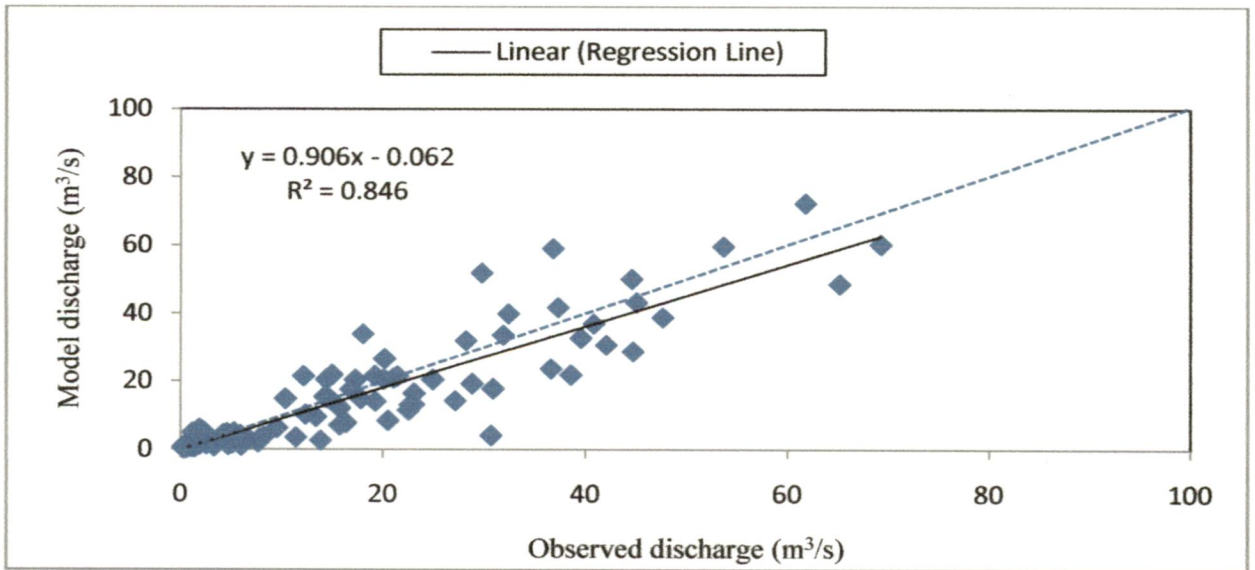| Parametes | Discharge | |
|---|---|---|
| | Model | Observed |
| Mean | 20.68 | 22.87 |
| Standard deviation | 16.27 | 14.23 |
| Coeffient of corelation ($R^2$) | 0.726 | |
| Nash-Sutcliffe efficiency (NSE) | 0.769 | |
| Relative Error (RE) | -0.096 | |
| % Deviation | -9.569 | |

**Figure 5.9 Comparison of Simulated and Observed discharge for all year**
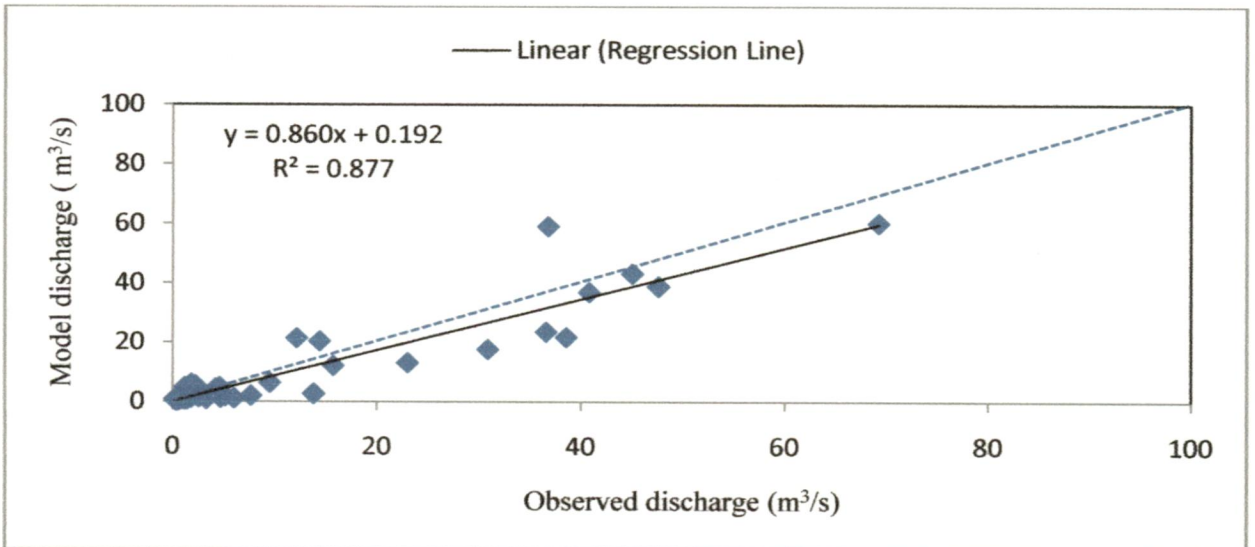


**Figure 5.10 Comparison of simulated and observed discharge for dry period**
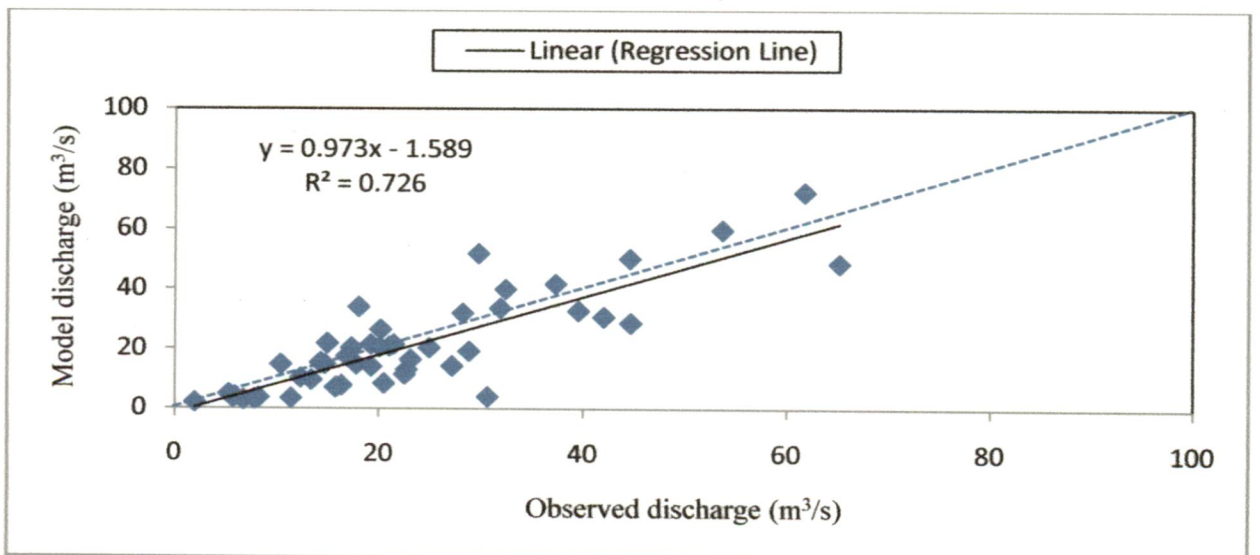


**Figure 5.11 Comparison of Simulated and observed discharge for rainy period**

## 5.3 Sensitivity analysis

The sensitivity analysis of SWAT parameters was carried out to have knowledge of how different parameters of SWAT influence the model output. The analysis was done, based on the hydrological simulation at the catchment outlet by varying the various parameters one by one and comparing the percentage deviation in the flow simulated.

Sensitivity analysis was carried out using those model parameters which were used for calibration of the watershed within their recommended range. The calibrated value of each parameter is selected as the base value for the sensitivity analysis. The base value of the each parameter is varied by increasing and decreasing them to certain percentage (+10, +20, +25, +50, -10, -20, -25, -50) within their recommended range. The parameters considered for sensitivity analysis are Available water capacity of soil layer (Sol_Awc), Threshold depth of water in shallow aquifer required for return flow to occur (Gwqmn), Soil evaporation compensation factor (Esco), Base flow recession alpha (Alpha_Bf), Threshold depth of water in shallow aquifer for percolation to the deep aquifer to occur (Revapmn), Manning's coefficient 'n' for channel (Ch_N2).

The various parameters and their range considered for sensitivity analysis are present in table (Table. 5.9).

**Table 5.9 Input SWAT parameter for sensitivity analysis for Mat watershed**

| Sl. No | Parameters | Short form | Range |
|--------|-----------|------------|-------|
| 1 | Base flow recession alpha ( days ) | Alpha_Bf | 0 - 1 |
| 2 | Threshold depth of water in shallow aquifer required for return flow to occur (mm H2O) | Gwqmn | 0 - 5000 |
| 3 | Threshold depth of water in shallow aquifer for percolation to the deep aquifer to occur | Revapmn | 0 - 500 |
| 4 | Soil evaporation compensation factor | Esco | 0.01 - 1.0 |
| 5 | Available water capacity of soil layer | Sol_Awc | 0 - 1 |
| 6 | Manning's coefficient 'n' for channel | Ch_N2 | 0.01 - 0.12 |

The sensitivity analysis reveals that the soil evaporation compensation factor is the most sensitive parameter and base flow recession alpha being the least sensitive parameter (Fig 5.12). The analysis reveals that the runoff (1.157 to 4.67) is sensitive to the soil evaporation compensation factor alone. The available water capacity of soil layer is also very sensitive to runoff (0.133 to 1.506), threshold depth of water in shallow aquifer for percolation to the deep aquifer to occur has a sensitivity of 0.008 to 0.426, and threshold depth of water in shallow aquifer required for return flow to occur has a sensitivity of 0.016 to 0.104. The two least sensitive parameters are Manning's coefficient (0.018 to 0.058) and Base flow recession alpha (0.004 to 0.029). Table 5.10 shows the details of sensitivity of various SWAT parameters.
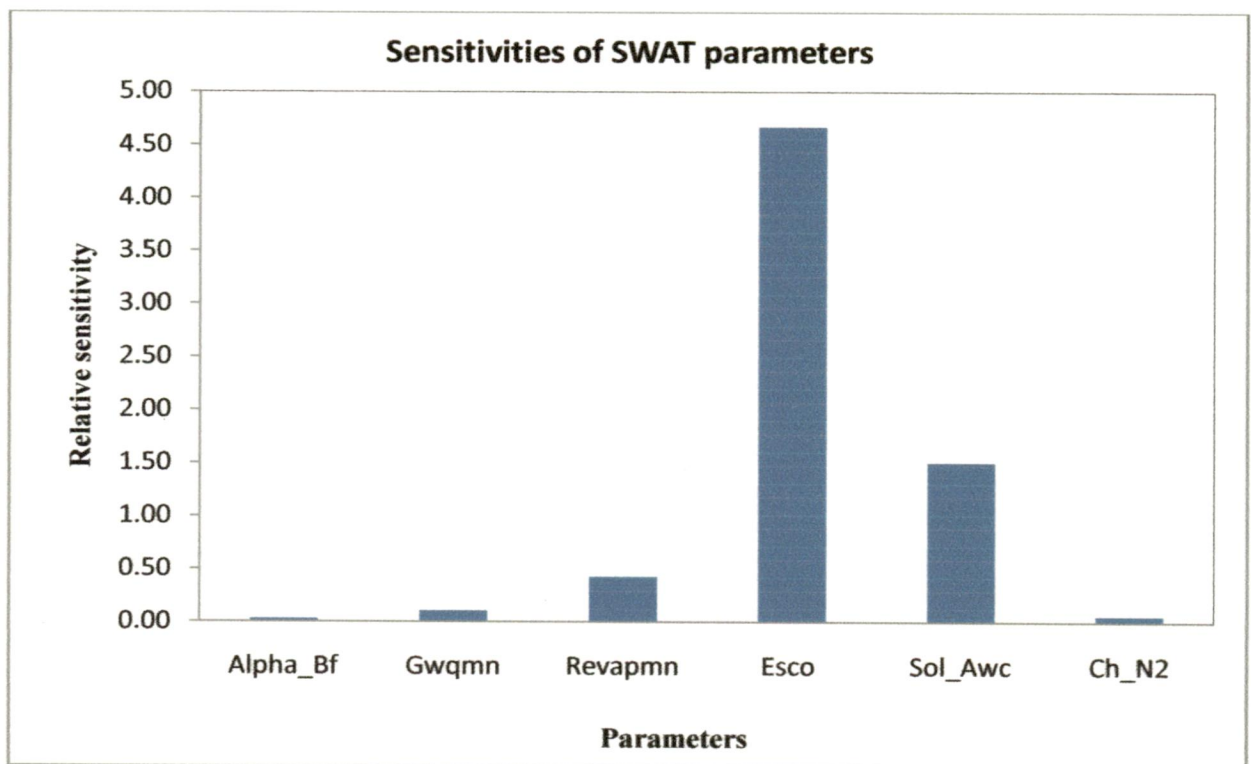


**Figure 5.12 Relative sensitivity of SWAT parameters**

**Table 5.10 Percentage deviation of discharge from the sensitivity analysis of the calibrated SWAT model**

| Sl. No | Parameters | Short form | -10 | -20 | -25 | -50 | 10 | 20 | 25 | 50 |
|---|---|---|---|---|---|---|---|---|---|---|
| 1 | Base flow recession alpha ( days ) | Alpha_Bf | -0.005 | -0.009 | -0.012 | -0.029 | 0.004 | 0.007 | 0.009 | 0.016 |
| 2 | Threshold depth of water in shallow aquifer required for return flow to occur (mm H2O) | Gwqmn | 0.016 | 0.033 | 0.043 | 0.104 | -0.017 | -0.036 | -0.045 | -0.103 |
| 3 | Threshold depth of water in shallow aquifer for percolation to the deep aquifer to occur | Revapmn | -0.066 | -0.100 | -0.122 | -0.426 | -0.016 | 0.008 | 0.022 | 0.068 |
| 4 | Soil evaporation compensation factor | Esco | -1.157 | -2.025 | -2.356 | -3.433 | 1.513 | 3.414 | 4.668 | - |
| 5 | Available water capacity of soil layer | Sol_Awc | 0.614 | 0.740 | 0.225 | 0.133 | 1.506 | 1.506 | 1.506 | 1.506 |
| 6 | Manning's coefficient 'n' for channel | Ch_N2 | -0.031 | -0.019 | -0.015 | 0.018 | -0.050 | -0.058 | - | - |

## 5.4    Selection of potential hydropower sites

The stream network of the Mat watershed was delineated using the SWAT model. by inputting a threshold value of 12000 flow accumulation to ascertain availability of flow. The model by default generates subbasin for every stream and generates subbasin outlet at each confluence point, giving information of the length and maximum and minimum elation of the stream. The elevation increased in the upstream was assessed by analyzing the DEM starting from the main outlet of the watershed. Outlets were added manually in the stream network where elevation requirement is satisfied from the previously assessed DEM, and the subbain were regenerated by the SWAT model. The information generated by the model is checked for the head and distance criteria and the subbasin outlet are readjusted till they satisfied the required criteria.

The sites were selected as potential sites when a head of 20 meter or above is available in the upstream within a river length between 500 meters and 3000 meters. Once the site is selected, assessment for the next potential site was again carried out from the last selected site and the process continues till the stream end.

Thirty three potential sites were identified in the Mat watershed (Table. 5.11). Their location is also shown along with the stream network of Mat River (Fig. 5.13)

**Table 5.11 Potential sites available in terms of Head**

| Site No. | Longitude in degree | Latitude in degree | Head in meter | Stream Length in meter |
|---|---|---|---|---|
| 1 | 92°48' 41.281" E | 23°19' 9.136" N | 20 | 596 |
| 2 | 92°49' 0.004" E | 23°19' 27.976" N | 20 | 882 |
| 3 | 92°49' 27.695" E | 23°19' 48.431" N | 20 | 1132 |
| 4 | 92°50' 19.316" E | 23°19' 54.716" N | 20 | 1725 |
| 5 | 92°49'38.614" E | 23°22' 5.84" N | 20 | 2974 |
| 6 | 92°49'57.952" E | 23°22' 53.253" N | 20 | 1819 |

Table 5.11 contd...

| Site No. | Longitude in degree | Latitude in degree | Head in meter | Stream Length in meter |
|---|---|---|---|---|
| 7 | 92°50'18.054" E | 23°26' 31.247" N | 20 | 2182 |
| 8 | 92°50'39.882" E | 23°28' 57.458" N | 20 | 685 |
| 9 | 92°50'49.441" E | 23°29' 26.407" N | 40 | 1688 |
| 10 | 92°51'6.642" E | 23°29' 50.076" N | 40 | 998 |
| 11 | 92°51'27.422" E | 23°30' 7.568" N | 40 | 919 |
| 12 | 92°50' 44.74" E | 23°19' 50.637" N | 20 | 800 |
| 13 | 92°50' 54.93" E | 23°19' 25.445" N | 20 | 646 |
| 14 | 92°50' 0.835" E | 23°20' 52.759" N | 20 | 577 |
| 15 | 92°49'24.185" E | 23°21' 55.171" N | 80 | 595 |
| 16 | 92°49'13.991" E | 23°21' 43.755" N | 20 | 505 |
| 17 | 92°48'56.309" E | 23°21' 39.528" N | 20 | 554 |
| 18 | 92°48'39.507" E | 23°21' 40.179" N | 60 | 539 |
| 19 | 92°48'52.917" E | 23°22' 45.456" N | 20 | 1302 |
| 20 | 92°48'35.366" E | 23°22' 47.311" N | 20 | 520 |
| 21 | 92°48'2.887" E | 23°23' 8.515" N | 20 | 1279 |
| 22 | 92°47'47.042" E | 23°23' 21.836" N | 20 | 690 |
| 23 | 92°47'27.342" E | 23°23' 31.576" N | 20 | 691 |
| 24 | 92°49'28.323" E | 23°24' 20.964" N | 20 | 886 |
| 25 | 92°49'5.513" E | 23°24' 25.83" N | 20 | 717 |
| 26 | 92°48'51.441" E | 23°24' 39.465" N | 40 | 622 |
| 27 | 92°48'31.019" E | 23°25' 0.906" N | 20 | 1013 |
| 28 | 92°49'38.433" E | 23°25' 36.82" N | 20 | 1113 |
| 29 | 92°49'15.016" E | 23°26' 12.035" N | 20 | 1621 |
| 30 | 92°50'46.169" E | 23°25' 42.88" N | 20 | 1408 |
| 31 | 92°49'57.259" E | 23°27' 2.097" N | 30 | 668 |
| 32 | 92°50'28.663" E | 23°28' 44.302" N | 40 | 500 |
| 33 | 92°50'46.928" E | 23°29' 41.877" N | 60 | 530 |
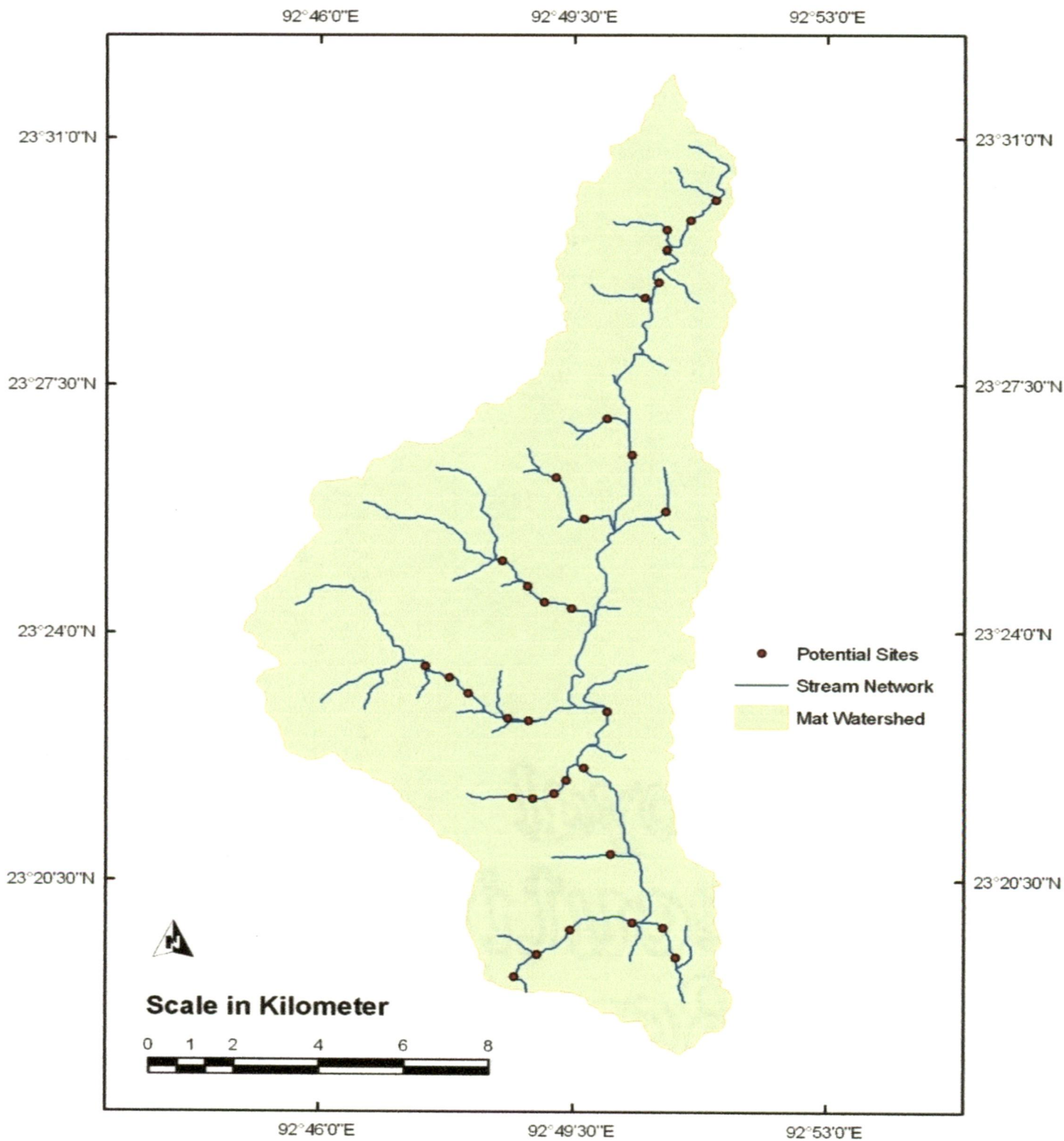
**Figure 5.13 Selected hydropower potential site in the Mat watershed**

## 5.6 Estimation of hydropower potential

The calibrated SWAT model was used to generate the flow for 10 years from 1988 to 1997. The discharge was simulated for the main watershed outlet for finding out the 90 % dependable year.

The 90% dependable year was calculated by rearranging in descending order, the annual runoff of all the years for which simulated discharge data is available and applied Weilbuls' formula (MNES/AHEC, 2008). The year 1992 is the 90 % dependable year (Table. 5.12 and Fig. 5.14).

**Table 5.12 Calculation of 90% dependable year**

| Year | Discharge m3/s | Descending order | Percentage Dependability | coresponding year |
|------|------|------|------|------|
| 1988 | 4264.34 | 5085.398 | 10 | 1993 |
| 1989 | 3684.94 | 4913.428 | 20 | 1991 |
| 1990 | 3763.82 | 4264.3416 | 30 | 1988 |
| 1991 | 4913.43 | 4106.8308 | 40 | 1996 |
| 1992 | 3391.48 | 3763.8182 | 50 | 1990 |
| 1993 | 5085.40 | 3684.9381 | 60 | 1989 |
| 1994 | 2483.13 | 3643.7491 | 70 | 1997 |
| 1995 | 3597.07 | 3597.0653 | 80 | 1995 |
| 1996 | 4106.83 | **3391.4847** | **90** | **1992** |
| 1997 | 3643.75 | 2483.1345 | 100 | 1994 |



**Figure 5.14 Flow duration curve for yearly discharge**

After the 90 percent dependable year is known, the discharge for each potential hydropower sites are generated by the validated SWAT model. Since the subbasin ou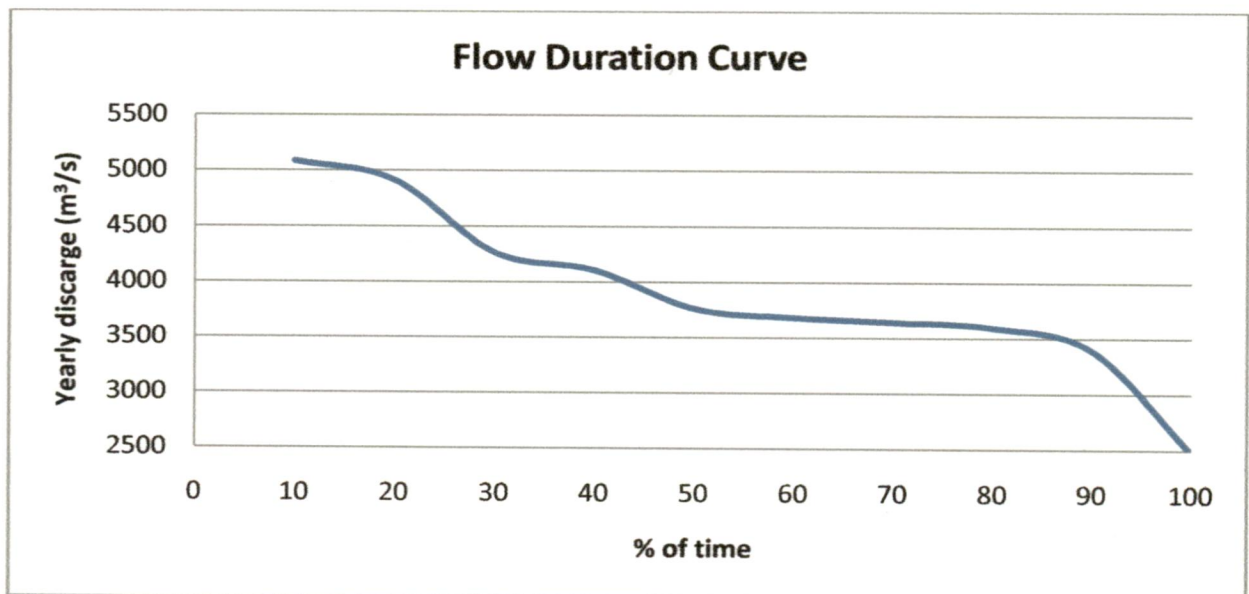tlet is added to each potential site at the time of head assessment, the model is able to generate discharge for each selected sites separately.

The watershed is relying mainly on the rainfall during monsoon period which results in large variation between the flow during dry and rainy periods. This result in variation of the power potential which are as high as 3039.47 kw during the rainy period and only 804.98 kw during the dry period respectively (Table. 13)

**Table. 5.13 Estimation of Hydropower potential in Mat watershed**

| Potential site No. | Power estimation in Kw | | |
|---|---|---|---|
| | 50 % dependability | 75 % dependability | 90 % dependability |
| 1 | 382.73 | 139.56 | 99.01 |
| 2 | 374.35 | 136.71 | 96.84 |
| 3 | 371.42 | 135.3 | 95.57 |
| 4 | 360.52 | 131.4 | 92.41 |
| 5 | 314.34 | 114.6 | 79.38 |
| 6 | 282.09 | 102.74 | 70.38 |
| 7 | 83.4 | 30.17 | 21.45 |
| 8 | 38.21 | 14.08 | 10.73 |
| 9 | 50.11 | 22.54 | 16.65 |
| 10 | 29.55 | 11.64 | 8.38 |
| 11 | 25.86 | 10.39 | 7.55 |
| 12 | 15.09 | 5.60 | 4.30 |
| 13 | 12.21 | 4.85 | 3.92 |
| 14 | 8.22 | 2.92 | 2.3 |
| 15 | 65.27 | 26.3 | 20.91 |
| 16 | 29.61 | 12.27 | 9.78 |
| 17 | 11.36 | 4.7 | 3.75 |
| Sub Total | 2454.34 | 905.77 | 643.31 |

| Potential site No. | Power estimation in Kw | | |
|---|---|---|---|
| | 50 % dependability | 75 % dependability | 90 % dependability |
| 18 | 31.33 | 12.49 | 10.18 |
| 19 | 62.94 | 25.47 | 18.91 |
| 20 | 62.39 | 25.25 | 18.73 |
| 21 | 47.55 | 20.03 | 14.74 |
| 22 | 45.63 | 19.33 | 14.32 |
| 23 | 36.29 | 15.69 | 12.01 |
| 24 | 45.14 | 15.68 | 10.6 |
| 25 | 42.00 | 14.68 | 9.93 |
| 26 | 80.96 | 28.3 | 19.26 |
| 27 | 33.51 | 11.09 | 8.18 |
| 28 | 17.04 | 5.22 | 3.46 |
| 29 | 9.16 | 2.53 | 1.66 |
| 30 | 9.44 | 3.23 | 2.38 |
| 31 | 16.77 | 5.46 | 3.77 |
| 32 | 12.66 | 4.85 | 3.65 |
| 33 | 32.32 | 12.09 | 9.89 |
| Sub Total | 585.13 | 221.39 | 161.67 |
| Total | 3039.47 | 1127.16 | 804.98 |

The hydropower was estimated considering three levels of dependability, 90 %, 75 %, and 50 % dependability respectively (MNES/AHEC, 2008). The total hydropower generation capacity at 50 %, 75 %, and 90 % dependability are 3039.47 kw, 1127.16 kw and 804.98 kw respectively (Table. 5.6). The total river length between the consecutive selected potential sites is 33.376 km, and the average distance between the consecutive selected potential sites is 1.011 km. The average slope of river bed between the selected site in mat watershed is 3.65 %.

# CHAPTER VI
# SUMMARY AND CONCLUSION

## 6.1 Catchment modeling using the SWAT model

The Mat watershed is shared by Aizawl and Serchhip Districts of Mizoram, India. The river Mat is a perennial river and is flashy and effluent. The river has a length of 127 km flowing in south direction flowing through Lunglei District and finally joins River Tuipui (also known as Kolodyne river). The study area covers 147.325 $km^2$ and length of the river up to the considered outlet is 35 km. The annual average rainfall is 3000 mm, and 56 % of the watershed is covered by forest. The resources of water in this watershed have not been tapped for generation of hydropower till date.

The catchment modelling was carried out using the SWAT model. SWAT requires specific information about weather, soil properties, topography, vegetation, and land management practices occurring in the watershed. The SWAT model divides a watershed into sub basins which allow accounting of land uses and soil properties impact on hydrology. The model further subdivides the sub basins into smaller homogenous units known as Hydrologic Response Units (HRU). Model calibration was performed manually by adjusting six (6) parameters (within their prescribed range) until the model output matches the observed discharge. The gauge discharge for a period of 1988 was used for calibration.

The validation of the SWATmodel was performed by comparing the observed and model simulated discharge by comparing them graphically and the model performance was also evaluated using five (5) established indices $viz.$, Coefficient of determination ($R^2$), Nash and Sutcliffe Efficiency (NSE), index of agreement (d), relative error of the stream flow volume (RE), and % deviation. The model performance was evaluated for the year 1989, 1991 and 1992 separately. Further, validation was also carried out for full period, dry period and rainy period for the year 1991, 1994 along with the calibration period (1988 – 1989).

## 6.2 Identification of potential hydropower sites

The potential hydropower sites were identified from the stream network generated by the SWAT model with a threshold value of 12000 flow accumulation cells. The SWAT model, by default generate subbasin outlet at every confluence point of rivers, thereby giving information of all the locations of the subbasin outlet and the subbasins. At the same time the model also generates detailed information of each and every stream within the watershed regarding the corresponding subbasin, and length of the river between outlets. It also gives the minimum and maximum elevation of the stream or the elevation of the subbasin outlet. Therefore, this information was utilized in selecting the head rise along the river by measuring the stream network and adding subbasin outlet for assessing the elevation as the model gives the length, maximum and minimum elevation of the river.

The assessment of head rise was initiated with a search of 20m increase in river bed from the main watershed outlet proceeding towards the upstream. When head rise of 20 m is identified, then minimum and maximum distance criteria was checked, and if satisfied then the site is select as hydropower potential site. In this way, thirty three (33) potential sites were identified in Mat watershed. The sum of the length of river between the consecutive selected potential site is 33.376 km and the average distance between the consecutive selected potential sites is 1.011 km. The average slope of river bed between the selected sites in the Mat watershed is 3.65 %.

Once the sites are selected, with the subbasin outlet already added, the calibrated SWAT model is run to simulate model discharge for each hydropower potential site. The 90 % dependable year was found out using Weilbuls' formula (MNES/AHEC, 2008). After knowing the 90% dependable year, 90 %, 75 %, and 50 % dependable flow was generated for each of the selected potential sites from a 10 daily discharge using flow duration curve (FDC). The hydropower generation capacities for each 33 potential sites were estimated using established power equation (CEA, 1997).

The total capacity of hydropower estimated from the 33 potential sites selected at 90 %, 75 % and 50 % dependability are 804.98 kw, 1127.16 kw and 3039.47 kw respectively.

## 6.3    Conclusions

The following important conclusions are drawn from this study.

1. The sensitivity analysis reveals that the SWAT parameters very effective in calibrating the model. The various parameter of the SWAT model in respect of their sentivities for the Mat watershed are: (i) Soil evaporation compensation factor (Esco), (ii) Available water capacity of soil layer (Sol_Awc), (iii) Threshold depth of water in shallow aquifer for percolation to the deep aquifer to occur (Revapmn), (iv) Threshold depth of water in shallow aquifer required for return flow to occur (Gwqmn), (v) Manning's coefficient 'n' for channel (Ch_N2) and (vi) Base flow recession alpha (Alpha_Bf).

2. Thirty three (33) potential hydropower sites were identified within 147. 325 $km^2$ of the Mat watershed from which a total of 3039.47 kw, 1127.16 kw and 804.98 kw could be harnessed at 50 %, 75 % and 90 % dependability respectively.

3. Proposed methodology can be adapted to other remote areas for assessment of hydropower potential. This will save time, expenditure and ultimately boost the hydropower development.

4. The study has revealed that potential hydropower sites can be effectively assessed and evaluated using GIS, Remote Sensing and the SWAT model.

Abbaspour K. C., Yang J., Maximov I., Siber R., Bogner K., Mieleitner J., Zobrist J., Srinivasan R., 2007. Modelling hydrology and water quality in the pre-alpine/alpine Thur watershed using SWAT. Journal of Hydrology, (333)413– 430

Arnold J.G, Allen P.M., Bernhardt G., 1993. A comprehensive surface ground water flow model. J Hydrol, 142:47–69.

Arnold, J.G., J.R. Williams and D.R. Maidment. 1995. Continuous-time water and sediment-routing model for large basins. Journal of Hydraulic Engineering 121(2):171-183.

Arnold, J.G., P.M. Allen, and G. Bernhardt. 1993. A comprehensive surfacegroundwater flow model. J. Hydrol. 142:47-69.

Bagnold, R.A. 1977. Bedload transport in natural rivers. Water Resources Res. 13(2):303-312.

Belmonte S., Nunez V., Viramonte J.G., Franco J., 2009. Potential renewable energy resources of the Lerma Valley, Salta, Argentina for its strategic territorial planning. Renewable and Sustainable Energy Reviews (13) 1475–1484

Brown, L.C. and T.O. Barnwell, Jr. 1987. The enhanced water quality models QUAL2E and QUAL2E-UNCAS documentation and user manual. EPA document EPA/600/3-87/007. USEPA, Athens, GA.

Campbell, G. S. 1985. Soil physics with basic: transport model for soil plant system. Elsevier, Amsterdam.

Castellarin A, Galeati G, Brandimarte L, Montanari A, Brath A., 2004. Regional flowduration curves: reliability for ungauged basins. Adv Water Resour.953–65.

CEA, 1997. Small hydro power potential in India, central electrical authority, Ministry of Power Government of India, New Delhi.

Central Water Commission (CWC), 1997. The Mat valley multipurpose project report.

Chapra, S.C. 1997. Surface water-quality modeling. McGraw-Hill, Boston.

Coskun H. Gonca, Alganci Ugur, Eris Ebru, Agıralioglu N, Cigizoglu H. Kerem, Yilmaz Levent, Toprak Z. F. Remote Sensing and GIS Innovation with Hydrologic Modelling for Hydroelectric Power Plant (HPP) in Poorly Gauged Basins. Water Resour Manage, DOI 10.1007/s11269-010-9632-x

Dandekar M.M and Sharma K.N., 1979. Water power Engineering.

Darren L. Ficklin, Yuzhou Luo, Eike Luedeling, Minghua Zhang, 2009. Climate change sensitivity assessment of a highly agricultural watershed using SWAT. Journal of Hydrology, (374) 16–29

Das S, Paul PK, 2006. Selection of site for small hydel using GIS in the Himalayan region of India. J Spatial Hydrol;6(1):18–28.

Deogratias M.M. Mulungu, Subira E. Munishi, 2007. Simiyu River catchment parameterization using SWAT model. Physics and Chemistry of the Earth, (32) 1032–1039

Dudhani S., Sinha A.K., Inamdar S.S., 2006. Assessment of small hydropower potential using remote sensing data for sustainable development in India. Energy Policy, (34) 3195–3205

Fennesseyl Neil and Vogel Richard M., 1990, Regional Flow-Duration Curves for ungauged sites in Massachusetts. Journal of Water Resources Planning and Management, Vol. 116, No.4

Gassman P. W., Reyes M. R., Green C. H., Arnold J. G., 2007. The soil and water assessment tool : Historical development, applications, and future research direction. American Society of Agricultural and Biological Engineers ISSN 0001-2351, Vol. 50(4): 1211-1250

Gassman PW, Reyes MR, Green CH, Arnold J. G., 2007. The soil and water assessment tool: historical development, applications, and future research directions. Trans ASABE;50(4):1211–50.

Gismalia Y. A., 1996. Use of a GIS in reconnaissance studies for small-scale hydropower development in a developing country: a case study from Tanzania. HydroGIS 96: Application of Geographic Information Systems in Hydrology and Water Resources Management (Proceedings of the Vienna Conference, April 1996). IAHS Publ. no. 235, 1996. 307

Green C.H., A. Griensven van, 2008. Autocalibration in hydrologic modeling: Using SWAT2005 in small-scale watersheds. Environmental Modelling & Software, (23) 422-434

Green, W.H. and G.A. Ampt. 1911. Studies on soil physics, 1. The flow of air and water through soils. Journal of Agricultural Sciences 4:11-24.

Haltiner, G. J. and Martin, F. L. 1957. Dynamical and meteorology. McGraw-Hill, New York.

Hongmei Xu, Richard G. Taylor, Daniel G. Kingston, Tong Jiang, Julian R. Thompson, Martin C. Todd, 2010. Hydrological modeling of River Xiangxi using SWAT2005: A comparison of model parameterizations using station and gridded meteorological observations. Quaternary International (xxx)1–6

Ioannis A. Niadas & Panos G. Mentzelopoulos, 2008. Probabilistic Flow Duration Curves for Small Hydro Plant Design and Performance Evaluation. Water Resource Manage (22)509–523

Jensen, M. E. (ed.) 1974. Consumptive use of water and irrigation water requirements. Rep. Tech. com. on irrig. Water requirements, irrig. and Drains. Div. ASCE.

Jones, C.A. 1983. A survey of the variability in tissue nitrogen and phosphorus concentrations in maize and grain sorghum. Field Crops Res. 6:133-147.

Kang M.S., Park S.W., Lee J.J., Yoo K.H., 2006. Applying SWAT for TMDL programs to a small watershed containing rice paddy fields. Agricultural Water Management, (79) 72–92

Kangsheng Wu, Johnston C. A., 2007. Hydrologic response to climatic variability in a Great Lakes Watershed: A case study with the SWAT model. Journal of Hydrology, (337)187– 199

Kannan N., White S.M., Worrall F., Whelan M.J., 2007. Hydrological modelling of a small catchment using SWAT-2000 – Ensuring correct flow partitioning for contaminant modelling. Journal of Hydrology, (334)64– 72

Kannan N., White S.M., Worrall F., Whelan M.J., 2007. Sensitivity analysis and identification of the best evapotranspiration and runoff options for hydrological modelling in SWAT-2000. Journal of Hydrology, (332) 456– 466

Kati L. White and Chaubey Indrajeet, 2005. Sensitivity analysis, calibration, and validation for a multi-site and multi-variable SWAT model. Journal of the American Water Resources Association.

Kusre B.C., Baruah D.C., Bordoloi P.K., Patra S.C., 2010. Assessment of hydropower potential using GIS and hydrological modeling technique in Kopili River basin in Assam (India). Applied Energy, (87) 298–309

Leonard, R.A., W.G. Knisel, and D.A. Still. 1987. GLEAMS: Groundwater loading effects on agricultural management systems. Trans. ASAE 30(5):1403-1428.

McElroy, A.D., S.Y. Chiu, J.W. Nebgen, A. Aleti, and F.W. Bennett. 1976. Loading functions for assessment of water pollution from nonpoint sources. EPA document EPA 600/2-76-151. USEPA, Athens, GA.

Ministry Of New And Renewable energy, Government of India standards / manuals / Guidelines for small hydro development: Manual on project Hydrology and installed capacity, 2008.

MNRE. Small hydro power programme, 2007. <www.mnre.gov.in/progsmallhydro.htm>.

Mohamoud Y.M., 2008. Prediction of daily flow duration curves and streamflow for ungauged catchments using regional flow duration curves. Hydrological Sciences–Journal–des Sciences Hydrologiques, 53(4)

Monteith, J.L. 1965. Evaporation and the environment. p. 205-234. In The state and movement of water in living organisms. 19th Symposia of the Society for Experimental Biology. Cambridge Univ. Press, London, U.K.

Ndomba P., Mtalo F., Killingtveit A., 2008. SWAT model application in a data scarce tropical complex catchment in Tanzania. Physics and Chemistry of the Earth, (33) 626–632

Neitsch SL, Arnold JG, Kiniry JR, Williams JR. 2005. Soil and water assessment tool – theoretical documentation.

Neitsch SL, Arnold JG, Kiniry JR, Williams JR. Soil and water assessment tool –version 2005 – user manual, Temple (TX, USA); 2001.

Nicks, A.D. 1974. Stochastic generation of the occurrence, pattern and location of maximum amount of daily rainfall. p. 154-171. In Proc. Symp. Statistical Hydrology, Tucson, AZ. Aug.-Sept. 1971. USDA Misc. Publ. 1275. U.S. Gov. Print. Office, Washington, DC.

Pandey A., Chowdary V.M., Mal B.C., Billib M., 2008. Runoff and sediment yield modeling from a small agricultural watershed in India using the WEPP model. Journal of Hydrology, (348)305–319

Pisinaras V., Petalas Christos, Georgios D. Gikas, Gemitzi A., Tsihrintzis V. A., 2010. Hydrological and water quality modeling in a medium-sized basin using the Soil and Water Assessment Tool (SWAT). Desalination, (250) 274–286

Pokharel S., 2000. Spatial analysis of rural energy system. int. j. geographical information science, vol. 14, no. 8, 855-873

Pokharel S., 2007. Water use opportunities and conflicts in a small watershed—a case study. Renewable and Sustainable Energy Reviews, (11)1288–1299

Priestley, C.H.B. and R.J. Taylor. 1972. On the assessment of surface heat flux and evaporation using large-scale parameters. Mon. Weather Rev. 100:81-92.

Ramachandra T.V., Rajeev Kumar Jha, Krishna S. V. and Shruthi B.V., 2004. Spatial Decision Support System for Assessing Micro, Mini and Small Hydel Potential. Journal of Applied Sciences, 4 (4): 596-604.

Ramachandra T.V., Shruthi B.V., 2007. Spatial mapping of renewable energy potential. Renewable and Sustainable Energy Reviews, (11) 1460–1480

Ramachandra TV, Jha RK, Vamsee Krishna S, Shruthi B.V., 2004. Spatial decision support system for assessing micro, mini and small hydel potential. J Appl Sci, 4(4):596–604.

Remegio B. Confesor Jr., Gerald Whittaker, 2007. Sensitivity Analysis And Interdependence Of The SWAT Model Parameters. ASABE, Paper No.: 072101

Ritchie, J.T. 1972. A model for predicting evaporation from a row crop with incomplete cover. Water Resour. Res. 8:1204-1213.

Rojanamon P., Chaisomphob T., Bureekul T., 2009. Application of geographical information system to site selection of small run-of-river hydropower project by considering engineering/economic/environmental criteria and social impact. Renewable and Sustainable Energy Reviews, (13) 2336–2348

Schmalz B. and Fohrer N., 2009. Comparing model sensitivities of different landscapes using the ecohydrological SWAT model. *Adv.* Geosci., (21)91–98, www.adv-geosci.net/21/91/2009.

Schuol J., Abbaspour K.C., 2007. Using monthly weather statistics to generate daily data in a SWAT model application to West Africa. ecological modelling, (201) 301–311

Schuol J., Karim C. Abbaspour, Raghavan Srinivasan, Yang H.,2008. Estimation of freshwater availability in the West African sub-continent using the SWAT hydrologic model. Journal of Hydrology, (352)30– 49

Shao Q., Zhang Lu, Yongqin D. Chen & Vijay P. S., 2009. A new method for modelling flow duration curves and predicting streamflow regimes under altered land-use

conditions. Hydrological Sciences–Journal–des Sciences Hydrologiques, 54(3) June.

Singh VP, Sharma N, Ojha C. S. P. (ed.), 2004. The Brahmaputra basin water resources. Kluwer Academic Publisher, Netherland.

Soil Conservation Service. 1972. Section 4: Hydrology in national Engineering handbook.SCS.

Strahler A.N., 1958. Dimensionless analysis applied to fluvially eroded landforms. Geol Soc Am Bull, (69)279–300.

Sung Yi, Jin-Hee Lee, Myung-Pil Shim, 2010. Site location analysis for small hydropower using geo-spatial information system. Renewable Energy, (35) 852–861

Tolson Bryan A., Christine A. Shoemakerb, 2007. Cannonsville Reservoir Watershed SWAT2000 model development, calibration and validation. Journal of Hydrology, (337)68– 86

Trevor Price, Douglas Probert, 1997. Harnessing hydropower: a practical guide. J Appl Energy, 57(2/3):175–251

Ullrich A., Volk Martin, 2009. Application of the Soil and Water Assessment Tool (SWAT) to predict the impact of alternative management practices on water quality and quantity. Agricultural Water Management, (96) 1207–1217

USDA Soil Conservation Service. 1972. National Engineering Handbook Section 4 Hydrology, Chapters 4-10.

USDA Soil Conservation Service. 1983. National Engineering Handbook Section 4 Hydrology, Chapter 19.

Vale M., Holman I.P., 2009. Understanding the hydrological functioning of a shallow lake system within a coastal karstic aquifer in Wales, UK. Journal of Hydrology, (376) 285–294

Vogel RM, Fennessey NM., 1994. Flow-duration curves. I: new interpretation and confidence intervals. J Water Resour Plan Manage ASCE. 120(4):485–504.

William, J. R. 1995. Chapter 25. The EPIC model. P. 909 – 1000. In V. P. Singh (ed.). Computer model of watershed hydrology. Water resources publications, highland ranch, CO.

Williams, J.R. 1969. Flood routing with variable travel time or variable storage coefficients. Trans. ASAE 12(1):100-103.

Williams, J.R. 1975. Sediment routing for agricultural watersheds. Water Resour. Bull. 11(5):965-974.

Williams, J.R. 1980. SPNM, a model for predicting sediment, phosphorus, and nitrogen yields from agricultural basins. Water Resour. Bull. 16(5):843-848.

Williams, J.R. and R.W. Hann. 1972. HYMO, a problem-oriented computer language for building hydrologic models. Water Resour. Res. 8(1):79-85.

Williams, J.R. and R.W. Hann. 1978. Optimal operation of large agricultural watersheds with water quality constraints. Texas Water Resources Institute, Texas A&M Univ., Tech. Rept. No. 96.

Winnaar G. de, Jewitt G.P.W., Horan M., 2007. A GIS-based approach for identifying potential runoff harvesting sites in the Thukela River basin, South Africa. Physics and Chemistry of the Earth, (32)1058–1067

Wischmeier, W.H., and D.D. Smith. 1978. Predicting rainfall losses: A guide to conservation planning. USDA Agricultural Handbook No. 537. U.S. Gov. Print. Office, Washington, D.C.

Yang J., Reichert P., Abbaspour K.C., Jun Xia, Yang H., 2008. Comparing uncertainty analysis techniques for a SWAT application to the Chaohe Basin in China. Journal of Hydrology, (358)1– 23